APPENDIX B

CAP MODELING

1.0 INTRODUCTION

Design of the Onondaga Lake sediment cap, specifically the chemical isolation component, was accomplished through a rigorous modeling effort. This appendix summarizes the objectives, application, input, results and recommendations from this modeling effort.

The models and modeling framework referenced in this appendix were developed by experts and have been published in peer-reviewed journals and publications such as the Journal of Soil and Sediment Contamination (Lampert, D. J. and Reible, D. 2009) and Guidance for *in situ* subaqueous capping of contaminated sediments (USEPA, 1998).

Design of the cap covering approximately 400 acres over five remediation areas and for 26 contaminants was accomplished using two models, a series of screening level evaluations, and both deterministic simulations and Monte Carlo analyses. An analytical model was used to evaluate steady state concentrations throughout the cap isolation and habitat layers. This model is similar in format to the model used during the Feasibility Study (FS) (Parsons, 2004), but offers several advantages over the FS model, including simultaneous modeling of advective and diffusive transport and concentration predictions throughout the habitat layer. A numerical model with a structure similar to the analytical model was employed in areas where cap amendments are under evaluation (requiring non-linear sorption) and for cases where a transient analysis was required.

The chemical isolation layer will consist primarily of sand. Based on treatability testing, elevated sediment pH is an indicator of where amendments to the sand consisting of activated carbon and siderite will be appropriate in order to achieve cap performance criteria. Amendments to the cap will be implemented in Remediation Areas B and D and in the northern portion of Remediation Area C in the vicinity of the SMU 2/SMU 3 boundary, where the pH is typically in the range of 10 to 11. The pH in portions of Remediation Area A and in the southern portion of Remediation Area C is elevated to a lesser degree, with some pH values in the 8 to 10 range. For the purpose of conceptual design, it is assumed that cap amendments will not be required in these areas. Results from ongoing bench-scale testing will be used to confirm this assumption.

Modeling was completed for both carbon-amended and non-amended caps. Appendix I provides a complete discussion of the geochemical modeling employed to assess the effectiveness of the pH buffering amendment.

Supporting documentation for the modeling evaluation is provided in the following attachments:

- Attachment 1– Model Inputs
  - 1.1 Model Input Table
  - 1.2 Correction Factors
  - 1.3 Description of Cumulative Distribution Function
  - 1.4 Groundwater Upwelling Distribution
- Attachment 2 – Partitioning Coefficients and Sediment to Porewater Calculations
- Attachment 3 – Biological Degradation Rate Evaluation
  - 3.1 VOC Biological Decay Rate Evaluation
  - 3.2 Phenol Biological Decay
- Attachment 4 – Model Files (provided electronically on attached CD)

2.0 MODELING EVALUATION

2.1 Objectives

Chemical isolation modeling was conducted to design an isolation layer that will meet the ROD requirements and ensure long-term effectiveness. Specifically, the objective of cap chemical isolation layer design is to meet the individual probable effects concentrations (PECs) for the 23 contaminants that were linked to toxicity on a lakewide basis and the New York State Department of Environmental Conservation (NYSDEC) sediment screening criteria (SSC) for benzene, toluene, and phenol[1] throughout the habitat layer.

As stated in the ROD, the compliance point for the cap is the bottom of the habitat layer. To ensure protectiveness, the isolation layer will be designed to prevent unacceptable concentrations of contaminants throughout the habitat restoration layer.

2.2 Modeling Areas

Remediation Areas A, D and E were evaluated as part of the conceptual design modeling effort. These areas are shown on Figures B.1 through B.6. Remediation Areas A and E constitute the majority of the capped areas where a traditional sand cap will be constructed. Remediation Area D constitutes the majority of the area where an amended cap will be constructed.

FILE

[1] Benzene and Toluene are not associated with lake-wide toxicity. Model results for Benzene and Toluene are compared to 50 times the NYSDEC chronic sediment screening criteria as well as NYSDEC acute criteria. Comparison to acute criteria is consistent with comparison to PEC values which are based on acute toxicity. Use of 50 times the chronic criteria is the recommended approach for compounds that do not have established acute criteria (NYSDEC, 1999).

Remediation Areas A and E were each divided into two model areas for volatile organic compound (VOC) modeling purposes due to the relatively higher porewater concentrations of VOCs observed in Remediation Area A at the mouth of Ninemile Creek and in Remediation Area E immediately adjacent to Remediation Area D. These modeled areas have been designated as Modeling Areas A1, A2, E1 and E2, as shown on Figures 1 through 5.

Remediation Area D was divided into four sub-areas based on chemical concentrations and distributions. Appendix G of this IDS presents the basis for development of these sub-areas, designated as the SMU 2, West, Center, and East sub-areas of Remediation Area D, as shown on Figure 5. Due to the measured differences in contaminant distributions and predicted groundwater upwelling velocities, each of the Remediation Area D sub-areas was modeled independently.

Remediation Areas B and C are relatively small and were not modeled as part of the conceptual design. Modeling of these areas will be completed as part of the intermediate design.

2.3 Modeling Approach

The modeling approach described herein was developed to allow for the evaluation of cap performance in the different remediation areas of the lake and to consider the individual fate and transport behavior of the 26 contaminants for which cap performance criteria were established. Design considerations and contaminant characteristics in each remediation area dictated the modeling approach and model framework employed. Two different models were used; an analytical steady state model and a numeric model, as discussed below. A summary of the types of modeling evaluations conducted by remediation area and contaminant is provided in Table 1. The habitat layer was modeled as a 1 ft. thick layer for all model runs, consistent with ROD requirements.

In the steady state model, an analytical solution is computed, representing the vertical concentration profile that would be anticipated to persist indefinitely in the cap and habitat layer. The steady state analytical model, as detailed below, was used to model VOC transport in Remediation Areas A and E, and to model VOC transport in Remediation Area D over long time-scales (i.e., following the initial period which will be controlled by transport through the carbon mat, pH equilibration, and anticipated onset of biodegradation). It is appropriate for these applications because transient conditions have a relatively minimal effect on cap performance (i.e., steady-state conditions are reached fairly quickly due to the chemicals' relatively high mobility). The analytical model was also used in a screening level evaluation for poly-aromatic hydrocarbons (PAHs) and poly-chlorinated biphenols (PCBs) in Remediation Areas A, D, and E, as discussed in Section 2.4.

Modeling of an amended cap, such as that envisioned in Remediation Area D, requires a model that computes contaminant concentrations over time and allows for evaluation of non-linear processes associated with sorption to amendment material. Therefore, the numerical model was used for Remediation Area D. The numerical model includes all of the underlying mechanisms represented in the steady state model, as well as non-linear sorption to a carbon amendment and the simulation of the contaminated underlying sediment layer.

Following a screening level evaluation for PAHs and PCBs using the analytical model, the numerical model was also employed for those compounds where exceedances were predicted at steady state and therefore required a more thorough evaluation of transient processes. The numerical model was also used to evaluate mercury transport given the long timeframes required for mercury to reach steady state conditions due to its relatively high partitioning coefficient.

2.3.1 Analytical Steady State Model

The analytical model was developed to simulate cap performance and evaluate an appropriate design for containment of contaminated sediments. Simulated transport processes within the typically homogeneous chemical isolation layer include porewater advection, diffusion, reaction, and equilibrium partitioning between the dissolved and sorbed phases of the contaminant. Within the overlying habitat layer, the steady state model includes these same processes, as well as sediment mixing and porewater pumping via bioturbation. The steady state model thus allows the complexities of the biologically active layer to be considered while maintaining an analytical form for convenient and rapid evaluation. The schematic below indicates the general structure and processes included in the steady state analytical cap model.

ILLUSTRATION OF CAP PROCESSES MODELED AND STRUCTURE OF STEADY STATE MODEL

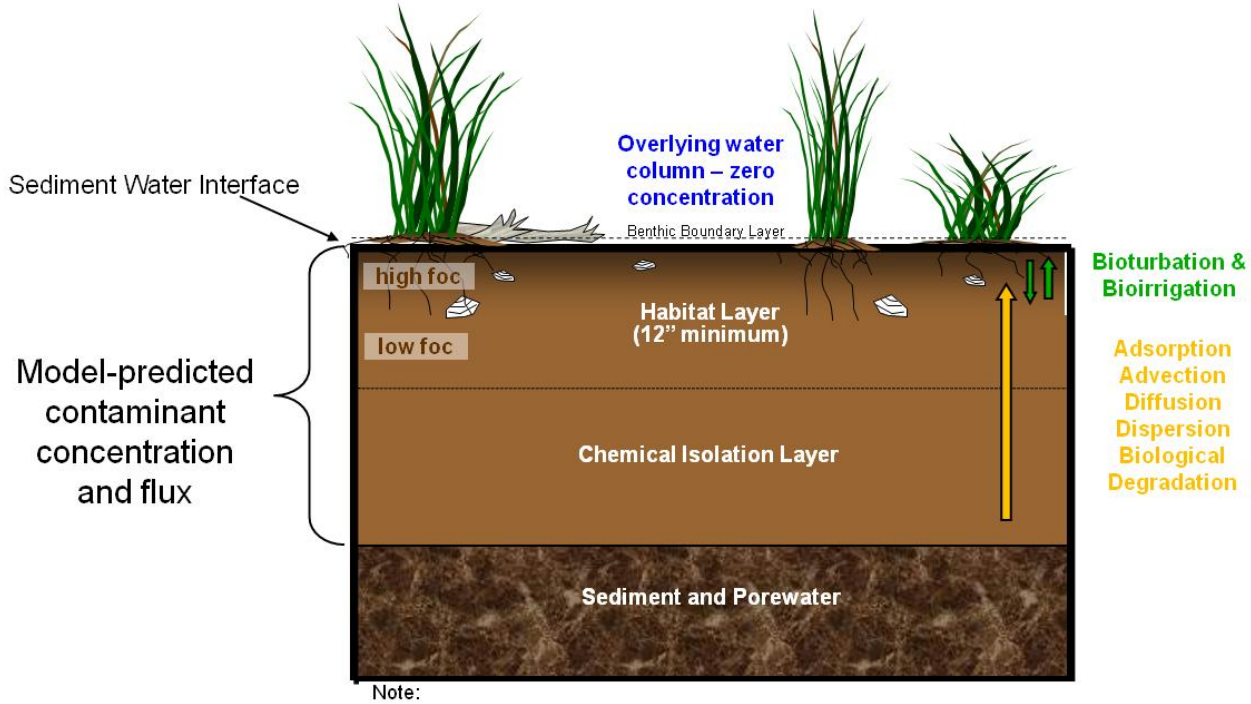

Note:
1) Buffer Layer, Mixing Layer and Overplacement not included in modeling.
2) Compliance evaluated throughout habitat layer
3) foc - fraction organic carbon
4) Constant source modeled in underlying sediment/porewater.

The analytical model was developed by experts, and has been published in the peer-reviewed *Journal of Soil and Sediment Contamination* (Lampert, D. J. and Reible, D. 2009). Validation of the analytical model code was completed in accordance with Parsons standard procedures for software verification and validation. Model results for various test cases were compared with calculations from well-documented 1-D solute transport equations by an independent reviewer; the model gave the same results using similar parameters and boundary conditions.

2.3.2 Numerical Model

The numerical model simulates the same processes as the analytical steady-state model, but uses numerical methods to solve the governing equations. This allows for time-variable simulations and incorporation of complexities such a non-linear sorption to amendment materials. The USEPA guidance document entitled "Guidance for *In Situ* Subaqueous Capping of Contaminated Sediments: Appendix B: Model for Chemical Containment by a Cap" describes the modeling processes and basis the numerical model (USEPA, 1998). This model allows for robust design analysis of multi-layered sediment caps, including simulation of underlying sediment conditions and incorporation of activated carbon amendments. The University of Texas has developed the numerical modeling code in MATLAB based on the calculation of one-dimensional vertical transport of a contaminant through a sediment cap considering the processes of advection, diffusion, dispersion, reaction, bioturbation, settlement induced advection, deposition and retardation with local equilibrium between sediment, porewater, and dissolved organic matter. The schematic below illustrates the general structure and processes included in the Onondaga Lake numerical cap carbon model.

ILLUSTRATION OF CAP PROCESSES MODELED AND STRUCTURE OF MODEL

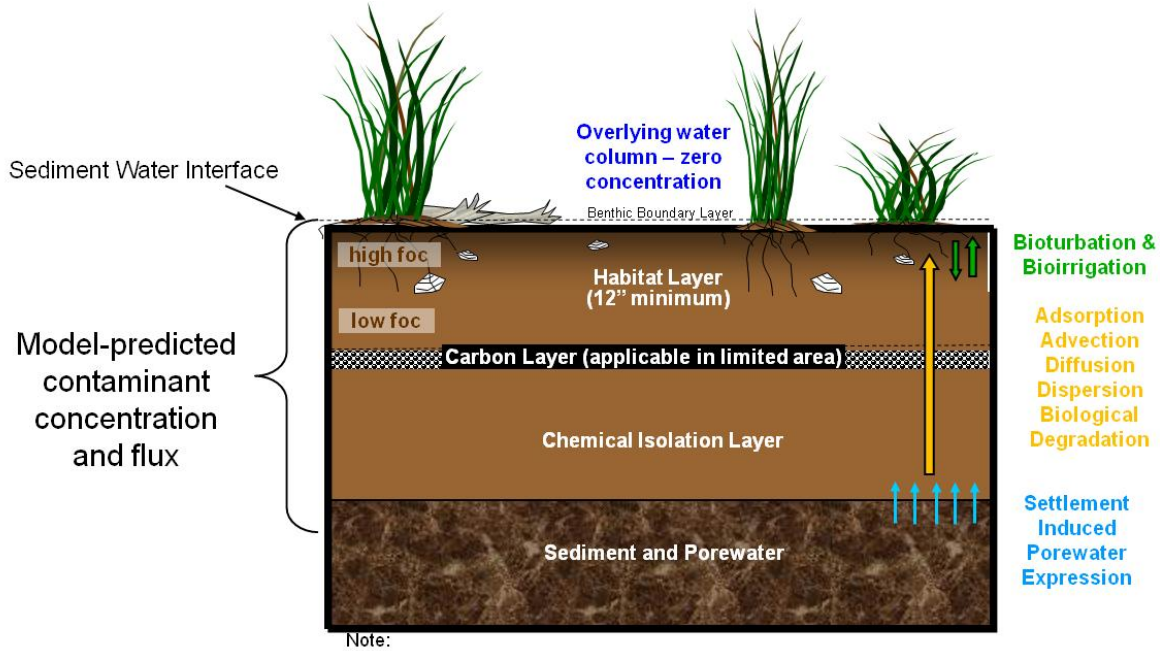

Note:

1) Buffer Layer, Mixing Layer and Overplacement not included in modeling.
2) Compliance evaluated throughout habitat layer
3) Carbon amendment modeled as carbon mat, but bulk carbon placement is also under consideration.
4) Diffusional gradient in top 2.5 meters of sediment included in numerical model, below which a constant source was modeled.
5) foc - fraction organic carbon
6) pH Amendment layer not shown, evaluated with a separate model.

Upwelling velocities in the cap areas are low, so transport from underlying sediments upwards into the cap is dominated by diffusion. This causes a concentration gradient to develop at the sediment-cap interface, which can result in a decrease in chemical concentration in the sediments just below the sediment-cap interface over time. This, in turn, can affect the overall rate of upward transport. In order to represent this process, the sediment underlying the cap is explicitly included as a layer in the numerical model. The sediment layer is modeled as 250 cm thick, with an infinite source boundary condition at the bottom. The processes modeled in the underlying sediment include advective and diffusive transport. Biological decay or other source depletion processes in the underlying sediment are conservatively not included in this modeling evaluation; however, the numerical model construct is capable of incorporating these processes as applicable in future design evaluations.

Validation of the numerical model was completed in accordance with Parsons standard procedures for software validation and verification. An independent validation of this model was performed by S.S. Papadopulos and Associates. Multiple test scenarios were simulated with the numerical model and compared to results from MT3D (Zheng and Wang, 1998), a widely used groundwater transport model that has been extensively verified, as well as an analytical solution to the governing equation of the model (Neville, 2005). Additional validation was provided by

Parsons/Anchor QEA, who found that the results of long-term simulations of the numerical model compared favorably with the results of the steady state model.

2.4 Evaluation Framework

The overall modeling strategy for the IDS includes the use of both the analytical steady state model and the numerical model, depending on the remediation area and the particular contaminant being modeled. As discussed in further detail below, variability in model input parameters was addressed using a series of Monte Carlo evaluations. Deterministic simulations were employed for comparison purposes. Screening level assessments were conducted using overly-conservative conditions to streamline the modeling effort and eliminate low mobility compounds from further analysis, if appropriate.

In general, biologically degradable and relatively less sorptive contaminants were modeled in the absence of a carbon amendment using the analytical steady state model. These compounds included benzene, toluene, ethylbenzene, xylenes, chlorobenzene, dichlorobenzenes, phenol and naphthalene.[2] These compounds are the more mobile contaminants and therefore tend to drive the cap isolation layer design.

Other contaminants evaluated include mercury, total PCBs and 15 PAHs. The modeling strategy for these contaminants included a screening level evaluation to reduce the total number of modeling runs required. Screening level evaluations included analysis of each of the 15 PAHs and total PCBs using steady-state deterministic model runs, and conservative assumptions, including maximum porewater concentration, no biological degradation, and no carbon layer (in Remediation Area D evaluations). Mercury screening modeling was also conducted using conservative input parameters. The numerical model was used for the mercury screening runs given the exceedingly long times to reach steady state for mercury. If a PEC exceedence was predicted under the conservative conditions used in the screening analyses for a given contaminant, a more detailed transient evaluation was conducted.

In Remediation Area D the numerical model was employed to evaluate the design life of a carbon mat. Design lives were evaluated for VOCs, and for PAHs that did not pass the screening level evaluation. The numerical model was also used to simulate a carbon mat for mercury modeling in Remediation Area D. A summary of the types of modeling evaluations conducted by remediation area and contaminant is provided in Table 1.

2.5 Input Parameter Development

Model inputs were derived from extensive site sampling efforts, bench scale testing, and literature. Attachment 1.1 includes a table summarizing the input parameters used in the modeling evaluation, the basis for the input including applicable references and data sources, and the basis for statistical distributions used in the Monte Carlo evaluation.

FILE

[2] Based on a review of concentration data and literature-based biological degradation rates, trichlorobenzene was assumed to behave similarly to dichlorobenzene and was therefore not modeled separately. Concentrations of TCB in lake porewater were generally much lower than concentrations of DCB, and a review of literature rates for TCB suggests that TCB will degrade at a rate equivalent to or faster than DCB (Pavlostathis, 2000).

Based on the initial modeling conducted during the FS, as well as analyses conducted since that time, model predictions have been found to be most sensitive to the following input parameters: underlying porewater concentration, groundwater upwelling velocity, biological decay rate, and sorption parameters (including partitioning to sand cap materials and to carbon amendments). Therefore, an extensive data collection effort and series of bench-scale evaluations have been ongoing since 2006 to increase understanding and provide site-specific information for these key parameters, which are discussed in detail in the following subsections.

Data relevant to cap modeling was collected as part of the 2009 Phase V PDI; however, not all of these data were available in time to incorporate into this modeling effort. A summary of the inclusion status of the Phase V PDI data is provided below:

- Remediation boundaries and corresponding cap area boundaries were established inclusive of validated Phase V sediment data.
- Sediment data used to predict porewater concentrations based on partitioning theory included unvalidated Round 1 Phase V sediment data in Remediation Area A.
- Porewater and groundwater upwelling velocity data collected as part of the Phase V PDI were not included in the cap modeling data sets.

Future model revisions will incorporate Phase V data.

2.5.1 Porewater Concentrations

Multiple sampling methods have been used to measure porewater concentrations within the remediation areas of the Lake. These methods are described further in the Onondaga Lake Phase I Pre-Design Investigation Porewater Methods Evaluation Report (Parsons, 2006). Sampling methods included in situ diffusion samplers (peepers), groundwater upwelling pumps and porewater generated via centrifugation of sediment. Peepers and centrifuged samples, in general, produced consistent results and provided readily implementable approaches for collecting a large number of porewater samples.

In consultation with the NYSDEC, correction factors were developed and applied to the porewater data to account for any potential losses during sample collection, handling or analysis. Correction factors varied by compound and sampling methodology. Correction factors for peeper data are based on the results of the Phase II Pre-Design Investigation: Data Summary Report, Appendix J - Diffusion Sampler Equilibrium Study. For porewater samples generated via centrifugation, correction factors were based on average MS/MSD recoveries. Groundwater data collected from upwelling pumps in 2002/2003 was discarded, with the exception of mercury results, due to the potential for losses along the pump tubing. Groundwater data collected from the upwelling pumps, following modification of the tubing during the Phase I Pre-design investigation (PDI), were incorporated into the model data set without correction factors[3]

FILE

[3] VOC data from groundwater upwelling pumps in the ILWD were inadvertently not included in the model input files. This data will be added to the data set during the intermediate design. Addition of this data does not significantly impact the modeling results.

Attachment 1 provides additional detail on the porewater dataset used as model input as well as a summary of the correction factors employed.

For certain contaminants, the ability to collect porewater sample was limited by the volume required for analysis. Therefore, in the case of PAHs, phenol and PCBs, sediment data from the lake PDI as well as the Remedial Investigation (RI) were used (in conjunction with measurements of TOC, bulk density, and porosity) to calculate porewater concentrations based on equilibrium partitioning equations for use in the modeling effort. Attachment 2 describes the calculation of porewater concentrations for these compounds.

2.5.2 Groundwater Upwelling Velocities

Appendix C to this IDS details the field effort and results of the extensive groundwater upwelling investigation conducted on the Lake. This work was completed to characterize the groundwater upwelling velocities that the sediment cap will be subjected to following construction.

In Remediation Areas A and E, direct measurements of groundwater upwelling velocity were taken, as detailed in Appendix C (Appendix C includes Phase V PDI data which were not available in time for inclusion in the modeling described herein). Direct measurements of groundwater upwelling velocities collected in the capping areas of Remediation Area A and E were used to generate the groundwater upwelling data set used in the cap modeling. The specific upwelling velocities used in the model runs are provided in the model input files included in Attachment 4.

Unlike Remediation Areas A and E, there are no direct measurements of groundwater upwelling rates within Remediation Area D. Rather, the upwelling rates used in the cap modeling for this area were based on predictions of conditions that would exist once the upland hydraulic containment system is in place. These estimates were developed from multiple lines of evidence by integrating existing geological information, boring data, and groundwater modeling. These estimates indicate that upwelling rates within Remediation Area D would be less than 2 cm/yr, with values being smaller in areas where the silt and clay layer that underlies Remediation Area D is thicker. Additional discussion is provided in Attachment 1 to this Appendix as well as in Appendix C.

Settlement calculations indicate that there will be some expression of porewater associated with sediment consolidation due to cap placement. This porewater expression would be equivalent to an additional advective flux into the cap. That flux will occur over a relatively short timeframe, after which the long-term conditions represented by the steady-state model would prevail. For steady state model behavior, such an initial expression of porewater does not change the ultimate steady state concentration profile calculated by the model. Therefore, consolidation effects were not included in the steady state analytical modeling included in this IDS. Similarly, this porewater expression would have minimal effect on the numerical modeling results for PAHs and mercury because it represents a very small portion of the flow that would occur over the very long design lives predicted for these contaminants, and therefore is not included in the modeling for these contaminants.

Porewater expression may have a more significant impact on the design life predicted by transient numerical modeling used to simulate carbon amendments in the Remediation Area D cap. Therefore, porewater expression is included in the modeling of carbon life for the Remediation Area D cap. Appendix E of the IDS presents predictions of settlement induced porewater expression as a function of time (Section 4.2 and Figure 17 of Appendix E-2), which has been incorporated into the model code for the numeric model.

2.5.3 Biological Decay Rates

Biological decay is an important fate process for the overall design of the sediment cap. Several stages of bench-scale experiments were conducted during the PDI to evaluate site-specific biological decay rates, as detailed in the IDS. The results and recommendations from these studies are presented in Attachment 3. Additional column and batch testing experiments are on-going. As the design progresses, the results of these ongoing studies will be used to refine the predictions of biological decay rates.

Bench-testing did not produce site-specific decay rates for phenol and TCB due to the very low concentrations of TCB in lake porewater and the large sample volume requirements for phenol. Therefore, literature surveys were conducted. Results and an analysis of literature decay rates for phenol are provided in Attachment 3. As noted above in Section 2.4, TCB was not modeled because results are expected to be consistent with DCB results based on lower porewater concentration and literature which suggests faster or equivalent biological decay rate estimates (Pavlostathis, 2000).

An extensive literature review was also conducted to assess PAH degradation. The findings of this review suggested that PAH degradation is likely to occur under the conditions present in the lake. However, for modeling purposes, PAH degradation was conservatively assumed to be zero.

2.5.4 Sorption Parameters

Sediment porewater concentrations used for modeling were based on porewater data as well as sediment data and partitioning theory, as described in Section 2.5.1. Partitioning theory was also used to predict partitioning between porewater and the sediment cap and to predict the concentration gradient that develops within the underlying sediments and porewater over time (for use in numerical model simulations). The basis for the sorption parameters is detailed below.

2.5.4.1 VOCs

For porewater sampling conducted using the centrifugation method described above in Section 2.5.1, chemical concentrations were also measured in the sediments from which the porewater was extracted. This provided data that were used to estimate site-specific partition coefficients. These coefficients were estimated using a regression approach. Carbon-normalized sediment concentration was plotted against the paired porewater concentration for all PDI Phase I through IV data, and the slope of a least squares regression line (log-transformed) was

used to define the partition coefficient (i.e., log Koc). Additional detail on VOC partitioning coefficient development is provided in Attachment 2.

Resulting coefficients were found to differ between ILWD and non-ILWD areas, likely due to the effects of high pH and/or dissolved organic carbon within the ILWD. These effects are assumed to be mitigated by the proposed cap amendments and the establishment of biological decay processes in the Remediation Area D cap. Therefore, the partitioning coefficients estimated based on data from Remediation Areas A and E were used to model partitioning to isolation sand in all areas of the lake.

Partitioning coefficients estimated from the ILWD data were used to model partitioning between porewater and sediment/waste material for the underlying sediment layer simulated in Remediation Area D carbon amendment modeling.

2.5.4.2 Mercury

Simulations of mercury partitioning to sand capping material was based on measurements collected during site-specific isotherm studies conducted as part of the Phase IV PDI (Parsons, 2009). Isotherm studies were designed to predict the adsorption capacity of cap material for a variety of compounds over range of concentrations. Isotherm studies were conducted using lake porewater from Remediation Areas D and E, and sand from a local source. Simulation of mercury partitioning to carbon mats (for Remedial Area D) was also based on isotherm study data conducted with site porewater and activated carbon (Parsons, 2009).

Site-specific data generated through porewater and sediment sampling, were used to estimate partition coefficients for mercury in the sediment underlying the cap. These partitioning coefficients were used in the transient numerical modeling. Additional detail on mercury partitioning coefficient development is provided in Attachment 2.

2.5.4.3 PAHs and PCBs

Given the large volumes of porewater required for PAH and PCB analysis an extensive porewater data set was not generated for these compounds. Rather, sediment data from the RI and five phases of PDI, was used to calculate underlying porewater concentrations in each remediation area using site-specific organic carbon measurements and literature based partitioning coefficients. Literature based coefficients from the NYSDEC sediment screening guidance (NYSDEC, 1999) were corrected based on field measurements as discussed in Attachment 2.

Literature based coefficients (not corrected) were used to define partitioning to the cap material.

Additional detail on applied literature partitioning coefficients and porewater calculations for PAHs and PCBs are as presented in Attachment 2.

2.5.5 Carbon Adsorption Parameters

Site-specific isotherms were generated for VOCs and naphthalene during the Phase IV PDI (Parsons, 2009). Data from these studies were used in the modeling evaluation of carbon amendments Model inputs include site-specific Freundlich isotherm parameters (Kf and 1/n) for each compound. Site-specific isotherm data and the corresponding input parameters for phenol and PAHs were not included in the scope of site-specific evaluations. In order to model these compounds, the site-specific results for benzene were used for phenol and the site-specific results for naphthalene were used for PAHs and PCBs.

Phenol is composed of a benzene ring with a hydroxyl group in place of one of the hydrogen atoms. Initial examination of its molecular structure would suggest that the polarity of the hydroxyl group would negatively influence the adsorption of phenol compared to benzene. However, a review of the available literature reveals that the mechanism of phenol adsorption is widely hypothesized to be the chemisorption of the double bonded π-orbital electrons of the aromatic ring with active sites on the adsorbent surface (Mattson, et. al, 1969; Jung, ***et. al***, 2001; Terzyk and Kowalczyk, 2005). These forces overcome the polarity caused by the hydroxyl group and serve to enhance its adsorption characteristics.

Due to the fact that the primary mechanism of phenol adsorption involves the aromatic ring, as opposed to the hydroxyl group, benzene was chosen as a surrogate compound to represent the adsorption of phenol. This choice is supported based on a review of available studies in which comparative isotherms were performed on both phenol and benzene, including the studies completed using water generated through contact with the ILWD for evaluating treatment of water generated during dewatering of ILWD material following dredging (EPA, 1980; Patterson, 1985; O'Brien & Gere, 2009; Calgon, 2009; Norit, 2009). A literature review of both phenol (Snoeyink and Weber, 1968; Sorial, ***et. al,*** 1993) and benzene (Weber and Pirbazari, 1982; Stenzel and Merz, 1988) adsorption isotherms yielded similar conclusions. For example, in the EPA study, the equilibrium sorbed concentration for benzene and phenol at a water concentration of 2 mg/L were determined to be 3 mg/g and 30 mg/g, respectively.

All of these studies indicate that phenol is at least as favorably adsorbed to carbon as benzene. Therefore, applying the site-specific Freundlich parameters for benzene to phenol will yield a conservative modeling estimate for the carbon cap amendment.

PAHs are composed of multiple benzene rings bonded in a planar configuration. With only two bonded benzene rings, naphthalene is the simplest and smallest of the PAH compounds. All other PAHs consist of greater numbers of bonded benzene rings and are therefore of higher molecular weight, larger molecular size, and greater hydrophobicity. These characteristics all lend themselves to higher relative carbon sorbability than naphthalene. For example, in one study the equilibrium sorbed concentration values for naphthalene and phenanthrene at a water concentration of 0.1 mg/L were determined to be 50 mg/g and 80 mg/g, respectively (EPA, 1980).

Since the addition of each benzene ring will increase the relative sorptivity of a PAH relative to naphthalene, applying the site-specific derived Freundlich parameters for naphthalene to the other PAHs will yield a conservative modeling estimate for the carbon cap amendment..

2.6 Accounting for Variability in Model Input Parameters

Model input parameters were established using a combination of site-specific data and published studies. A single value was used for parameters to which model results were relatively insensitive. For key parameters to which the model was relatively sensitive, parameter variability was addressed based on an analysis of the underlying data and through completion of Monte Carlo modeling simulations.

Monte Carlo analysis is commonly used to account for input variability and in models with multiple parameters (e.g., EPA 1997). The first step in performing a Monte Carlo analysis is to estimate a statistical distribution for each key parameter, based on the data (for example, a normal distribution). Next, a model simulation is performed, selecting randomly from the distribution for each parameter. This represents one "realization," and produces one possible outcome, in this case, one estimate of sediment and porewater concentration within the cap. The model calculation is then repeated many times (5,000 realizations were used in the current modeling evaluation), each time selecting a new value for each input parameter from its distribution. This produces a frequency distribution of computed concentrations.

Management decisions can then be made using a chosen percentile of this distribution (e.g., 80th, 90th or 95th percentile). The appropriate percentile for cap design to provide a high level of confidence that the cap will be effective everywhere can be chosen based upon an understanding of the overall conservatism of the model and input parameters (a lower percentile may be appropriate in a model that is designed and implemented conservatively).

Distributions for the Monte Carlo Analysis were developed for each key input parameter based on an analysis of the site data, in light of the underlying physical, chemical, and biological processes. Variability in the data used to estimate parameter values originated from two sources: 1) measurement variability associated with sampling, processing and laboratory analysis, and data interpretation; and 2) spatial variability due to natural and anthropogenic processes such as contaminant loadings to the lake and heterogeneity in permeability, deposition and erosion. Modeling was completed accounting for this variability based on an analysis of the data and considering the underlying physical, chemical, and biological processes as discussed further in Section 2.6.1 and 2.6.2.

For comparison to the Monte Carlo simulation results, deterministic model runs (i.e. single model runs without Monte Carlo analysis) were also completed using the 80^{th}, 90^{th} and 95^{th} percentiles for porewater concentration while all other parameters were assumed to be the mean of their respective values. Results from both the Monte Carlo simulations and deterministic runs are provided in Section 3.0 through 6.0.

2.6.1 Spatial Variability

The distributions of measured porewater concentrations in all Remediation Areas and groundwater upwelling velocity in Remediation Areas were likely dominated primarily by spatial variability. Spatial variability was addressed in two steps. First, the remediation areas were separated into smaller model areas to account for major differences in upwelling velocity and/or contaminant distribution (i.e., A1 and A2, E1 and E2, and the four sub-areas of Remediation Area D). Second, independent Monte Carlo analyses were performed for each area, using the distribution of data from that area.

The model parameters that were identified to vary spatially across a modeling area included:

- Porewater contaminant concentration in each modeling area;
- Groundwater upwelling velocity in each Remediation Area D sub-area; and
- Groundwater upwelling velocity in Remediation Area A.

Contaminant distributions in Remediation Area A, D and E were used to define two model areas within each Remediation Area A and E, and four model sub-areas in Remediation Area D. In general, higher concentrations at the mouth of Nine Mile Creek were used to define Model Area A-2 and higher concentrations adjacent to the ILWD were used to define model Area E-2. The ILWD sub-area delineation is described in Appendix G.

Spatial variability in upwelling velocities within Remediation Area D is predicted to occur due to differences in the thickness of the underlying silt and clay unit. To represent these anticipated conditions, the contour map of upwelling rates presented in Appendix C was used to develop a statistical distribution for each Remediation Area D sub-area. These distributions were developed by calculating the percentage of acreage covered by the various upwelling ranges within each Remediation Area D sub-area. Additional details on the development of these distributions are provided in Attachment 1.

In Remediation Area A, while spatial variability is likely given the underlying geologic conditions, the measured upwelling velocities did not exhibit discernable spatial patterns conducive to defining a specific smaller modeling area. Therefore, the full distribution of measured upwelling velocities in Remediation Area A was used to represent the variability of upwelling velocities for both Model Areas A-1 and A-2.

Upwelling velocities and porewater concentration distributions were developed using a cumulative distribution function (CDF). The CDF method uses the data to represent the distribution over the full range of measurements and does not assume a specific distribution type. More detailed discussion of development of the CDFs is provided in Attachment 1.3.

2.6.2 Measurement Variability

For several parameters, it was judged that variability arose primarily from measurement or data interpretation variability, as opposed to true spatial variability. These included the following:

- groundwater upwelling velocity in Remediation Area E;
- the organic carbon partition coefficient for each chemical (log Koc);
- the biological decay rate of each chemical (lambda);
- the benthic mixing coefficients for particulate matter (bioturbation) and porewater (bioirrigation) within the habitat layer;
- the fraction of organic carbon anticipated to be established within the cap's bioturbation layer at some time in the future (focbio); and
- carbon isotherm sorption parameters (i.e., the parameters Kf and 1/n in the Freundlich isotherm equation).

The distributions used in the analysis represent the uncertainty in the best estimate, which is described by the mean. The uncertainty in the mean is characterized by the standard error, as opposed to the standard deviation which characterizes the variability of individual values. Therefore, the distributions used in the Monte Carlo analysis for these parameters were normal or lognormal distributions developed using the mean and the standard error (= standard deviation / sqrt(number of observations)) of the data (or the log transformed data in the case of a lognormal distribution).[4]

2.7 Model Conservatism

There are a number of conservative assumptions incorporated into this cap modeling and design effort. Several of the more significant conservative assumptions are discussed below.

ROD point of compliance (bottom of habitat layer) is set below organism exposure zone

The cap performance criteria were developed based on consideration of contaminant toxicity to benthic organisms. These organisms move throughout the benthic activity zone of sediment, which for Onondaga Lake has been characterized as approximately the top 6 inches of sediment. As such, they are exposed to average conditions within this zone. Additionally, literature suggests exposure may be more heavily weighted toward the surface of this zone (Strommer and Smock, 1989).

The cap design and recommended chemical isolation layer thickness is based on the ROD-specified point of compliance at the bottom of the habitat layer, as well as throughout the habitat layer where the critical modeling point tends to be the bottom of the benthic activity zone. The habitat layer thickness ranges from one to two feet thick, depending on the habitat module, while the active zone for benthic organisms is the uppermost 6 inches of the habitat layer. Due to the effects of bioturbation, aerobic biodegradation, and bioirrigation, average concentrations in the benthic activity zone will be less than the maximum concentrations predicted at the ROD point of compliance and less than those predicted at the bottom of the benthic activity zone.

FILE

[4] For parameters with small sample sizes (the decay rate [n=2 to 9] and the porewater mixing coefficient n= 6]), a Student's t distribution was used, with the degrees of freedom determined by the data.

Recommended cap thicknesses are developed based on predicted maximum concentrations at the point of compliance and throughout the habitat zone, which is inherently conservative based on consideration of where the benthic activity zone is located.

Cap material over-placement results in greater thicknesses for each cap layer

The actual thickness of each cap layer constructed in the field will typically exceed the minimum required design thickness due to operational considerations of how the cap materials will be placed in the lake. The contract requirements will specify that the contractor will need to place a minimum thickness for each layer. To ensure that the minimum required cap thickness is obtained, the capping construction contract will allow for over-placement beyond the minimum target cap layer thickness. This over-placement allowance addresses the tolerances contractors can achieve given the water depths, bathymetry, currents, waves, capping equipment and other factors. For each specific layer (*e.g.* chemical isolation, erosion protection, and habitat) the contract documents will specify the minimum thickness and the allowable amount of over-placement. The result of this approach will be that the final thickness of each layer will be more than the specified minimum thickness in each area. The overplacement thickness is assumed to be at least 3 inches on average, and will be significantly more than this in some areas. This added thickness will provide additional chemical isolation, but is not considered in the model.

Mixing layer allowance adds thickness but is not considered

The bottom 3 inches of the chemical isolation layer material is assumed to mix with the underlying sediment, and is not considered when meeting the minimum required isolation layer thickness. This material will mix with the underlying sediment and reduce contaminant concentrations immediately underlying the cap. However, this impact is not considered for modeling purposes.

ROD-specified minimum thickness is significantly greater than required thickness based on modeling

The ROD requires a minimum chemical isolation layer thickness. However, current modeling indicates that a minimum thickness of 6 inches or even less would be sufficient to provide chemical isolation. The added thickness required to meet the minimum thickness required by the ROD provides significant conservativism in the overall cap design.

An infinite source mass is assumed in modeling

The steady-state model assumes a constant source at the cap/sediment interface. However, mass conservation principles dictate that as advection and diffusion move contaminant mass out of the underlying sediment and into the cap, the mass in the underlying sediment will decrease, resulting in lower sediment and porewater concentrations immediately beneath the cap. Mass transport out of the sediment as well as any source depletion due to natural decay processes are not considered in the steady state model.

The numerical model assumes an infinite concentration 2.5 meters below the sediment cap interface. Diffusion processes are considered in the top 2.5 meters below the sediment cap interface. Natural decay processes, or mass transport out of the underlying sediment below 2.5 meters due to advection, are not incorporated into the numerical model.

Initial concentration data conservatively selected

In instances where multiple results existed for a given sampling location, maximum sample concentrations were selected from the analytical database. For example, if multiple samples were collected over a modeled interval or if duplicate samples were collected at a particular location, the maximum value measured was used in the modeled dataset.

Depth intervals for developing the porewater input data sets were selected considering the proposed dredge plan and generally include the data from two meters above to two meters below the maximum dredge cut in an area, exclusive of hot spot dredging in Remediation Area D. This is conservative because it includes data from sediments which will be dredged, including those sediments identified as hot spots, which generally contain higher porewater contaminant concentrations than the remaining sediments.

One dimensional model does not consider multi-directional diffusive transport

In general, the dominant form of contaminant transport modeled under the in-lake groundwater upwelling conditions is molecular diffusion. Diffusion is a molecular based phenomenon describing the net movement of molecules across a concentration gradient, toward regions of lower concentration. In the cap model diffusion is assumed to be out of the sediment up into the clean cap material. This assumption is based on a constant well-mixed concentration in the underlying sediment. However, given the non-homogeneous nature of the underlying lake sediment and porewater, there are areas and depths within the underlying sediment of higher and lower concentrations. Therefore, when considering model results based on 80^{th}, 90^{th} and/or 95% initial concentrations it is likely that diffusional transport may not be entirely in one direction up into the cap but may also result in transport laterally or deeper into regions of lower concentrations within the underlying sediment matrix, which would tend to lower the most-elevated concentration levels especially over the long timescales considered in this modeling.

Consolidation Impacts on Underlying Sediment Porosity

The numerical model considers diffusion/dispersion processes in the underlying sediment, though this is conservatively limited to the top 2.5 meters of sediment below the cap. In actuality, these processes are in part dependant on sediment porosity. However, in the model porosity set at a fixed value which does not change during the model run (the value based on sediment samples collected in Remediation Area D). Subsequent to cap placement, consolidation processes will actually reduce the porosity of the underlying sediments. The change in porosity would reduce permeability and the effective diffusion coefficient in the underlying sediments. The reduction in porosity would result in a reduction in contaminant flux.

3.0 STEADY STATE VOC MODELING SUMMARY AND RESULTS

As discussed above, the steady state analytical model was used to simulate VOCs in Remediation Areas A, D and E. Cap amendments are not incorporated in Remediation Areas A and E. While cap amendments are incorporated in Remediation Area D, the steady state model was employed to evaluate the required cap thicknesses for VOCs under conditions where pH has been controlled and biological decay has been established. As shown in Tables 2 and 3, the model predictions indicate that a 0.5 ft. chemical isolation layer would be effective in all modeled areas. A chemical isolation layer of 1 ft. as required by the ROD would provide a safety factor of at least 2.

Table 2 summarizes the Monte Carlo results for VOCs in each modeling area, and illustrates the percentile of realizations that meet the performance criteria. For comparison purposes, deterministic model runs (i.e. single model runs without Monte Carlo analysis) were also completed for each Model Area using the 80th, 90th, and 95th percentiles of the porewater concentration distributions. For these runs, all other parameters were assumed to be the mean of their respective values. Results from these runs are provided in Table 3.

4.0 CARBON AMENDMENT VOC MODELING SUMMARY AND RESULTS

The numerical model was applied to predict the design life based on VOCs for a cap amended with activated carbon in Remediation Area D. Modeling of the carbon design life for SVOCs is discussed in Section 6. Design life of the activated carbon is defined as the time elapsed before an exceedance of the cap performance criteria is reached at any location within the habitat layer. These simulations were conducted assuming no biodegradation. For modeling purposes it was assumed that carbon would be placed in a single mat, which is one method of applying carbon to a cap. The carbon mat acts as a permeable composite layer consisting of activated carbon encapsulated in a non-woven core matrix bound by two geotextiles. A single mat, as modeled herein, is assumed to contain 0.41 lb/ft^2 of activated carbon, which is consistent with the carbon mat manufactured by CETCO Corporation.

Table 4 summarizes the results for each modeling area, and illustrates the design life predictions associated with a single carbon mat under different input scenarios. Design lives are presented as the 80^{th}, 90^{th} and 95^{th} confidence intervals based on the various model input distributions, as described in Attachment 1. For comparison purposes, deterministic model runs (i.e., single model runs without Monte Carlo analysis) were completed using 80^{th}, 90^{th} and 95^{th} percentile concentrations. For these runs, all other parameters were assumed to be the mean of their respective values.

Both the Monte Carlo and deterministic model simulations led to significantly long design life predictions for a single carbon mat. Design lives greater than 1,000 years were calculated for most of the compounds and on the order of hundreds of years for nearly all other compounds and simulations. Naphthalene was the one exception and tended to drive the model results in most subareas. Design lives for Naphthalene varied by subarea but ranged from 84 years to greater than 1,000 years, as shown in Table 4.

5.0 MERCURY MODELING

Mercury modeling was conducted using a conservative "screening" approach in which the underling porewater concentration and groundwater upwelling velocity were both set to their maximum values within a given area. The numerical model was used to evaluate the "breakthrough time", as defined as the time at which the mercury concentration at any point within the habitat layer (it was always highest at the bottom) exceeded the 2.2 mg/kg PEC, if observed. Table 5 provides a summary of the model results.

As shown in Table 5, conservative screening-level modeling indicates that 0.5 ft. is a sufficient chemical isolation layer thickness to provide long-term chemical isolation for mercury in all modeled areas.

6.0 PAH AND PCB MODELING

PAH and PCB modeling was initially conducted using a conservative "screening" approach in which the underlying porewater concentration was set to the maximum values within a given area and no biological decay was considered. In Remediation Area E, the mean upwelling velocity was used since the observed variability there was determined to be the result of measurement effects rather than representative of spatial variability, in Remediation Area A the maximum velocity was modeled. The model was run with a 0.5 ft. chemical isolation layer for all model areas. The analytical steady state model was used to evaluate contaminant concentrations throughout the habitat layer and compare the resulting concentrations to the individual PEC for each compound. Table 6 provides a summary of the model results.

From the results shown in Table 6, the screening level assessment indicates that for Remediation Areas A and E, 0.5 ft. is a sufficient chemical isolation layer thickness to meet the individual PEC for total PCBs and most PAHs. In Remediation Area E, only fluorene and acenapthalene were predicted to not meet the criteria at steady state under the conservative input specifications. Therefore, a more rigorous modeling effort was performed for these two compounds using the transient numerical model with both Monte Carlo and deterministic analyses. As shown in Table 7, the more rigorous modeling effort indicated that a 0.5 ft. thick isolation layer will provide long-term isolation of fluorene and acenapthalene.

In Remediation Area D, the screening evaluation indicated that PCBs and many of the PAHs will meet the criteria at steady state; however, a number of PAHs did not pass the steady state screening evaluation. These compounds were therefore evaluated with the transient numerical model, which for this area also considered the added sorption capacity from the carbon mat. As shown in Table 7, the chemical isolation layer in combination with activated carbon will provide long-term chemical isolation of PAHs in Remediation Area D.

7.0 SUMMARY OF RESULTS

Results from the modeling based on site-specific conditions and incorporating conservative assumptions, are summarized in the table below.

Chemical Isolation Layer Design Summary

Remediation Cap Area	Required Thickness Based on Modeling (feet)	Design Thickness (feet)[a]	Comment
A (77 acres)	Less Than 0.5	1	Applies to Model Areas A1 and A2.
B (16.1 acres)	Not Modeled	1	Will include amendments. Assume 1 ft. for conceptual design.
C (18.9 acres)	Not Modeled	1	Will include amendments in northern portion. Assume 1 ft. for conceptual design.
D (98.5 acres)	Less Than 0.5	1	Will include amendments. Applies to all modeled sub-areas.
E (173.8 acres)	Less Than 0.5	1	Applies to Model Areas E1 and E2.

a Consistent with the ROD, the minimum thickness of the chemical isolation layer will be 1 ft. Where cap modeling indicated less than 1 ft. was necessary to achieve cap performance criteria, the design thickness was increased to 1 ft.

8.0 REFERNCES

Aronson, D., Howard, P.H., 1997. "Anaerobic Biodegradation of Organic Chemicals in Groundwater: A Summary of Field and Laboratory Studies." Syracuse Research Corporation, North Syracuse, New York.

Boudreau, B. 1996. The Diffusive Tortuosity of Fine-Grained Unlithified Sediments: Geochimica et Cosmochimica Acta 60, no. 16: 3139-3142.

Ginevan, Michael E., and Douglas E. Splitstone, 2004. Statistical tools for environmental quality measurement. CRC Press LLC. p. 229.

Lampert, D. J. and Reible, D. (2009) An Analytical Modeling Approach for Evaluation of Capping of Contaminated Sediments, Soil and Sediment Contamination: An International Journal,18:4,470 – 488.

Millington, R.J., 1959. Gas diffusion in porous media. Science, Vol. 130:100-102.

National Program Office, Chicago, Il. Available at http://www.epa.gov/grtlakes/sediment/iscmain/appndb.pdf.

NYSDEC and USEPA. 2005. Record of Decision Onondaga Lake Bottom Subsite of the Onondaga Lake Superfund Site. Town of Geddes and Salina, Villages of Solvay and Liverpool, and City of Syracuse, Onondaga County, New York.

NYSDEC. 1999. Technical Guidance for Screening Contaminated Sediments. New York State Department of Environmental Conservation, Albany, N.Y.

NYSDEC and USEPA. 2005. Record of Decision Onondaga Lake Bottom Subsite of the Onondaga Lake Superfund Site. Town of Geddes and Salina, Villages of Solvay and Liverpool, and City of Syracuse, Onondaga County, New York.

Neville, C., 2005. ADFL Analytical Solution – Version 4, User's Guide. S.S. Papadopulos & Associates, Inc. Bethesda, MD.

Palermo, M.R., S. Maynord, J. Miller, and D. Reible, 1996. Guidance for in-situ subaqueous capping of contaminated sediments. Environmental Protection Agency, EPA 905-B96-004, Great Lakes.

Parsons, 2004. Onondaga Lake Feasibility Study Report, Onondaga County, New York. Prepared for Honeywell, in association with Anchor Environmental and Exponent. May.

Parsons, 2007. Onondaga Lake Phase IV Pre-Design Investigation Work Plan, Addendum 2 Isotherm Studies with Activated Carbon, Organoclay and Peat. Prepared for Honeywell. Draft report under review.

Parsons. 2008. Remedial Design Work Plan for the Onondaga Lake Bottom Subsite Prepared for Honeywell.

Parsons. 2009. Onondaga Lake Pre-Design Investigation: Phase II Data Summary. Prepared for Honeywell.

Parsons. 2009. Onondaga Lake Pre-Design Investigation: Phase III Data Summary. Prepared for Honeywell.

Parsons. 2009. Onondaga Lake Pre-Design Investigation: Draft Phase IV Data Summary. Prepared for Honeywell.

Strommer and Smock, 1989. Freshwater Biology (1989) 22, 263-274

USEPA. 1997. Guiding Principles for Monte Carlo Analysis. Risk Assessment Forum, U.S. Environmental Protection Agency. EPA/630/R-97/001.

USEPA. 1997. Guiding Principles for Monte Carlo Analysis. Risk Assessment Forum, U.S. Environmental Protection Agency. EPA/630/R-97/001.

Zheng, C. and P. Wang, 1998. MT3DMS, A modular three-dimensional multispecies transport model for simulation of advection, dispersion and chemical reactions of contaminants in groundwater systems. Documentation and User's Guide. U.S. Army Corps of Engineers Technical Report, June 1998.

TABLES

Table 1

Cap Design Modeling Evaluation Framework

Remediation Area/Contaminant	Steady State Model Screening	Steady State Analytical Model with full Monte Carlo and Deterministic Evaluation	Numerical Model Screening	Numerical Model with full Monte Carlo and Deterministic Evaluation
Remediation Area A				
PAHs (Acenaphthene, Acenaphthylene, Anthracene, Benz[a]anthracene, Benzo[a]pyrene, Benzo[b]fluoranthene, Benzo[ghi]perylene, Benzo[k]fluoranthene, Chrysene, Dibenz[a,h]anthracene, Fluoranthene, Fluorene, Indeno[1,2,3-cd]pyrene, Phenanthrene, Pyrene)	X			
Total PCBs	X			
Mercury			X	
Remediation Area D				
VOCs		X		X[1]
PAHs	X		X[1]	X[1, 2]
Total PCBs	X		X[1]	
Mercury			X[1]	
Remediation Area E				
VOCs		X		
PAHs	X			X[2]
Total PCBs	X			
Mercury			X	

1. Carbon amendment simulated in model runs.

2. Select PAH compounds modeled with numerical model following initial screening level evaluation.

Table 2

VOC Analytical Modeling Results for Monte Carlo Simulations - Percentage of Modeled Results Meeting the Standard

Contaminant	Standard	Units	Model Area							
			SMU 2	West	Center	East	A1	A2	E1	E2
Benzene	10500	µg/L	100.00	100.00	100.00	99.98	100.00	100.00	100.00	100.00
Benzene	760	µg/L	100.00	99.94	99.78	98.06	100.00	100.00	100.00	92.92
Chlorobenzene	428	µg/kg	100.00	100.00	100.00	99.96	100.00	100.00	100.00	99.98
Diclorobenzene	239	µg/kg	100.00	99.98	99.94	99.94	100.00	100.00	100.00	99.98
Ethylbenzene	176	µg/kg	99.98	100.00	99.90	99.96	100.00	99.98	100.00	100.00
Naphthalene	917	µg/kg	100.00	100.00	99.98	99.98	100.00	100.00	100.00	100.00
Toluene	5000	µg/L	100.00	100.00	100.00	100.00	100.00	100.00	100.00	100.00
Toluene	480	µg/L	99.98	99.42	99.28	99.92	100.00	100.00	100.00	100.00
Xylene	561	µg/kg	100.00	99.92	99.82	99.98	100.00	100.00	100.00	100.00
Phenol	250	µg/L	100.00	99.82	99.98	99.98	100.00	100.00	100.00	100.00

Note: All simulations based on a 6-inch chemical isolation layer and a 12-inch habitat layer thickness. Reported results are the percentage of modeled scenarios, based on 5,000 iterations over the range of potential model input parameters that result in concentrations equal to or less than the performance standard throughout the habitat layer.

Table 3

VOC Analytical Modeling Results for Deterministic Simulations - Maximum Predicted Concentrations in the Habitat Layer

Porewater Concentration Percentile	Contaminant	Standard	Units	Model Area							
				SMU 2	West	Center	East	A1	A2	E1	E2
C_95	Benzene	10500	µg/L	10.84	49.83	101.56	46.16	1.05	1.15	0.69	4.24
	Benzene	760	µg/L	10.84	49.83	101.56	46.16	1.05	1.15	0.69	4.24
	Chlorobenzene	428	µg/kg	0.07	0.47	0.53	3.28	0.00	0.03	0.04	0.78
	Dichlorobenzene	239	µg/kg	0.02	0.47	0.49	1.49	0.01	0.02	0.04	1.43
	Ethylbenzene	176	µg/kg	0.63	0.92	1.82	1.17	0.01	2.40	0.10	0.59
	Naphthalene	917	µg/kg	2.01	3.93	5.79	3.43	0.01	0.01	0.47	4.96
	Toluene	5000	µg/L	5.39	41.26	55.55	17.63	0.07	0.30	0.09	2.81
	Toluene	480	µg/L	5.39	41.26	55.55	17.63	0.07	0.30	0.09	2.81
	Xylene	561	µg/kg	1.66	5.78	11.12	3.83	0.03	2.41	0.12	1.62
	Phenol	250	µg/L	4.31	36.63	18.34	15.17	2.46	2.46	0.24	0.24
C_90	Benzene	10500	µg/L	7.52	36.70	60.94	41.75	0.15	0.87	0.39	3.86
	Benzene	760	µg/L	7.52	36.70	60.94	41.75	0.15	0.87	0.39	3.86
	Chlorobenzene	428	µg/kg	0.05	0.37	0.36	2.22	0.00	0.01	0.03	0.59
	Dichlorobenzene	239	µg/kg	0.01	0.29	0.40	1.21	0.01	0.02	0.02	1.36
	Ethylbenzene	176	µg/kg	0.46	0.71	1.33	0.91	0.01	0.43	0.03	0.49
	Naphthalene	917	µg/kg	1.14	3.21	3.72	2.40	0.00	0.00	0.18	2.95
	Toluene	5000	µg/L	3.91	34.99	45.13	13.76	0.02	0.26	0.06	2.22
	Toluene	480	µg/L	3.91	34.99	45.13	13.76	0.02	0.26	0.06	2.22
	Xylene	561	µg/kg	0.79	5.05	10.09	3.19	0.02	2.18	0.08	1.37
	Phenol	250	µg/L	2.27	26.15	14.01	11.70	0.29	0.29	0.14	0.14
C_80	Benzene	10500	µg/L	3.74	29.36	38.95	24.66	0.04	0.62	0.21	2.97
	Benzene	760	µg/L	3.74	29.36	38.95	24.66	0.04	0.62	0.21	2.97
	Chlorobenzene	428	µg/kg	0.01	0.23	0.17	0.70	0.00	0.00	0.01	0.35
	Dichlorobenzene	239	µg/kg	0.01	0.13	0.33	0.85	0.01	0.01	0.01	0.64
	Ethylbenzene	176	µg/kg	0.23	0.57	1.05	0.62	0.01	0.41	0.01	0.36
	Naphthalene	917	µg/kg	0.83	2.61	2.90	1.90	0.00	0.00	0.06	1.55
	Toluene	5000	µg/L	1.65	18.27	30.68	8.45	0.01	0.23	0.03	1.25
	Toluene	480	µg/L	1.65	18.27	30.68	8.45	0.01	0.23	0.03	1.25
	Xylene	561	µg/kg	0.54	3.43	7.41	2.50	0.01	2.01	0.03	0.95
	Phenol	250	µg/L	1.65	21.08	10.16	7.94	0.03	0.03	0.04	0.04

Note: All simulations based on a 6-inch chemical isolation layer and a 12-inch habitat layer thickness. Mean values used for all input parameters except porewater concentration in underlying sediment which was based on the percentile value in the first column of the table. Reported results are the maximum concentrations predicted in the habitat layer.

Table 4
Numerical Modeling Results for Carbon Amendment Design Life Assuming No Biological Degradation

ILWD Subarea/Contaminant	Performance Standard	Units	Carbon Mat Design Life (years)					
			Deterministic			Monte Carlo		
West			C-80	C-90	C-95	80th %	90th %	95th %
Chlorobenzene	428	µg/kg	>1,000	>1,000	>1,000	>1,000	>1,000	901
Dichlorobenxzene	239	µg/kg	>1,000	>1,000	>1,000	>1,000	748	360
Ethylbenzene	176	µg/kg	>1,000	>1,000	>1,000	>1,000	>1,000	>1,000
Benzene	10,500	µg/L	>1,000	>1,000	>1,000	>1,000	>1,000	>1,000
Benzene	760	µg/L	>1,000	>1,000	>1,000	>1,000	>1,000	>1,000
Toluene	5,000	µg/L	>1,000	>1,000	>1,000	>1,000	>1,000	>1,000
Toluene	480	µg/L	>1,000	>1,000	>1,000	>1,000	>1,000	>1,000
Naphthalene	917	µg/kg	250	200	160	213	149	113
Xylene	561	µg/kg	>1,000	>1,000	>1,000	>1,000	>1,000	702
Center								
Chlorobenzene	428	µg/kg	>1,000	>1,000	>1,000	>1,000	>1,000	627
Dichlorobenxzene	239	µg/kg	>1,000	>1,000	>1,000	>1,000	>1,000	853
Ethylbenzene	176	µg/kg	>1,000	>1,000	>1,000	>1,000	>1,000	>1,000
Benzene	10,500	µg/L	>1,000	>1,000	>1,000	>1,000	>1,000	>1,000
Benzene	760	µg/L	>1,000	>1,000	>1,000	>1,000	>1,000	>1,000
Toluene	5,000	µg/L	>1,000	>1,000	>1,000	>1,000	>1,000	>1,000
Toluene	480	µg/L	>1,000	>1,000	>1,000	>1,000	>1,000	>1,000
Naphthalene	917	µg/kg	230	175	105	187	116	84
Xylene	561	µg/kg	785	515	450	665	441	343
East								
Chlorobenzene	428	µg/kg	960	140	82	603	112	65
Dichlorobenxzene	239	µg/kg	760	470	355	562	340	250
Ethylbenzene	176	µg/kg	>1,000	>1,000	>1,000	>1,000	>1,000	>1,000
Benzene	10,500	µg/L	>1,000	>1,000	>1,000	>1,000	>1,000	>1,000
Benzene	760	µg/L	>1,000	>1,000	>1,000	>1,000	>1,000	>1,000
Toluene	5,000	µg/L	>1,000	>1,000	>1,000	>1,000	>1,000	>1,000
Toluene	480	µg/L	>1,000	>1,000	>1,000	>1,000	>1,000	>1,000
Naphthalene	917	µg/kg	425	315	200	288	182	126
Xylene	561	µg/kg	>1,000	>1,000	>1,000	>1,000	>1,000	>1,000
SMU 2								
Chlorobenzene	428	µg/kg	>1,000	>1,000	>1,000	>1,000	>1,000	>1,000
Dichlorobenxzene	239	µg/kg	>1,000	>1,000	>1,000	>1,000	>1,000	>1,000
Ethylbenzene	176	µg/kg	>1,000	>1,000	>1,000	>1,000	>1,000	>1,000
Benzene	10,500	µg/L	>1,000	>1,000	>1,000	>1,000	>1,000	>1,000
Benzene	760	µg/L	>1,000	>1,000	>1,000	>1,000	>1,000	>1,000
Toluene	5,000	µg/L	>1,000	>1,000	>1,000	>1,000	>1,000	>1,000
Toluene	480	µg/L	>1,000	>1,000	>1,000	>1,000	>1,000	>1,000
Naphthalene	917	µg/kg	>1,000	725	350	>1,000	488	270
Xylene	561	µg/kg	>1,000	>1,000	>1,000	>1,000	>1,000	>1,000

Note: All design life simulations based on the full 12- inch chemical isolation required by the ROD and a 12-inch habitat layer thickness. Model runs were capped at 1,000 years to limit processing time. Reported results for deterministic model runs are the predicted carbon mat design lives expressed for specific initial concentrations, i.e. 80, 90th and 95 percentile. The results for the Monte Carlo simulations represent the design life for a particular confidence interval, based on 5,000 realizations over the range of potential model input parameters that results in concentrations equal to or less than the performance standard throughout the habitat layer.

Table 5

Results of Numerical Screening-Level Mercury Modeling

Area	Break-through Time (yrs)
A1	844
A2	>1,000
E1	>1,000
E2	>1,000
D (east) without carbon	>1,000
D (east) with carbon	>1,000
D (center, west and SMU 2) without carbon	>1,000
D (center, west and SMU 2) with carbon	>1,000

Notes: Initial concentrations and upwelling velocity were modeled as the maximum observed in each model area. Remediation Area D west, center and SMU 2 subareas grouped for screening given the results for the eastern subarea modeling and the comparatively lower maximum mercury concentration in these subareas. All simulations based on a 6-inch chemical isolation layer and a 12-inch habitat layer thickness.

Table 6

Analytical Model Results for PAH and PCB Screening Evaluation – Maximum Predicted Concentrations in the Habitat Layer

Contaminant	PEC µg/kg	Model Area: Remediation Area A µg/kg	Remediation Area E µg/kg	Remediation Area D: West µg/kg	Remediation Area D: Center µg/kg	Remediation Area D: East µg/kg	SMU 2 µg/kg
Flourene	264	4	872	1,947	2,121	940	1,242
Phenanthrene	543	18	194	4,808	5,593	700	1,562
Acenaphthene	861	10	305	790	1,512	144	678
Acenaphthylene	1301	23	1,497	1,543	1,914	278	583
Anthracene	207	6	84	1,289	1,939	176	463
Pyrene	344	11	94	208	386	57	84
Benzo(a)anthracene	192	6	57	234	213	27	72
Benzo(b)flouranthene	908	9	79	152	136	25	54
Benzo(k)Flouranthene	203	1	25	62	57	9	24
Chrysene	253	7	42	193	192	25	56
Flouranthene	1436	15	643	783	781	98	244
Benzo(a)pyrene	146	5	68	131	113	21	45
Dibenz(a,h)anthracene	157	1	32	30	16	3	8
Indeno(1,2,3-cd)pyrene	183	4	16	65	38	10	18
Benzo(g,h,i)perylene	780	5	42	67	33	11	18
PCBs	295	45	69	1	16	17	14

Note: Initial concentrations and upwelling velocity were modeled as the maximum observed in each model area. Chemical isolation layer thickness was set to 6-inches in all model areas. Habitat layer thickness was modeled as 12-inches. Biological decay was not included in model simulations. Results represent the maximum concentration observed at steady state in the habitat layer post-capping

Table 7
Numerical Model Results for Refined Modeling Evaluation of PAHs

Contaminant	Monte Carlo Evaluation: % indicates the percentage of simulations meeting the PEC @ 1,000 years	Deterministic Evaluation: Time to Exceedance
Remediation Area E		
Flourene	98.80%	>1,000 years
Acenaphthylene	99.78%	>1,000 years
Remediation Area D – West		
Flourene	98.72%	>1,000 years
Phenanthrene	98.44%	>1,000 years
Anthracene	99.48%	>1,000 years
Benzo(a)anthracene	100.00%	>1,000 years
Acenaphthylene	99.99%	>1,000 years
Remediation Area D – Center		
Flourene	99.78%	>1,000 years
Phenanthrene	99.72%	>1,000 years
Acenaphthene	100.00%	>1,000 years
Acenaphthylene	100.00%	>1,000 years
Anthracene	99.82%	>1,000 years
Benzo(a)anthracene	100.00%	>1,000 years
Pyrene	100.00%	>1,000 years
Remediation Area D – East		
Flourene	100.00%	>1,000 years
Phenanthrene	100.00%	>1,000 years
Remediation Area D – SMU 2		
Flourene	99.50%	>1,000 years
Phenanthrene	99.99%	>1,000 years
Anthracene	100.00%	>1,000 years

Note: Chemical isolation layer thickness was set to 6-inches in Model Areas E, in Remediation Area D carbon design lives were calculated based on a 12-inch layer. Habitat layer thickness was modeled as 12-inches. Biological decay was not included in model simulations. Results in the Monte Carlo evaluation column represent the percentage of model simulations meeting the PEC at 1,000 years. Results in the deterministic evaluation column represent the time to steady state based on the 95th percentile concentration with other input parameters fixed at their mean values.

FIGURES

OL-VC-50052
OL-VC-50053
OL-VC-50054
OL-VC-50056
OL-VC-50055
SMU 5
SMU 4
OL-VC-40188
OL-VC-40142
OL-VC-40189
OL-PP-40062
OL-VC-40190
OL-VC-30080
OL-VC-30082
OL-VC-40191
SMU4
SMU3
OL-PP-40061
Model Area A-1
OL-PP-40063
OL-PP-40065
OL-VC-30081
OL-VC-30084
OL-VC-40192
OL-PP-40064
TR01-C
OL-VC-40193
OL-VC-40194
OL-PP-40066
OL-PP-40070
OL-PP-40068
OL-PP-40067
OL-VC-40195
Model Area A-2
OL-PP-40069
OL-VC-40196
OL-VC-40197
TR01-B
OL-PP-40071
OL-VC-40198
OL-PP-40073
OL-VC-40199
OL-VC-40200
OL-PP-40072
TR01-A

Cap Area

Remediation Area Boundary

Notes:
1. Porewater data was used for VOCs and naphthalene where available.
2. Location OL-VC-40197 was not included in modeling evaluation. Additional data collected during the Phase V PDI will be used to further delineate the cap boundary and porewater conditions in this area. OL-VC-30084 was not included in modeling evaluation and some locations outside the cap area were included in evaluation, in part as a result of changes in remediation area boundaries occurring after modeling was initiated. Future modeling evaluations will be updated accordingly.

0 50 100 200 300 400
Feet

N

FIGURE B-1

Honeywell

Onondaga Lake
Syracuse, New York

Remediation Area A
Porewater Sample Locations

PARSONS

301 PLAINFIELD RD, SUITE 350, SYRACUSE, NY 13212 Phone:(315) 451-9560

Q:\GIS\GIS_Lake\OL-porewater\PW Cap Modeling\Rem_A_PW_locs.mxd

SMU2 ILWD Area

SMU1 ILWD Western Area

SMU1 ILWD Center Area

SMU1 /SMU7 ILWD Eastern Area

OL-PP-20101
OL-PP-20011
OL-PP-20107
OL-PP-20104
OL-PP-20079
OL-VC-20108
OL-PP-20106
OL-PP-20006
OL-VC-10158
OL-PP-10036
TR02-B-PW
OL-STA-10008-PP
OL-STA-10008-PW
OL-PP-10034
OL-VC-10152
OL-VC-10153
OL-VC-10136
TR03-A-PW
OL-STA-10001-PP
OL-STA-10001-PW
TR02-C-PW
OL-VC-10159
OL-PP-10042
OL-PP-10040
OL-PP-10040A
OL-VC-10160
TR03-D-PW
OL-STA-10013-PP
OL-STA-10013-PW
OL-VC-10137
TR03-C-PW
TR03-B-PW
OL-VC-10138
OL-VC-10140
OL-STA-10018-PP
OL-STA-10018-PW
OL-STA-10020-PW
OL-PP-10055
OL-VC-10139
OL-STA-10022-PP
OL-STA-10022-PW
OL-VC-10141
OL-STA-10010-PP
OL-STA-10010-PW
TR04-B-PW
OL-VC-10143
OL-PP-10063
OL-STA-10004-PP
OL-STA-10004-PW
TR04-D-PW
OL-VC-10142
TR04-C-PW
OL-PP-10071
OL-PP-10095
OL-STA-10006-PP
OL-STA-10006-PW
OL-VC-10154
OL-VC-10155
OL-VC-70087
OL-VC-10145
OL-PP-70017
OL-STA-10024-PP
OL-STA-10024-PW
OL-VC-10156
OL-PP-10096
OL-VC-10148
OL-STA-10007-PW
OL-STA-10007-PP
OL-VC-10157
OL-STA-10011-PW
OL-VC-10146
OL-PP-70021
OL-PP-70021A
TR04-A-PW
OL-VC-10144
OL-VC-10149
OL-VC-10147
OL-STA-10012-PW
OL-VC-10150
TR05-B-PW
OL-VC-10151
TR05-A-PW

Cap Area

Remediation Area Boundary

ILWD Boundary

Note:
Porewater data was used for VOCs, naphthalene and phenol where available.

0 60 120 240 360 480
Feet

FIGURE B-2

Honeywell

Onondaga Lake
Syracuse, New York

Remediation Area D
Porewater Sample Locations

PARSONS
301 PLAINFIELD RD, SUITE 350, SYRACUSE, NY 13212 Phone (315) 451-9560

Q:\GIS\GIS_Lake\OL-porewater\PW Cap Modeling\Rem_D_PW_locs.mxd

SMU 5
SMU 6
OL-VC-60203
OL-STA-60033-PP
OL-STA-60033-PW
OL-STA-60034-PP
OL-STA-60034-PW
OL-STA-60035-PP
OL-STA-60035-PW
OL-STA-60031-PP
OL-STA-60031-PW
OL-VC-60204
OL-VC-60205
OL-VC-60206
OL-STA-60040-PP
OL-STA-60040-PW
OL-STA-60039-PP
OL-STA-60039-PW
OL-STA-60038-PP
OL-STA-60038-PW
OL-STA-60037-PP
OL-STA-60037-PW
OL-STA-60036-PP
OL-STA-60036-PW
OL-VC-60222
OL-VC-60207
OL-VC-60208
OL-VC-60209
OL-VC-60210
OL-VC-60223
OL-STA-60045-PP
OL-STA-60045-PW
OL-STA-60044-PP
OL-STA-60044-PW
OL-STA-60043-PP
OL-STA-60043-PW
OL-STA-60042-PP
OL-STA-60042-PW
OL-VC-60224
Model Area E-1
OL-VC-60211
OL-STA-60041-PP
OL-STA-60041-PW
OL-VC-60212
OL-VC-60214
OL-VC-60213
OL-PP-60109
OL-STA-60050-PP
OL-STA-60050-PW
OL-PP-60104
OL-VC-60215
OL-STA-60049-PP
OL-STA-60049-PW
OL-PP-60108
OL-STA-60048-PP
OL-STA-60048-PW
OL-VC-60103
OL-VC-70120
OL-VC-60216
OL-PP-60106
OL-PP-70031
OL-STA-60047-PP
OL-STA-60047-PW
OL-VC-60107
OL-VC-60107A
OL-STA-70050
OL-STA-60046-PP
OL-STA-60046-PW
OL-VC-70086
OL-PP-70050
OL-PP-60105
OL-VC-60102
OL-VC-70123
OL-VC-70119
OL-VC-60217
SMU1
SMU7
OL-VC-70122
OL-VC-60110
OL-VC-70085
OL-PP-70022
OL-PP-70022A
OL-STA-70049
OL-VC-60101
TR06-C
OL-VC-70110
OL-VC-70111
OL-PP-70024
SMU6
SMU7
TR06-B
OL-VC-70109
OL-VC-70049
Model Area E-2
OL-VC-70108
OL-VC-70084
OL-STA-70048
OL-PP-70048
TR06-A

Cap Area
Remediation Area Boundary
ILWD Boundary

0 50 100 200 300 400
Feet

N

Notes:
1. Porewater data was used for VOCs and naphthalene where available.
2. Some sample locations outside the cap area were included in modeling evaluation, in part as a result of changes in remediation area boundaries occuring after modeling was initiated. Future modeling evaluations will be updated accordingly.

FIGURE B-3

Honeywell
Onondaga Lake
Syracuse, New York

Remediation Area E
Porewater Sample Locations

PARSONS
301 PLAINFIELD RD, SUITE 350, SYRACUSE, NY 13212 Phone:(315) 451-9560

Q:\GIS\GIS_Lake\OL-porewater\PW Cap Modeling\Rem_E_PW_locs.mxd

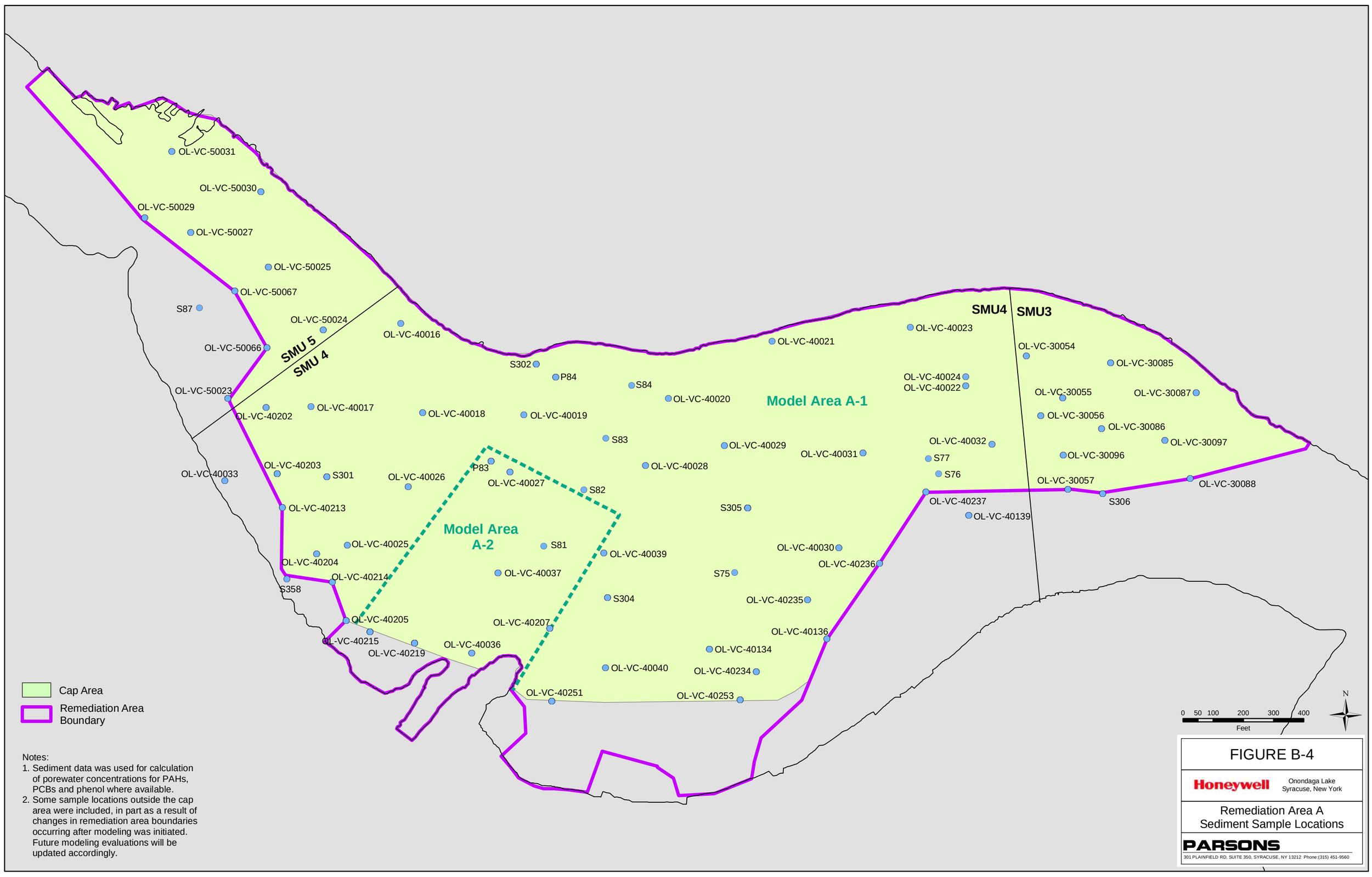

Notes:
1. Sediment data was used for calculation of porewater concentrations for PAHs, PCBs and phenol where available.
2. Some sample locations outside the cap area were included, in part as a result of changes in remediation area boundaries occurring after modeling was initiated. Future modeling evaluations will be updated accordingly.

FIGURE B-4

Honeywell — Onondaga Lake, Syracuse, New York

Remediation Area A
Sediment Sample Locations

PARSONS
301 PLAINFIELD RD, SUITE 350, SYRACUSE, NY 13212 Phone:(315) 451-9560

Q:\GIS\GIS_Lake\CAP\IDS\SED Model Area Locs\Rem_A_Sed_locs_11302009.mxd

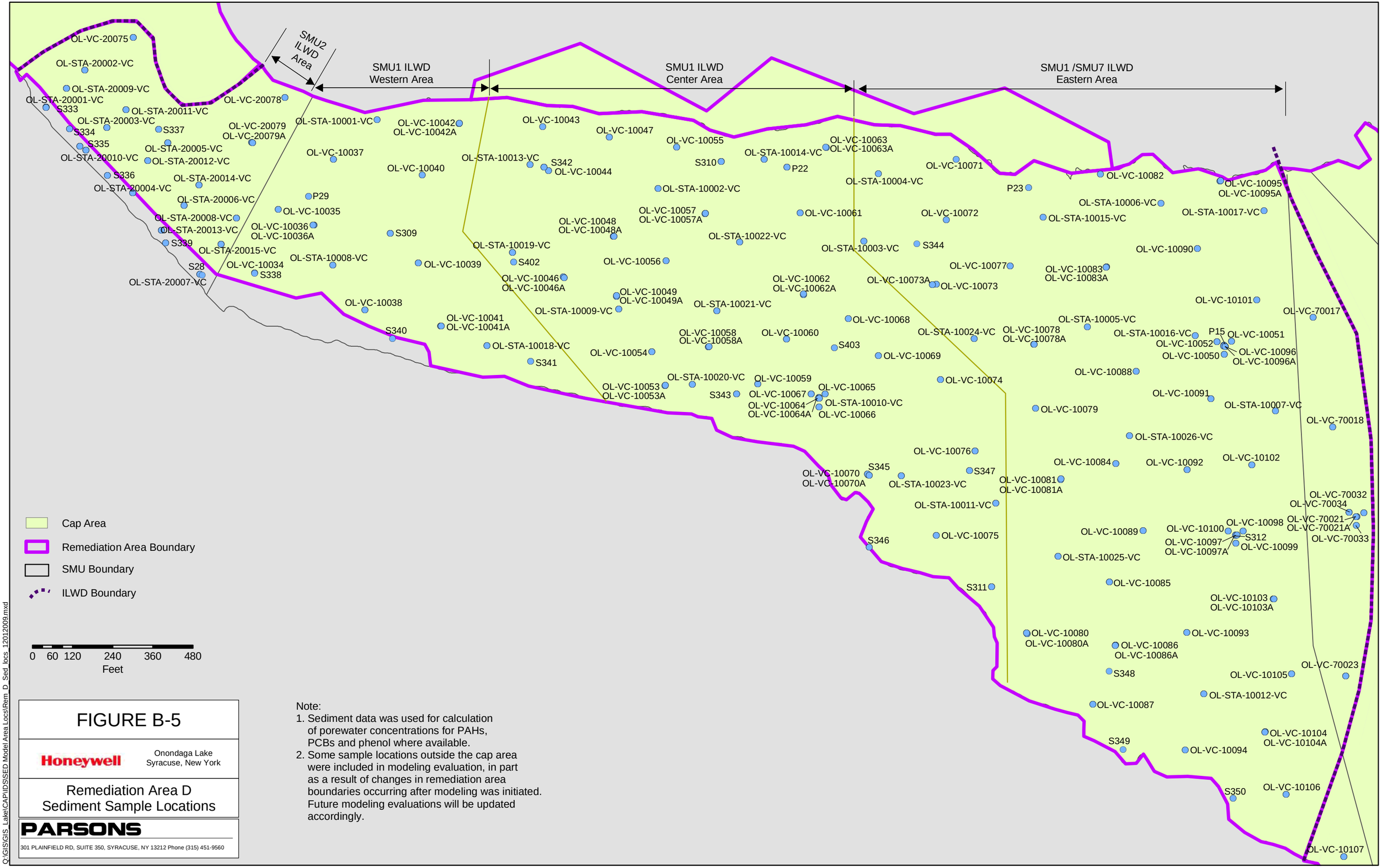

Note:
1. Sediment data was used for calculation of porewater concentrations for PAHs, PCBs and phenol where available.
2. Some sample locations outside the cap area were included in modeling evaluation, in part as a result of changes in remediation area boundaries occurring after modeling was initiated. Future modeling evaluations will be updated accordingly.

FIGURE B-5

Honeywell

Onondaga Lake
Syracuse, New York

Remediation Area D
Sediment Sample Locations

PARSONS
301 PLAINFIELD RD, SUITE 350, SYRACUSE, NY 13212 Phone (315) 451-9560

Q:\GIS\GIS_Lake\CAP\DS\SED Model Area Locs\Rem_D_Sed_locs_12012009.mxd

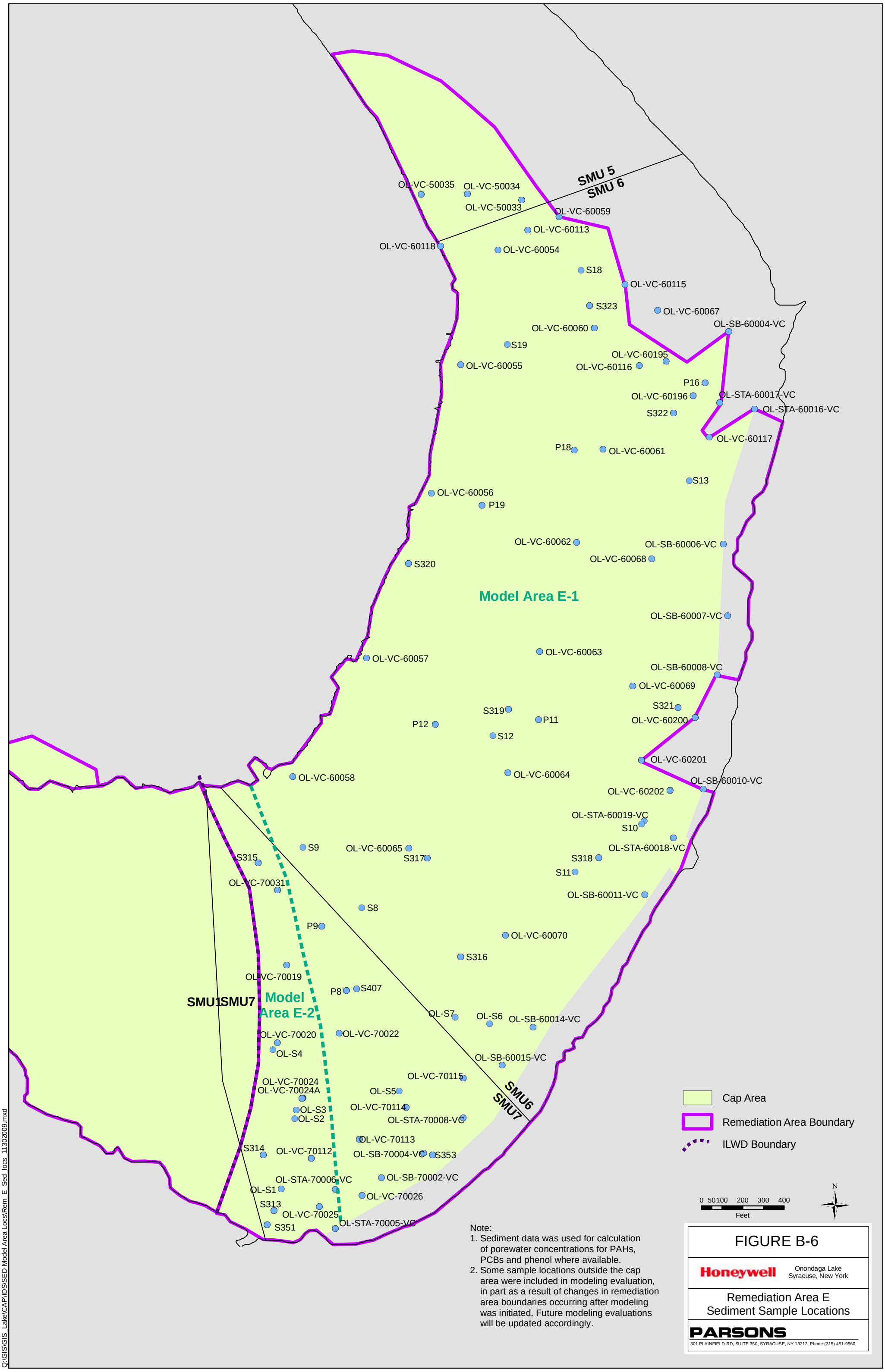

Note:
1. Sediment data was used for calculation of porewater concentrations for PAHs, PCBs and phenol where available.
2. Some sample locations outside the cap area were included in modeling evaluation, in part as a result of changes in remediation area boundaries occurring after modeling was initiated. Future modeling evaluations will be updated accordingly.

FIGURE B-6

Honeywell

Onondaga Lake
Syracuse, New York

Remediation Area E
Sediment Sample Locations

PARSONS
301 PLAINFIELD RD, SUITE 350, SYRACUSE, NY 13212 Phone:(315) 451-9560

Q:\GIS\GIS_Lake\CAP\IDS\SED Model Area Locs\Rem_E_Sed_locs_11302009.mxd

ATTACHMENT 1

MODEL INPUT

A1.1
MODEL INPUT PARAMETERS AND BASIS

Model Input	Fixed or Monte Carlo Distribution	Site-specific or Literature Based	Reference	Rationale
Initial porewater concentration in underlying sediment	Distribution (Fixed for deterministic simulations and screening evaluations)	Site-specific	Based on concentrations measured in porewater for the following Contaminants: Benzene, Toluene, Ethylbenzene, Xylene, Chlorobenzene, Dichlorobenzenes and Naphthalene. Porewater concentrations for the following contaminants were calculated based on sediment concentrations and equilibrium partitioning formulae: phenol, PAHs, and total PCBs (see Attachment 2). Phenol data from groundwater upwelling pumps were used, where available, to supplement values calculated from phenol sediment data. Data were selected from the following depth intervals: the top 0 to 5 meters in SMU 2 ILWD, 1 to 5 meters in the West and East, 0 to 4 meters in the Center, and 0-3 m in Remediation Areas A and E. Correction factors were applied as appropriate, see Attachment A1.2. Depth intervals were selected considering the proposed dredge plan and generally include the data from two meters above to two meters below the maximum dredge cut in an area, exclusive of hot spot dredging in the ILWD. This is conservative because it includes data from sediments which will be dredged, which generally contain higher porewater contaminant concentrations than the remaining sediments. Under Honeywell's proposed approach, no removal is proposed in portions of the ILWD Center and ILWD West subareas. For the ILWD West subarea, porewater data from depths of 1 to 5 meters were used to generate an area-wide data set. Data from the top meter in the West were excluded as this layer will be removed over a significant portion of the western subarea. Concentrations in the top meter are generally lower than or consistent with the deeper porewater data, and therefore exclusion of this data does not have a significant impact on the porewater distribution used in the modeling. *Honeywell Onondaga Lake Locus Database, 2009.*	Spatial variability exists across the isolation cap areas. The ILWD has been broken into four subareas to account for larger-scale differences in contaminant concentration distributions. Likewise, Remediation Areas A and E have been broken into Modeling Areas A1, A2 and E1, E2 based on differences in pore water concentration. Monte Carlo simulations are based on empirical cumulative distribution functions developed from the concentration datasets for each COC within a given modeling area. Further explanation of the derivation of the CDF is provided in Attachment A1.3. Figures 1 through 6 illustrate porewater sampling locations and modeling areas.

Model Input	Fixed or Monte Carlo Distribution	Site-specific or Literature Based	Reference	Rationale
Molecular diffusion coefficient	Fixed	Literature	Fixed value by compound. *Lyman, W.J, Reehl, W.F. and Rosenblatt D.H. 1990. Handbook of Chemical Property Estimation Methods. American Chemical Society, Washington, D.C.*.	Little to no spatial variability or uncertainty anticipated.
Hydrodynamic dispersivity	Fixed	Literature	Conservative value fixed at 10% of the total cap thickness. *Domenico and Schwartz (1990), Physical and Chemical Hydrogeology, John Wiley. Homogenous cap layer expected to exhibit significantly smaller dispersivity.*	Upper bound employed, not expected to significantly impact cap design
Porosity (Isolation and Habitat Layers)	Fixed	Literature	Fixed value of 0.4. Theoretical maximum porosity for uniform spherical particles is 0.4765 (cubic packing); if the particles are rhombohedrally packed, then the uniform maximum porosity is 0.2595. Baseline value based on a typical value for loosely packed, medium-grain sand.	Little to no spatial variability or uncertainty anticipated.
Porosity (carbon mat)	Fixed	Literature	Fixed value of 0.35. Based on F400 dry bulk density of 0.52 g/cc and an assumed particle density of 0.8 g/cc.	Little to no spatial variability or uncertainty anticipated.
Porosity (underlying sediment)	Fixed	Site-specific	Average porosity in the ILWD of 79.26%. *Honeywell Onondaga Lake Locus Database, 2009.*	The critical model input parameter is the initial porewater concentration (Co), which was either measured or calculated from sediment data. Since the calculated value is a function of sediment characteristics such as fraction organic carbon, porosity and particle density (along with sediment contaminant level), it is difficult to coherently apply distributions to all these parameters simultaneously. The decision was made to prioritize Co, and use fixed values for the underlying sediment characteristics. Using a fixed value for porosity is not expected to significantly impact cap design.

Model Input	Fixed or Monte Carlo Distribution	Site-specific or Literature Based	Reference	Rationale
Particle density	Fixed	Literature	Fixed value of 2.6 g/cm^3. *Freeze, R.A., Cherry, J.A. 1979. Groundwater. Prentice-Hall, Inc., Englewood Cliffs, New Jersey.*	Little to no spatial variability or uncertainty anticipated. Not expected to significantly impact cap design.
foc (Isolation Layer)	Fixed	Site-specific	Remediation Area D - Fixed value of 0.022% based on average effective foc measured in column study experiments on SMU 1 sediments. *Parsons, 2009. Phase III PDI Data Summary Report.* Remediation Area A and E - Fixed value of 0.098% as measured on sands from Syracuse Region. Parsons, 2009. *Phase III PDI Data Summary Report.*	Little to no spatial variability or uncertainty anticipated.
foc (Underlying Sediment)	Fixed	Site-specific	Individual sample results. *Honeywell Onondaga Lake Locus Database, 2009.*	The critical model input parameter is the initial porewater concentration (Co), which was either measured or calculated from sediment data. Since the calculated value is a function of sediment characteristics such as fraction organic carbon, porosity and particle density (along with sediment contaminant level), this makes it difficult to coherently apply distributions to all these parameters simultaneously. The decision was made to prioritize Co, and use fixed values for the underlying sediment characteristics. Using a fixed value for foc is not expected to significantly impact cap design.

Model Input	Fixed or Monte Carlo Distribution	Site-specific or Literature Based	Reference	Rationale
Boundary layer mass transfer coeff.	Fixed	Site-specific	Fixed value of 0.363 cm/hr. Eqn 11 of *Thibodeaux and Becker, 1982 (4 m/s windspeed, 5m water depth, benzene, 500m fetch). Thibodeaux, L. J., and Becker, B., (1982). "Chemical transport rates near the sediment of a wastewater impoundments", Environmental Progress, Vol 1; no. 4, p 296-300.*	Little to no spatial variability or uncertainty anticipated.
Koc for isolation sand and underlying sediment	Distribution for VOCs, fixed value for mercury, phenol, PCBs, PAHs as well as for all deterministic simulations,	Site-specific for VOCs and mercury, literature for PCBs, PAHs, phenol	Values for VOCs (mean and standard error) calculated using regression of paired sediment/pore water measurements from Phase 1-4 data. Paired data were also used for estimating mercury Kd's in the native sediments (for use in numerical modeling) *See Attachment 2.* Literature value used for phenol based on *NYSDEC Technical Guidance for Screening Contaminated Sediment (NYSDEC, 1999)).* Values used for PAHs and PCBs based on NYSDEC screening guidance values to represent partitioning to cap material, and corrected literature values to represent partitioning to underlying sediment , as described in Attachment 2. Mercury partitioning coefficients for sand based on data from: Reible, D., 2009. *Phase IV Addendum 2 Report –Isotherm Experiments with Organic Contaminants of Concern with Sand, Organoclay and Peat and for Mercury with Sand, Organoclay, Peat and Activated Carbon.*	The variability observed is a function of parameter uncertainty due to sampling methodology and analytical limitations. To evaluate the impact of this uncertainty the distribution for Koc is modeled by a mean and normal distribution defined by the standard error, the standard error representing uncertainty about the mean value. For literature-based values used in PAH, PCB, and phenol modeling, uncertainty was not represented, since there is little information available to estimate site-specific variation in these parameters. These values were derived from NYSDEC Guidance.

Model Input	Fixed or Monte Carlo Distribution	Site-specific or Literature Based	Reference	Rationale
foc (Bioturbation zone of Habitat Layer)	Distribution/Fixed for deterministic simulations	Site-specific	Distribution based on mean and standard error of site-specific TOC data in the top six inches of lesser-impacted non-ILWD SMUs (SMU 4 and 5), length weighted averages were developed for cores where multiple sample intervals were collected in the top 0-6" . *Honeywell Onondaga Lake Locus Database, 2009.*	Inherent uncertainty exists in trying to estimate the ultimate post-remedy TOC in the upper layer of the sediment cap. Site-specific data may provide a suitable estimate of this input parameter in areas of the lake not impacted (or impacted to a lesser degree) by METRO processes and Solvay Waste materials, which tend to produce higher TOC values. To address the uncertainty around future TOC levels in the upper layer of the cap data in the 0-6" interval from SMUs 4 and 5 were used to develop a range of surficial TOC. The SMU 4/5 data do not exhibit any spatial structure and are expected to be an overestimate of post-remedy TOC given recent decreases in organic loading and lake productivity associated with METRO upgrades. This data set was described by a normal distribution represented by the mean and standard error.

Model Input	Fixed or Monte Carlo Distribution	Site-specific or Literature Based	Reference	Rationale
Freundlich coefficients	Distribution/ Fixed for deterministic simulations	Site-specific	Isotherm experiments were conducted by Carnegie-Mellon to establish sorption characteristics of the proposed activated carbon to be used. Mean values for Kf and 1/n were used for the deterministic runs. Monte Carlo modeling based on sampling from the 95% confidence regions for those parameters. *Draft report for Phase IV Addendum 2 PDI Work Plan, Isotherm Experiments for Activated Carbon, Organoclay and Peat (February 2009).* For modeling of phenol, isotherm parameters for benzene were used, and naphthalene isotherm parameters were used to represent the other PAHs.	The best estimates of Kf and 1/n were used for deterministic model runs. In order to quantify uncertainty around the mean values used for Kf and 1/n, a 95% confidence region was generated around the means, and estimates of the coefficient pairs randomly taken from within that range were used for the Monte Carlo simulations. The 95% confidence interval was generated directly from experimental data (a two parameter (Kf, 1/n) nonlinear sorption isotherm).
Particle Biodiffusion Coefficient (Habitat Layer)	Distribution/Fixed for deterministic simulations	Literature	Normal distribution of log transformed values. *Thoms, S.R., Matisoff, G., McCall, P.L., and Wang, X. 1995. Models for Alteration of Sediments by Benthic Organisms, Project 92-NPS-2, Water Environment Research Foundation, Alexandria Virginia*	Uncertainty associated with size, depth and distribution of benthic organisms. Data from freshwater sites employed to generate a log-normal distribution.
Pore Water Biodiffusion Coefficient (Habitat Layer)	Distribution/Fixed for deterministic simulations	Literature	Student's t distribution of log transformed values with standard error (to account for small sample size) based on literature. *Wood, L.W. (1975) Role of oligochaetes in the circulation of water and solutes across the mud-water interface. Verhandlungen der Internationalen Vereinigung fur Theoretische und Angewandte Limnologie. 19: 1530-1533. Svensson, J.M., and L. Leonardson. (1996) Effects of bioturbation by tube-dwelling chironomid larvae on oxygen uptake and denitrification in eutrophic lake sediments. Freshwater Biology. 35: 289-300. Cunningham (2003) Unpublished PhD dissertation, Louisiana State University, D. Reible, Advisor.*	Uncertainty associated with size, depth and distribution of benthic organisms. Data from freshwater sites employed to generate a log-normal distribution.

Model Input	Fixed or Monte Carlo Distribution	Site-specific or Literature Based	Reference	Rationale
Darcy Velocity	Distribution/ Fixed	Site-specific	Site-specific groundwater upwelling data used to generate an empirical cumulative distribution function for the data sets in Remediation Areas A and E. Upwelling rates used in Remediation Area D were based on the best estimate of conditions that would exist once the upland hydraulic containment system is in-place. To represent these anticipated conditions in the ILWD cap modeling, the contour map of upwelling rates presented in Appendix C was used to specify a statistical distribution for each ILWD sub-area, further detail is provided in Attachment A1.4.	Within Remedial Area D, simulation of separate sub-areas captures major spatial variation in upwelling rate (resulting from differences in underlying clay thickness). The impacts of smaller-scale variations in upwelling within these subareas are quantified by the Monte Carlo results (i.e., the distribution in outputs captures parameter uncertainty as well as spatial variability). Likewise, within Remedial Areas A and E, distributions characterize the observed variations in upwelling from the site data (which represent a combination of measurement uncertainty and true spatial variation).
Biological decay rate (Isolation and Habitat Layers)	Distribution	Site-specific for VOCs, literature for phenol	Student's t distribution of log transformed values with standard error (to account for small sample size) based on Phase III Column Studies data. See Attachment 3 for addition detail. For phenol, Student's t distribution of log transformed values with standard error (to account for small sample size) was developed based on values reported in the literature (see Attachment 3).	Uncertainty associated with estimates of reactivity. Data generated from experimental columns by assuming (conservatively) detection limit in effluent. See Attachment 3 for additional information.

A1.2
CORRECTION FACTORS FOR POREWATER CONCENTRATIONS

Porewater Sample Collection Method	Correction Factor
Peepers (Phases I, II & III)	
Xylenes (total)	1.1
Chlorobenzene	1.1
Toluene	1.1
Ethylbenzene	1.1
Benzene	1.1
1,3-Dichlorobenzene (phases I & II)	1.2
1,3-Dichlorobenzene (phase III)	1.1
1,4-Dichlorobenzene (phases I & II)	1.2
1,4-Dichlorobenzene (phase III)	1.1
1,2-Dichlorobenzene (phases I & II)	1.2
1,2-Dichlorobenzene (phase III)	1.1
Naphthalene (phases I & II)	1.2
Naphthalene (phase III)	1.1
Mercury (Tuffryn)	1.1
1,2,4-Trichlorobenzene (phases I & II)	1.2
1,2,4-Trichlorobenzene (phase III)	1.1
1,2,3-Trichlorobenzene (phases I & II)	1.2
1,2,3-Trichlorobenzene (phase III)	1.1
1,3,5-Trichlorobenzene (phases I & II)	1.2
1,3,5-Trichlorobenzene (phase III)	1.1
Centrifuge (Phases I, II, III & IV)	
Xylenes (total)	1.11
Chlorobenzene	1.11
Toluene	1.08
Ethylbenzene	1.07
Benzene	1.09
1,3-Dichlorobenzene	1.10
1,4-Dichlorobenzene	1.14
1,2-Dichlorobenzene	1.15
Naphthalene	1.54
Mercury	1.06
1,2,4-Trichlorobenzene	1.45
1,2,3-Trichlorobenzene	1.53
1,3,5-Trichlorobenzene	1.07

A1.3

CUMULATIVE DISTRIBUTION FUNCTION

The contaminant concentrations in the pore water of the sediments underlying the cap were characterized by data collected in Onondaga Lake. There were certain cases where the presence of a relatively high proportion of non-detect results introduced uncertainty at the lower end of the concentration distribution. For example, Figure T1 shows the distribution of ethylbenzene concentrations in SMU 2, with non-detect sample concentrations plotted at the detection limit (5 ug/L) as grey symbols. Clearly, assuming all non-detect results are equal is inappropriate, whether at the detection limit which would be overly conservative or at zero which is equally inappropriate.

The approach used to estimate the full distribution of contaminant concentrations was based on the observation that the detected concentrations generally follow a log-normal distribution (that is, the detected data are roughly linear in Figure T1); thus a reasonable and logical assumption is that the non-detect concentrations follow this same distribution. A cumulative distribution function was derived based on the detected concentrations, and this function was then used to estimate values for the non-detect results. Specifically, a truncated lognormal distribution was fit to only the detected concentrations by fitting a linear regression to predict log-concentration from the normal z-score values (see black line in Figure T1). Z-score values were assigned assuming all of the detected concentrations were higher than the non-detect sample results. The fitted regression line was then used to predict log-concentrations for the normal z-score values attributed to the non-detect samples (see open symbols in Figure T1). Finally, the empirical cumulative distribution function was used to characterize the distribution of pore water concentrations for the Monte Carlo simulations, restricted to the range of detected and estimated concentrations. This approach is recommended by Ginevan and Splitstone 2004.

Figure T1

Ethylbenzene concentrations in the pore water of sediment from SMU2

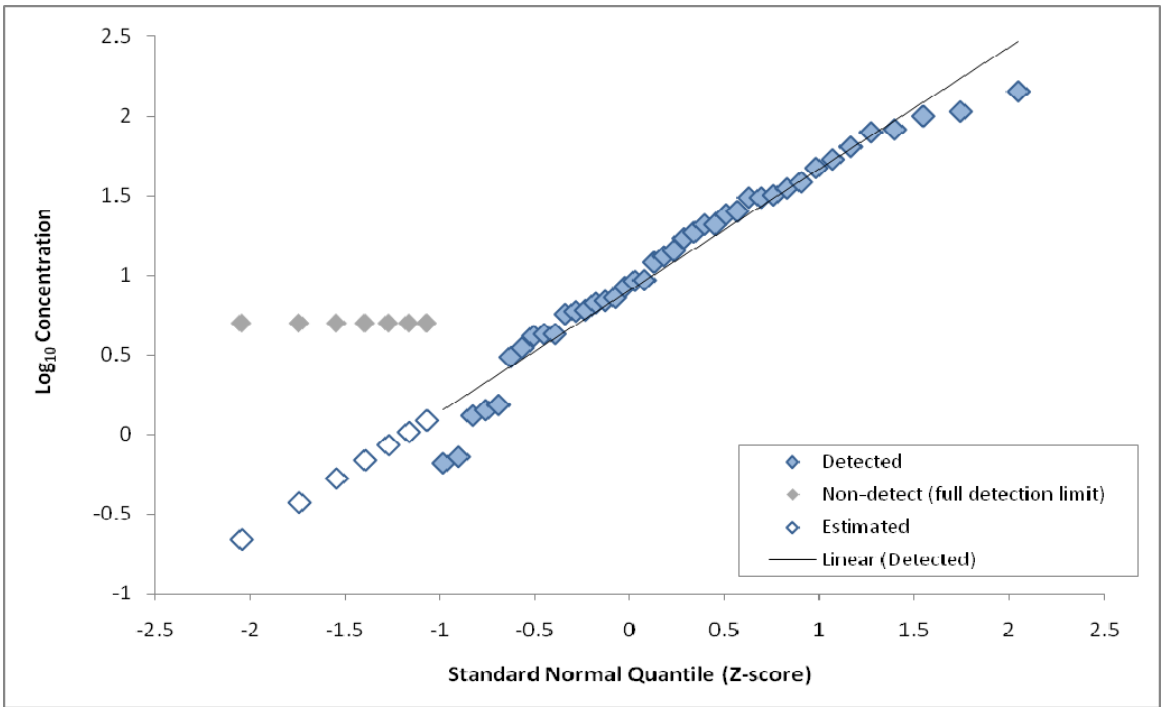

Reference:

Ginevan, Michael E., and Douglas E. Splitstone, 2004. Statistical tools for environmental quality measurement. CRC Press LLC. p. 229.

A1.4
ILWD UPWELLING VELOCITY DISTRIBUTIONS

Unlike Remedial Areas A and E, there are no direct measurements of groundwater upwelling rates within the ILWD. Rather, the upwelling rates used in the cap modeling for this area were based on the best estimate of conditions once the upland hydraulic containment system is in-place. These estimates were developed from multiple lines of evidence by integrating existing geological information, boring data, and groundwater modeling, as discussed in Appendix C of this IDS. These estimates indicate that upwelling rates within the ILWD would be 2 cm/yr or less, with lower values in areas where the silt and clay below the ILWD is thicker.

For cap modeling purposes, the anticipated conditions in the ILWD were simulated using the contour map of upwelling rates presented Appendix C. The contour map was used to specify a statistical distribution for each ILWD sub-area. These distributions were developed by first calculating the percentage of acreage covered by the various upwelling ranges within each ILWD sub-area, as shown in Figure 1 below.

Figure 1.
Estimated groundwater upwelling rates within the ILWD and associated acreages within ILWD sub-areas.

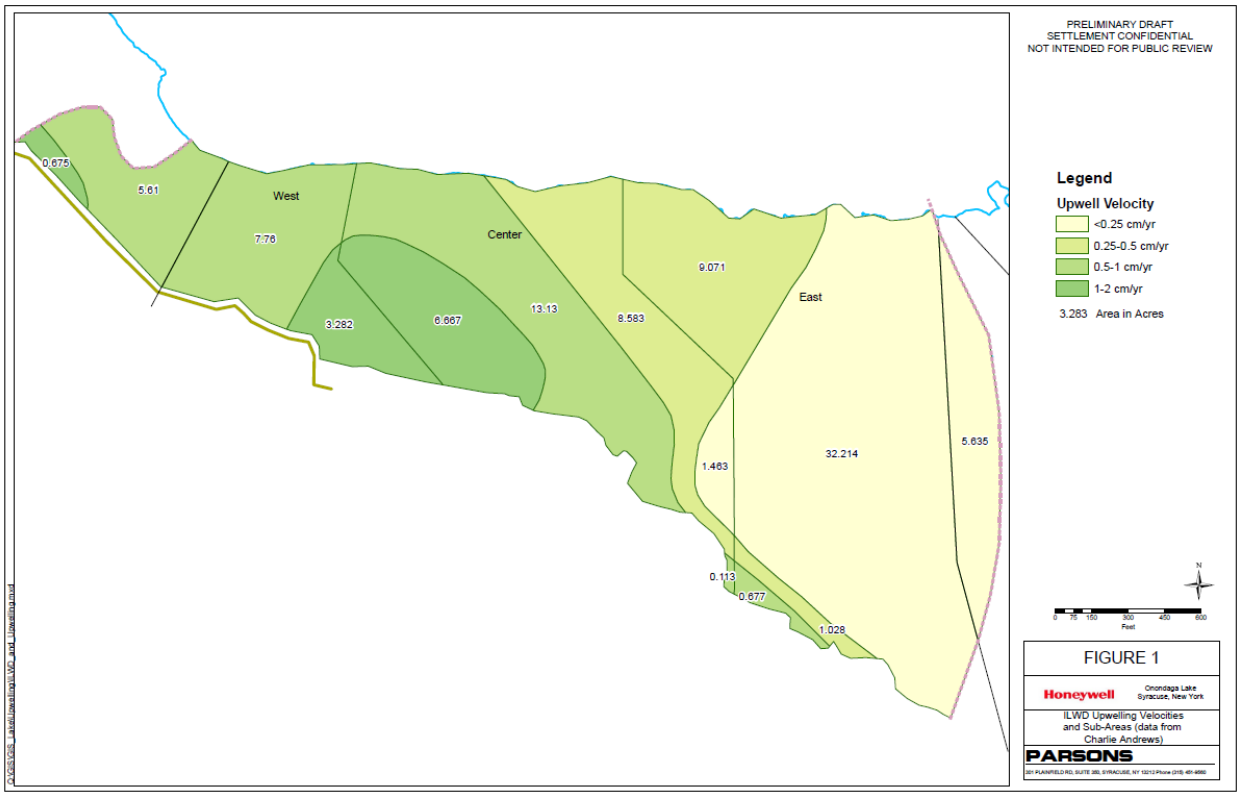

For each ILWD sub-area, the area-based percentage of each upwelling range was applied directly to the percentiles of a cumulative distribution function (CDF), with an assumed linear variation across the discrete ranges (with the exception of the <0.25 cm/yr range, which was held constant at 0.25 cm/yr). For example, for the ~30 acre ILWD Center sub-area, Figure 1 shows that 1.5 acres (5%) are in the <0.25 cm/yr range, 8.6 acres (29%) are in the 0.25 to 0.5 cm/yr range, 13.1 acres (44%) are in the 0.5 to 1 cm/yr range, and 6.7 acres (22%) are in the 1 to 2 cm/yr range. Thus, for this sub-area, the upwelling CDF was based on:

- The lowest 5% of the values are set at a constant of 0.25 cm/yr
- The 6th to 34th percentiles vary linearly from 0.25 to 0.5 cm/yr
- The 35th to 79th percentiles vary linearly from 0.5 to 1 cm/yr
- The 79th to 100th percentiles vary linearly from 1 to 2 cm/yr

The resulting cumulative distribution functions for the four ILWD sub-areas are shown in Figure 2.

Figure 2
Groundwater upwelling rates cumulative distribution functions for the ILWD sub-areas.

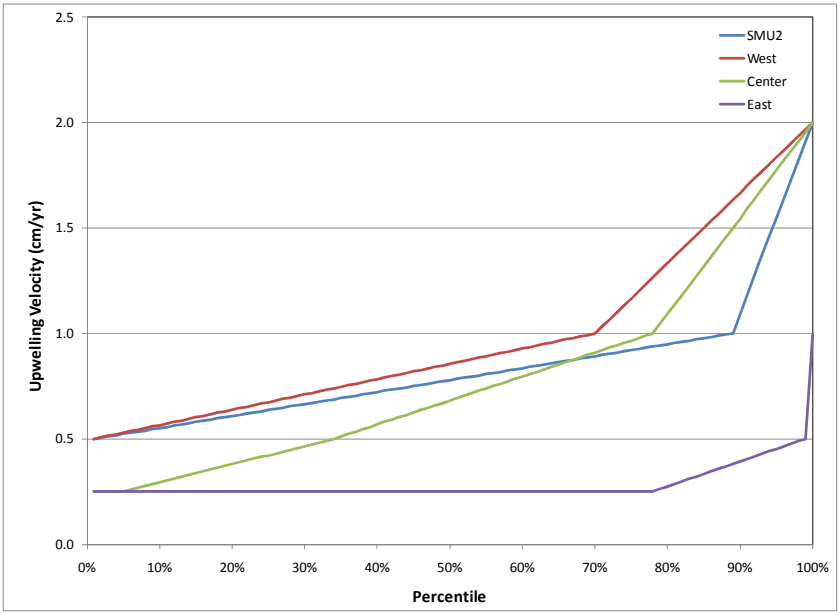

This approach results in a mean value for each ILWD sub-area that corresponds to the area-weighted average of the contoured upwelling rates within that sub-area, and a range that corresponds to those shown in the contour plots, as developed based on the thickness of the underlying silt and clay unit.

ATTACHMENT 2

PARTITIONING COEFFICIENTS AND SEDIMENT TO POREWATER CALCULATIONS

ATTACHMENT 2

PARTITIONING COEFFICIENT EVALUATION AND SEDIMENT TO POREWATER CALCULATION BASIS

Partitioning coefficients were employed in various aspects of the cap modeling evaluation to describe the equilibrium relationship between contaminant concentrations in the dissolved and sorbed-to-sediment phases within the cap materials as well as in the underlying sediments. This memorandum discusses the basis for the selected partitioning coefficients as well as the calculations used to derive porewater concentrations from sediment data or vice versa.

The following sections describe the methods used to estimate partition coefficients for use in the model based on site-specific data or literature studies. Due to differences in data availability, varying methods were used to develop partition coefficients for the different classes of modeled CPOIs (i.e., VOCs, mercury, phenol, PAHs and PCBs). As such, the classes of CPOIs are discussed separately in the sections below.

1.0 PARTITIONING COEFFICIENT EQUATIONS

Partitioning coefficients, by definition, relate equilibrium porewater concentrations to sorbed-to-sediment concentrations. Since the laboratory-reported sediment concentrations for this project account for contaminants in all phases (i.e., sorbed, dissolved, vapor, and NAPL) per dry weight of sediment, the calculation of a partitioning coefficient must relate to this total sediment concentration. The partitioning equation derived from the EPA's Soil Screening Guidance (EPA, 1996) equation 22 of Part 2 (reorganized) for non-NAPL-impacted material is:

$$K_d = \frac{C_{sed}}{C_{pw}} - \frac{\theta}{\rho_b}$$

where

C_{sed} equals the total sediment concentration (dry weight) of the CPOI (ug/kg),
C_{pw} equals the core dissolved porewater concentration (ug/l),
θ is porosity, and
ρ_b is dry bulk density (kg/L).

For hydrophobic organics, the equation is:

$$K_{oc} = \frac{\left[\frac{C_{sed}}{C_{pw}} - \frac{\theta}{\rho_b} \right]}{f_{oc}}$$

where

f_{oc} is the mass fraction of organic carbon of the raw sediment.

The equation, as laid out, assumes there is no NAPL in the sample. The principal reason for doing this is that it is not possible to test for the presence of NAPL using a sample's CPOI

concentrations without first knowing the Koc values. Therefore, the use of this equation would provide an overestimate of mean Koc values since a NAPL-impacted sample would exhibit a higher total sediment concentration than what would be indicated by equilibrium with its porewater phase. This issue affects the assessment of sediments in SMU 1, where NAPL has been observed. However , it is not expected that the presence of NAPL in some of the samples would materially affect the overall estimates, given the large number of usable data pairs in SMU 1 and the logarithmic distribution of the data.

As noted above, partition coefficients relate equilibrium porewater concentrations to sorbed-to-sediment concentrations, not to the total sediment concentration as measured in the PDI sampling program. While this distinction, which suggests it is important to account for contaminant mass in the dissolved-phase of a sample, is meaningful for low sorptivity compounds, it is not actually important for highly sorptive compounds. This is due to the fact that for highly sorptive compounds, such as PAHs and PCBs, very little contaminant mass is held in the dissolved-phase of a sediment sample. Therefore in calculating PAH and PCB porewater concentrations from measured sediment concentrations, it is only necessary to also know the f_{oc} of the sediment sample. This procedure actually adds a very small element of conservatism to the estimation of porewater concentration, since complete accounting for the dissolved-phase mass in the sample would lower the estimate of porewater concentration.

For PAHs and PCBs, the equation for calculating the local porewater concentration is:

$$C_{pw} = \frac{C_{sed}}{K_{oc} \bullet f_{oc}}$$

2.0 DEVELOPMENT OF SITE SPECIFIC PARTITIONING COEFFIENTS FOR VOCs

The analysis of paired sediment and porewater samples, generated via centrifugation procedures in Phases I, III and IV of the PDI, provided an opportunity to estimate site-specific partitioning coefficients for Onondaga Lake sediments, in the form of an organic carbon-water partitioning coefficient (K_{oc}) for Benzene, Toluene, Ethylbenzene, Xylene, Tri-cholorobenzene, Di-chlorobenzene, chlorobenzene and naphthalene. This section describes the sample processing procedures, and the calculations and analysis methods used to estimate the partitioning coefficients from the sample data (including filtering of the dataset to eliminate unusable results). Results are presented in graphical and tabular formats. The site specific partitioning coefficients generated as described in the following subsections were used in cap modeling to predict partitioning within the chemical isolation layer and habitat layer materials as well as within the underlying sediments for the numerical modeling conducted for Remediation Area D.

2.1 SAMPLE COLLECTION AND PROCESSING

In Phase I of the PDI, samples of sediment and porewater were collected at 13 locations in SMU 1 (at two depths, for a total of 26 data pairs), and 20 locations in SMU 6 (from the surficial zone only, providing 20 data pairs). No paired sampling was conducted in Phase II for the purpose of estimating partitioning coefficients. The total number of sample pairs was greatly increased by work conducted in Phase III, with an additional 238 sample pairs collected in

SMU 1, an additional 20 sample pairs in SMU 6, and also 44 sample pairs collected from SMU 7. During Phase IV, additional sampling was conducted within SMUs 4, 6, and 7, producing 51, 62, and 48 sample pairs, respectively. Samples have also been collected in other locations, including 29 sample pairs in SMU 3, 10 sample pairs in SMU 4, and 7 sample pairs in SMU 8.

In Phase I, three cores were collected at each location and depth interval to provide material for sediment and porewater analyses. Upon receipt in the lab, the cores were opened and freestanding water decanted and discarded. No homogenization of sediments occurred. One core was used for raw sediment analysis, and the other two were used to fill between four and six centrifuge bottles, which were then centrifuged to generate porewater. All generated porewater was then composited prior to sub-sampling for the various analyses. One of the centrifuged bottles provided material for the dewatered sediment analysis. A sample pair from Phase I, for the purposes of calculating partition coefficients, was comprised of a dewatered sediment sample and an associated porewater sample.

In Phase III and IV, long cores were cut into 2-ft sections. Upon receipt in the lab the 2-ft cores were opened, and freestanding water carefully decanted for compositing with porewater subsequently generated by centrifugation of the sediment sample. A portion of the sediment sample from the top of the core was sub-sampled for raw sediment analyses. The balance of the sediment from the 2-ft core was weighed and placed in centrifugation bottles. The sample bottle was centrifuged and supernatant water was separated and collected. The aqueous sample for volatile organic compounds (VOCs) was then centrifuged again, decanted and placed in volatile organic analyte (VOA) vials for analysis. A sample pair from Phase III and IV, for the purposes of calculating partition coefficients, was comprised of a raw sediment sample and an associated porewater sample.

2.2 AREA-WIDE PARTITION COEFFICIENT ANALYSIS

The partition coefficients estimated from the site data used in the cap modeling effort were developed based on the hypothesis that a single mean partition coefficient could be used to describe the site data within a given area, and that sample-to-sample differences within these areas stem primarily from measurement variability. This is consistent with the fact that partition coefficients are often taken to be chemical-specific properties (after properly normalizing for organic carbon content as appropriate). To estimate the effective partition coefficient for an area containing numerous sediment-porewater sample pairs, the sorbed-to-sediment phase concentration was first calculated for each sample pair. This concentration was calculated by taking the reported total dry weight concentration (Csed in the equations above) and subtracting off the porewater mass (using the measured porewater concentration, bulk density, and porosity):

$$C_s = C_{sed} - \left(C_{pw} \frac{\theta}{\rho_b} \right)$$

where Cs is the sorbed-to-sediment phase concentration of a CPOI (ug/g).

After calculating Cs for all samples within an area, the concentrations were normalized by foc and plotted against their paired porewater concentrations. Plotting these values against porewater concentration in linear space produces a relationship with a slope that is equivalent to Koc. Thus, a least squares regression analysis can be used to calculate the Koc for a given area (and the confidence interval of the regression line can describe variability). Preliminary analyses indicated that such regressions could be strongly influenced by the highest concentration data pairs. Given that porewater concentrations within the cap would be expected to be within a lower range, the underlying regression equation (Cs/foc = Koc*Cpw) was log-transformed to remove the effect of a few high concentration samples driving the regression and therefore all measurements were treated as having the same standard error. By doing this, it was equivalent to the model: log (Cs/foc) = log (Koc) + log (Cpw). Least squares regression formulae were derived for this case, which produced a best estimate of log Koc and an associated standard error. The log-transform was judged appropriate since Kocs are typically found to be log normally distributed (and hence typically reported as log Koc).

For the cap modeling effort, the analysis method described above was used to estimate a Koc value for each modeled CPOI. The data from Remedial Areas A and E were pooled together, and data from SMU 1 were analyzed separately since previous analyses had suggested partitioning within ILWD materials differed from that in sediments from other areas of the lake.

2.3 FILTERING OF DATA PAIRS

After compiling the data from Phases I, III and IV, any data pair (sediment and porewater) which involved a non-detect result was excluded from the analysis, given the uncertainty of the resulting calculation. Additionally, any result which produced a negative value for the sorbed-to-sediment concentration from the above equation was deleted. This would occur when the measured contaminant mass in all the phases (the sediment concentration) was not sufficient to produce the measured mass in the dissolved-phase (the porewater concentration). Another way of explaining the same situation would be to say that the CPOI mass measured in the porewater exceeded the total CPOI mass measured in the bulk sediment (i.e., solids plus porewater). Since such a scenario is not possible, even though the analytical results support it, the assumption is that there is some error in the one or more of the analyses, and therefore the data pair does not allow for a calculation of a partitioning coefficient. Such occurrences were rare, and primarily involved benzene, the least sorptive of the detected compounds.

In an effort to assess the potential effects of surface water on porewater concentrations in the surficial samples, the data set was also sorted and samples collected in the 0-1 ft interval were eliminated.

2.4 RESULTS

Following the filtering step described above, the log-transformed regression analyses described above were conducted. Figures 1 through 9 show the regressions and the resulting Kocs and standard errors (derived from the confidence limit on the regression line). The data and regression lines on Figures 1-9 indicate that while there is scatter in the data (the degree to which varies by CPOI), when taken together, the data from the different areas (i.e., Areas A/E

and SMU 1) tend to exhibit a single relationship between sorbed-to-sediment and porewater concentrations. The presence of such a relationship is consistent with the concept of the area-based approach used in this analysis. The resulting Koc values tend to differ a bit between SMU 1 and Areas A & E, with SMU 1 values being a bit higher – this is consistent with results from previous analyses and likely attributable to the effects of elevated pH and dissolved organic carbon (DOC) in these materials.

Table 1 lists for each CPOI the number of data pairs and the resulting Koc values and associated standard errors, and includes a comparison to a range of literature values. The differences in resulting Koc's among CPOI follow expected trends (e.g., Kocs of dichlorobenzenes are higher than that of chlorobenzene), and the calculated values are within the range of the literature values.

As such, the values listed in Table 1 for Areas A and E were used to describe the partitioning of VOCs to sand capping materials in all areas of the Lake. Likewise, the Koc's estimated from the SMU 1 data set were used to describe partitioning within the underlying sediment/waste materials in Remedial Area D for use in the transient numerical modeling. The differences in Koc between ILWD and non-ILWD materials are believed to be due to elevated pH and DOC in the ILWD as discussed above; however, the Koc's derived from non-ILWD data were used to simulate sorption to sand capping materials within the ILWD because the pH amendment to the cap is designed to lower pH in the isolation layer and the subsequent onset of biological degradation within that layer would result in lower DOC levels. Thus, the amended cap approach within the ILWD is expected to eliminate these effects and result in partitioning behavior within the isolation layer that is consistent with that in other capped areas of the lake.

2.5 MERCURY PARTITIONING COEFFIENTS

Unlike VOCs, the partition coefficients used for simulating mercury were expressed as a Kd value, since organic carbon is not the only significant sorbing phase for mercury. The values used in the transient numerical cap modeling conducted for mercury were developed as follows:

- Kd's for the underlying sediment were calculated from the values for paired sediment / porewater data (i.e., using the data sets/filtering methods described above for VOCs), and the average log Kd for each area was used in the model. Separate values were calculated for Remedial Areas A, E, and D. The resulting log Kd values were 4.5, 4.6, and 3.1, respectively. The lower Kd value estimated from the SMU 1data is believed to reflect differences in the nature of the ILWD materials, including elevated pH. This simpler method for calculating the sediment Kd (as compared to the regression-based approach used for VOCs) was used since this parameter only describes the partitioning within the underlying sediment in the numerical model, which has much less influence on predicted concentrations in the cap than the Kd's used to describe partitioning onto capping materials (which are described below).

- Kd's for sorption onto sand capping material in Remedial Areas A and E were estimated based on the data from isotherm studies conducted using porewater from SMU 6/7 sediments (Parsons, 2008). These data were found to best be described by a Freundlich isotherm equation (Parsons, 2008). As such, the best fit SMU 6/7 isotherm equation was used to calculate a Kd based on the maximum measured porewater concentration in each modeling area. It should be noted that this approach is conservative because at the lower concentrations that would be present in the cap (as compared to the maximum underlying porewater concentration), the SMU 6/7 isotherm relationship produces Kd values that are higher than those calculated for that maximum porewater concentration (thus resulting in even slower transport). The resulting log Kd values for Modeling Areas A1 and A2 were 3.0 and 3.2, respectively, while the Modeling Area E1 and E2 log Kd values were 3.9 and 3.8, respectively.

- Kd's for sorption onto sand capping material in Remedial Area D were also derived from data generated from isotherm studies performed with SMU 1 porewater (Parsons, 2008). These data were found to follow a linear relationship, so a regression-based approach was used, in which the slope of a linear regression line fit through a plot of sorbed-to-sediment phase mercury concentrations versus porewater concentrations was used to estimate the Kd. The resulting log Kd value was 3.1.

- In Remedial Area D, the effect of a carbon mat was also evaluated in certain model simulations – the Kd for activated carbon was also developed based on the isotherm study data, using the same approach as described above for sand. The resulting log Kd value was 4.0.

3.0 PHENOL PARTITIONING COEFFIENT

Site-specific porewater data for phenol were limited given the large volumes required or analysis. Additionally, sediment-porewater pairs were not available for the direct estimate of a phenol partitioning coefficient. In lieu of a site specific Koc value the NYSDEC Technical Guidance (NYSDEC, 1999) value for Phenol was used to describe partitioning of phenol to both the underlying sediment, to supplement existing porewater data, and to simulate partitioning to the cap material. Similar to VOC compounds, phenol partitioning in the cap model is simulated through use of a Koc value. The Technical Guidance document directly provides an octanol/water partition coefficient or Kow. The Technical Guidance suggests that when applying the equilibrium partitioning methodology Koc and Kow values are very similar, for un-chlorinated phenol the Log Kow value is 2.0 (NYSDEC, 1999). A fixed value was used for phenol in all model simulations.

4.0 PCB AND PAH PARTITIONING COEFFIENTS

Site specific porewater data were not available for PAH and PCB model simulations. Porewater collected during the 2002/2003 groundwater upwelling investigation were mostly non-detect for PAHs and PCBs (Parsons, 2003 and Parsons, 2007). In the absence of site-specific

data for PAHs and PCBs a literature review of partitioning of these compounds was conducted. This information was used to calculate initial porewater concentrations in model simulations as well as to describe partitioning to cap materials.

Modeling conducted during the Feasibility Study had used Kow values reported in New York State Department of Environmental Conservation Guidance (NYSDEC, 1999) as estimates of Koc and measured foc values to estimate the concentrations of PAHs and PCBs in sediment porewater beneath the cap. This same approach was taken in the IDS when modeling fate and transport of PAHs and PCBs within the sand capping material; however, a growing body of literature indicates that the conventional approach of calculating PAH and PCB porewater concentrations in underlying sediments will overestimate actual PAH or PCB porewater concentrations (for discussions see Arp et al., 2009; Hawthorne et al., 2006; and McGroddy *et al.*, 1996). The primary cause of this discrepancy is that natural sediments are composed of different types of organic carbon, with some phases of organic carbon ("hard" carbon) sorbing hydrophobic contaminants stronger but more slowly than other phases ("soft" carbon). For purposes of calculating initial porewater concentrations in the underlying sediment, measured foc values and field-derived effective Koc values measured in natural sediment at other sites that account for strongly-sorbing fractions of sediment, were used. Addendum 1 provides a detailed description of the literature review and partitioning coefficient recommendations.

Recommendations from the evaluation presented in Addendum 1 support the use of corrected PAH and PCB Koc values to most accurately model and predict porewater PAH and PCB concentrations within the underlying Lake sediment in the absence of direct measurements. Based on the data presented in Addendum 1 an increase in effective Koc values of 10X from PAH Kow values is recommended for derivation of PAH porewater concentrations in the non-ILWD impacted sediments at this time. Based on the data presented in Addendum 1, an increase in effective Koc values of 5X from PCB Kow values is recommended for derivation of PCB porewater concentrations in the non-ILWD impacted sediments. Effective Koc values are based on the values presented in the NYSDEC Technical Guidance. Partitioning in the underlying sediments of the ILWD is based directly on the Technical Guidance values, as the unusual pH and DOC conditions there create conditions at variance with the natural sediments and so are not addressed by the literature cited above. Partitioning to the cap material is simulated in the model using uncorrected values from the Technical Guidance. Fixed values were used for PAHs and PCBs in all model simulations.

5.0 REFERENCES

NYSDEC, 1999. Technical Guidance for Screening Contaminated Sediments. January 1999.

Parsons, 2003. Groundwater Upwelling Investigation for Onondaga Lake, Syracuse New York. Prepared for Honeywell, Morristown, New Jersey. Syracuse, New York.

Parsons, 2007. Onondaga Lake Pre-Design Investigation, Phase I Data Summary Report. Prepared for Honeywell, Morristown, New Jersey. Syracuse, New York.

Parsons, 2008. Onondaga Lake Pre-Design Investigation: Phase IV Work Plan - Addendum 2 Cap Amendment Isotherm Development. Prepared for Honeywell, Morristown, New Jersey. Syracuse, New York.

USEPA, 1996. Soil Screening Guidance: Technical Background Document, Part 2, page 36, EPA/540/R-95/128, May 1996.

TABLES

Table 1. Summary of Koc values determined by regression analysis, compared to literature-based values.

	SMU-1			Model Areas A & E			Range of LOG Koc from regression-based formulas in literature[1]		Range of LOG Koc from published studies (Mackay, et al.)[2]	
	No. of data pairs	LOG Koc	std error of regression	No. of data pairs	LOG Koc	std error of regression	Min	Max	Min	Max
Benzene	124	1.68	0.049	20	1.67	0.16	1.63	1.97	1.26	2.01
Toluene	184	2.35	0.030	40	2.27	0.11	2.31	2.64	2.25	2.39
Ethylbenzene	122	2.88	0.035	32	2.59	0.10	2.77	3.10	2.21	
Xylene	204	2.84	0.029	56	2.45	0.11	2.77	3.10	2.22	2.52
Chlorobenzene	160	2.55	0.039	49	2.14	0.11	2.46	2.79	1.92	2.73
1,2-Dichlorobenzene	160	3.10	0.036	35	2.74	0.14	3.00	3.32	2.26	3.51
1,3-Dichlorobenzene	3	3.00	0.10	48	2.43	0.12	--	--	--	--
1,4-Dichlorobenzene	167	3.18	0.036	47	2.59	0.12	3.00	3.32	2.78	3.26
Naphthalene	217	3.10	0.030	61	2.66	0.10	2.99	3.31	2.66	5.00

Notes:

1. Range from several representative regression formulas that correlate Kow to Koc (Log Kow values presented in the NYDEC's *Technical Guidance for Screening Contaminated Sediments* were used). These formulas were pooled from the following studies:
   - DiToro, D.M., 1985. A Particle Interaction Model of Reversible Organic Chemical Sorption. *Chemosphere 14* :1503-1538.
   - Karickhoff, S.W., 1981. Semi-empirical estimation of sorption of hydrophobic pollutants on natural sediments and soil. *Chemosphere 10:* 833-846.
   - Means, J.C., S.G. Wood, J.J. Hassett and W.L. Banwart, 1980. Sorption of polynuclear aromatic hydrocarbons by sediments and soils. *Environmental Science & Technology 14:* 1524-1528.
   - Shimizu, Y., S.Yamazaki and Y. Terashima, 1992. Sorption of anionic pentachlorophenol (PCP) in aquatic environments: The effect of pH. *Water Science & Technology 25:* 41-48.
2. Range of values taken from *Illustrated Handbook of Physical-Chemical Properties and Environmental Fate for Organic Chemicals,* Donald Mackay, Wan Ying Shiu, and Kuo Ching Ma, 1992. Only values from studies utilizing field measurements were included.

FIGURES

BENZENE – SMU-1

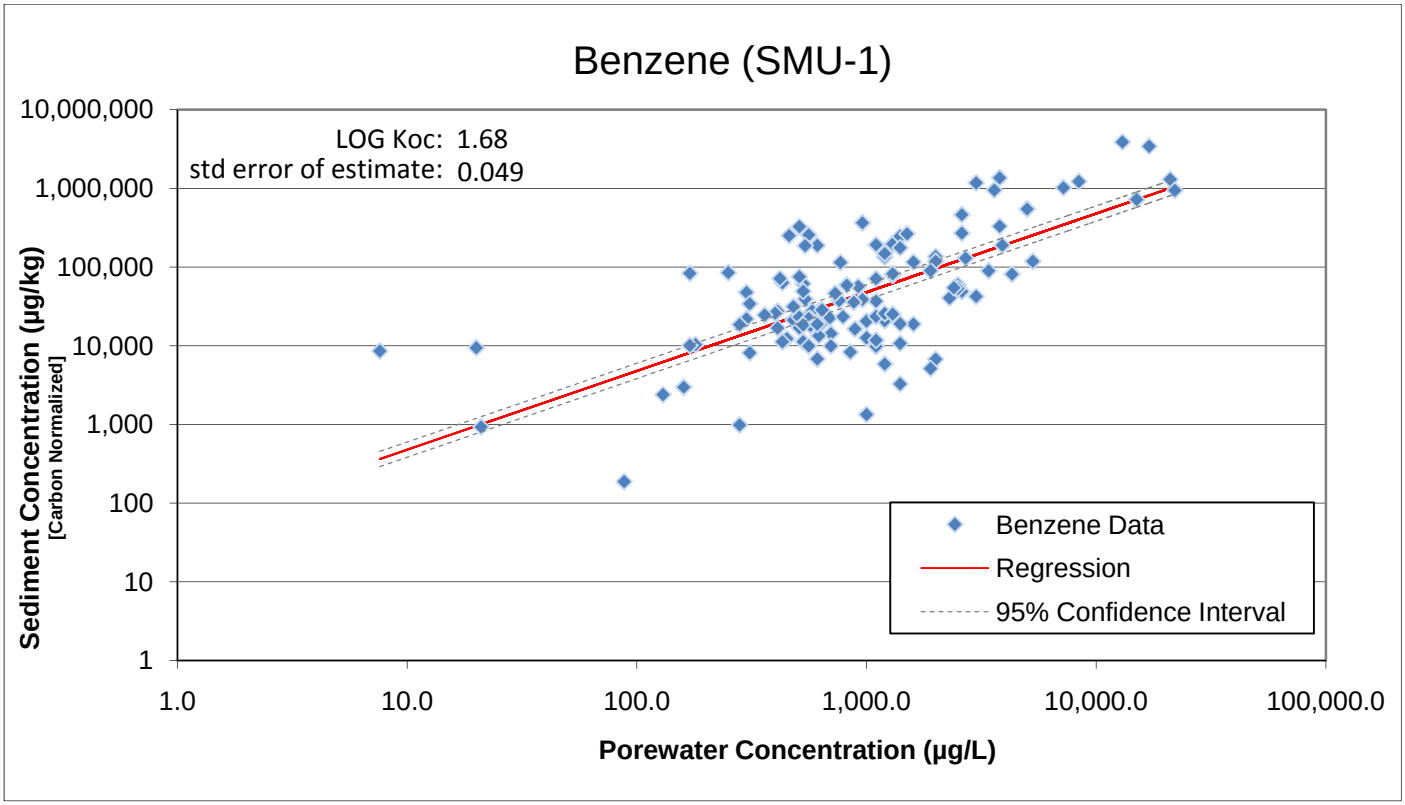

BENZENE – Model Areas A & E

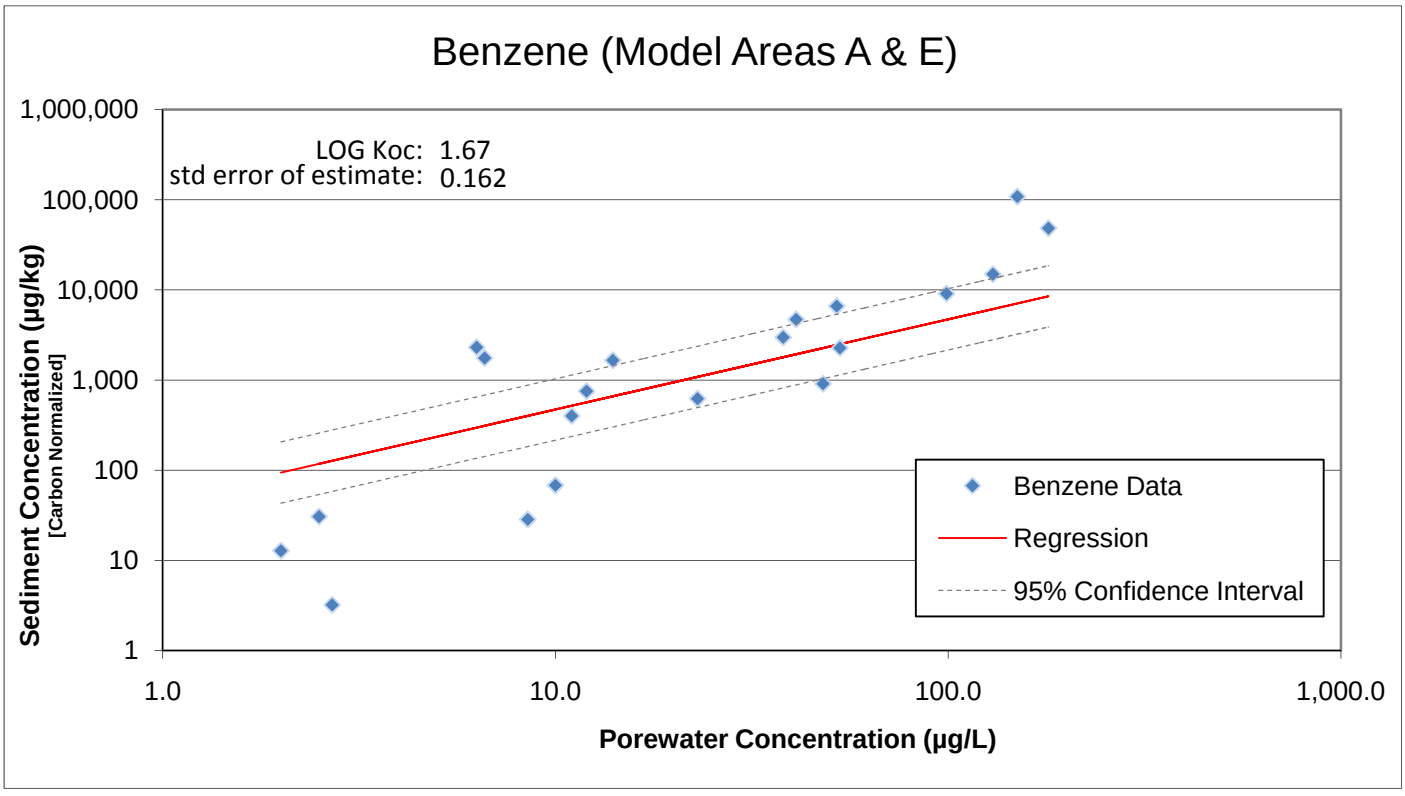

Figure 1. Relationship between *benzene* porewater concentration and carbon-normalized sediment concentration (with log-transformed regression).

TOLUENE – SMU-1

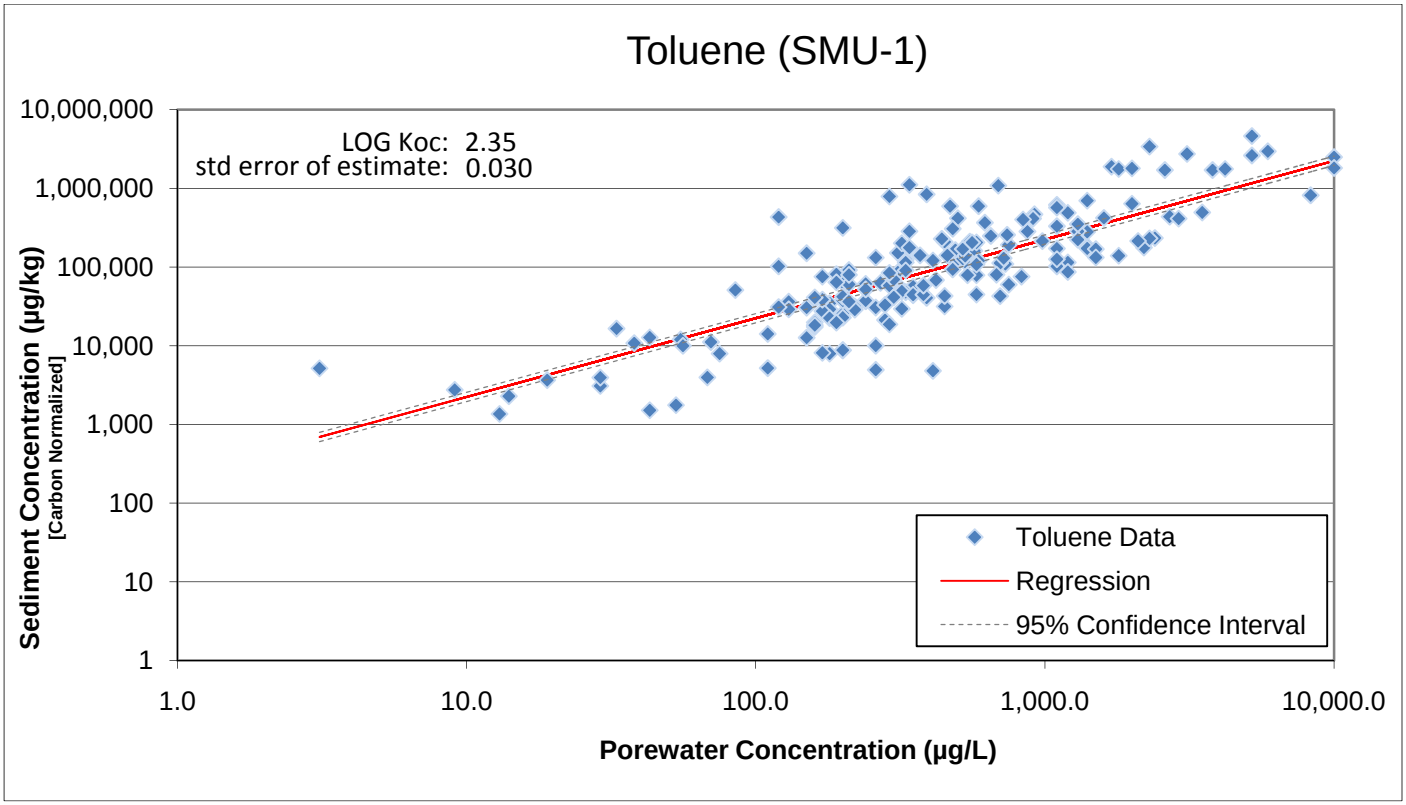

TOLUENE – Model Areas A & E

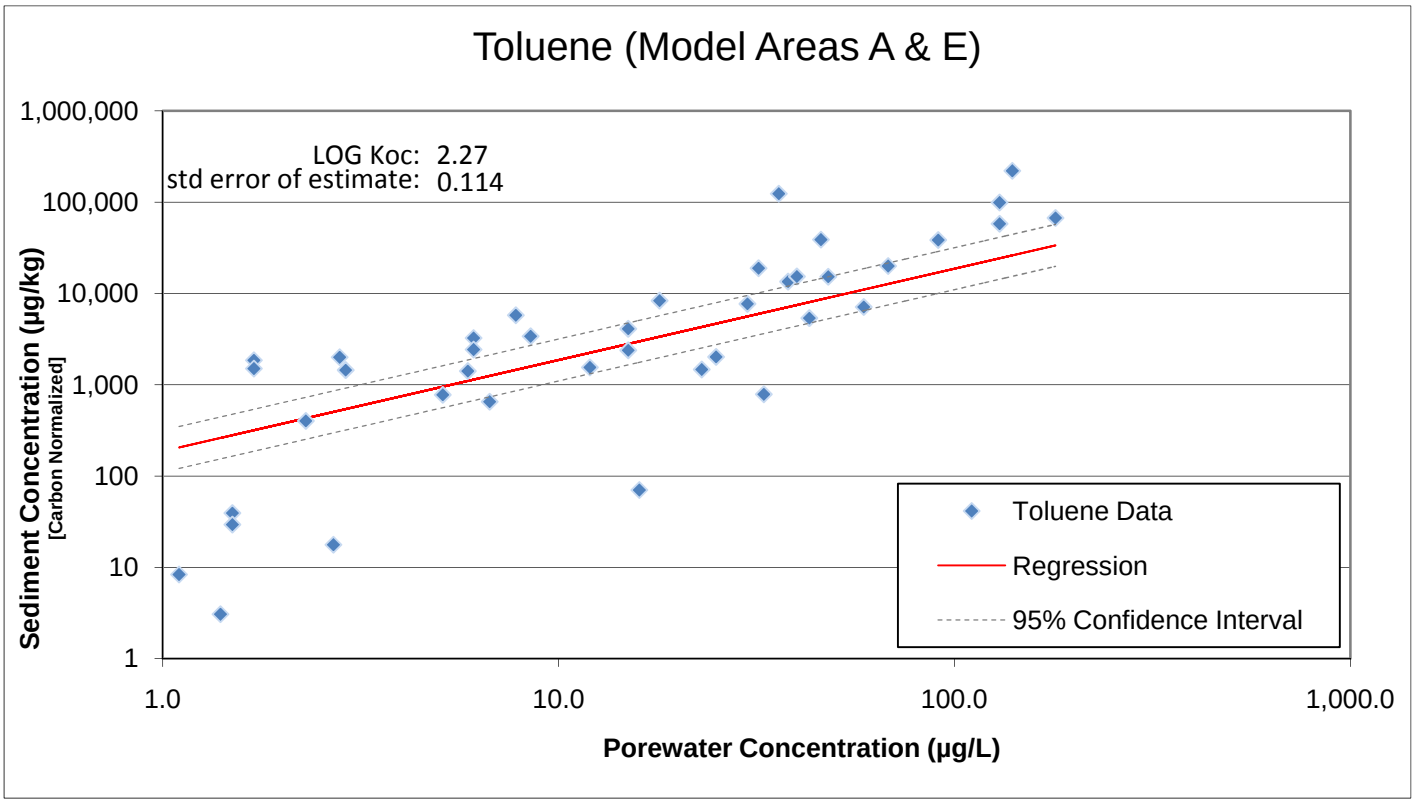

Figure 2. Relationship between *toluene* porewater concentration and carbon-normalized sediment concentration (with log-transformed regression).

ETHYLBENZENE – SMU-1

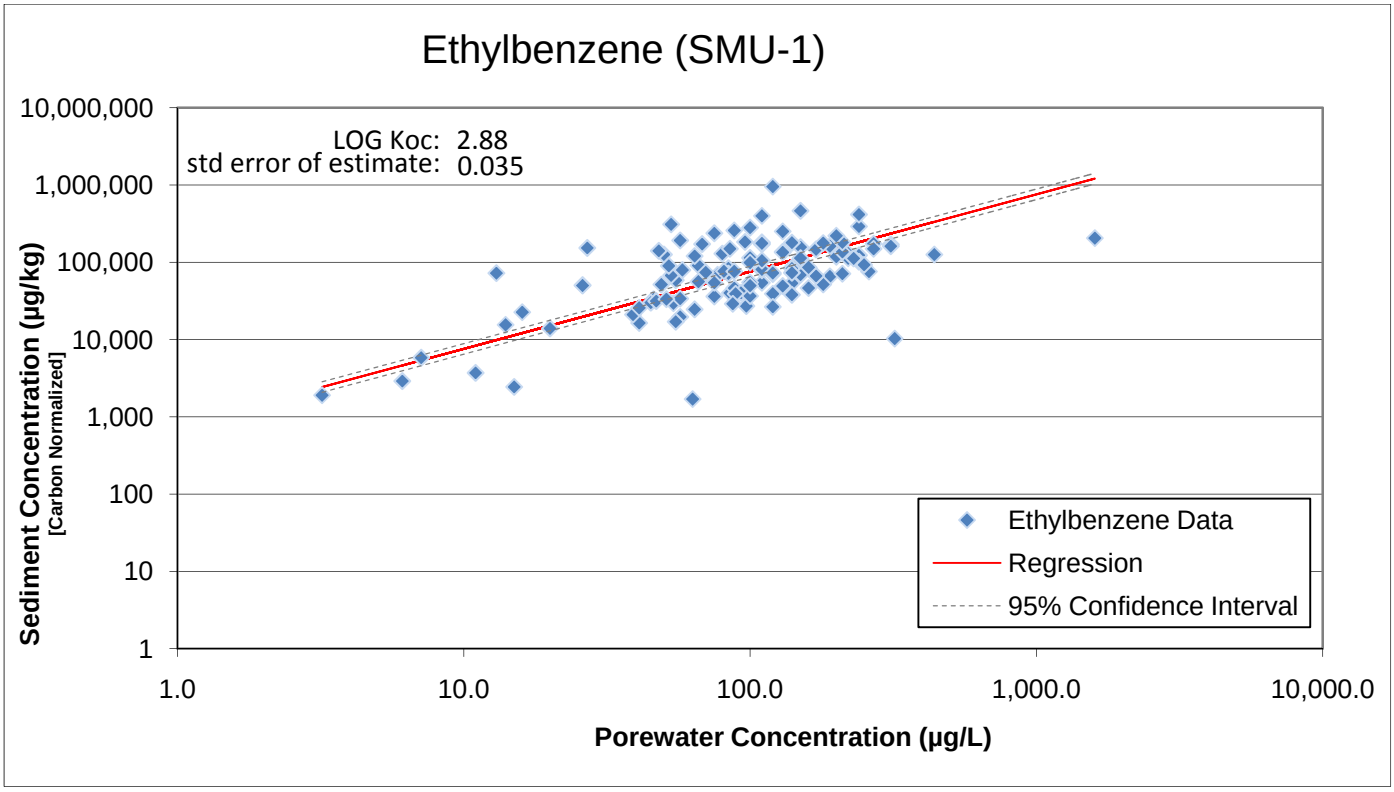

ETHYLBENZENE – Model Areas A & E

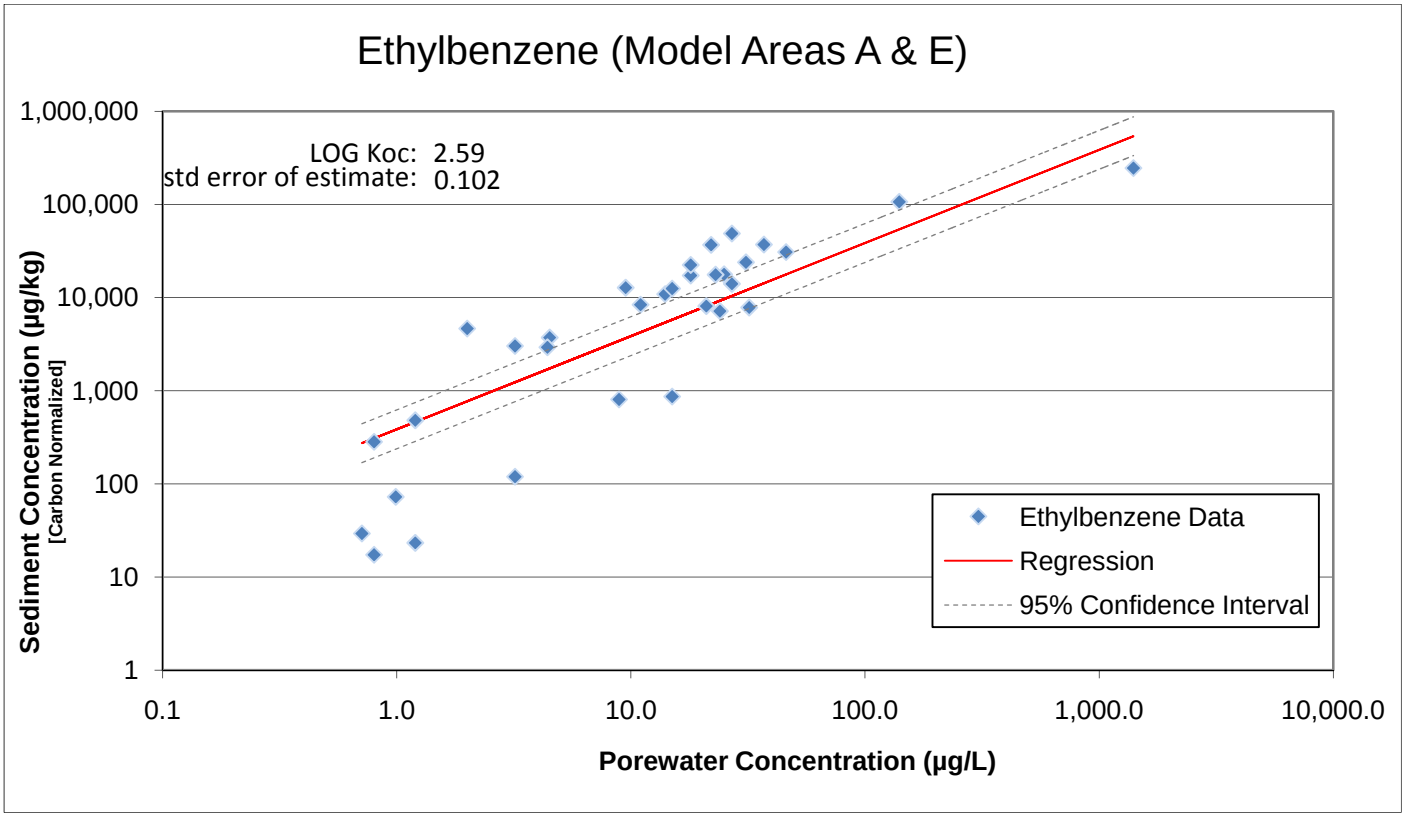

Figure 3. Relationship between *ethylbenzene* porewater concentration and carbon-normalized sediment concentration (with log-transformed regression).

XYLENE – SMU-1

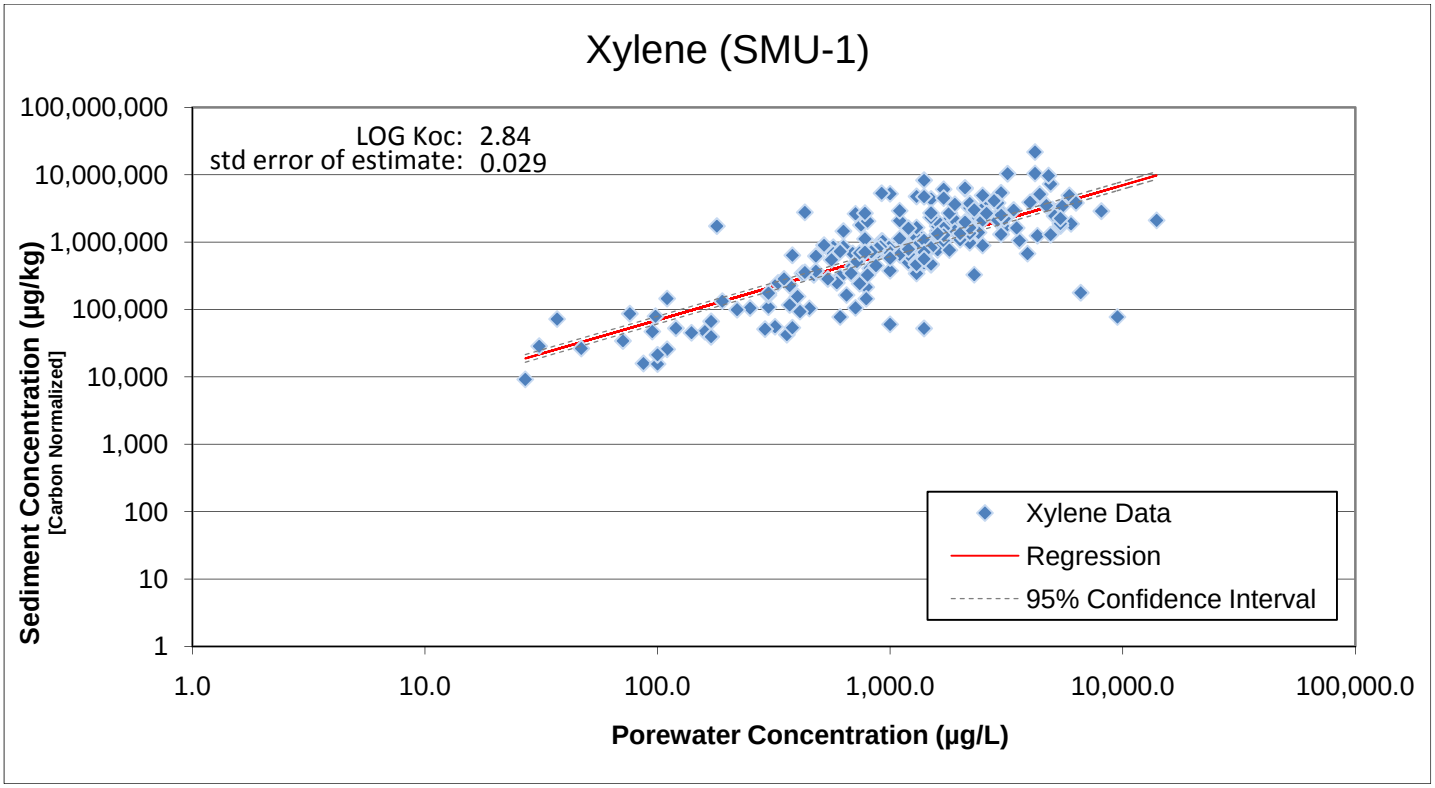

XYLENE – Model Areas A & E

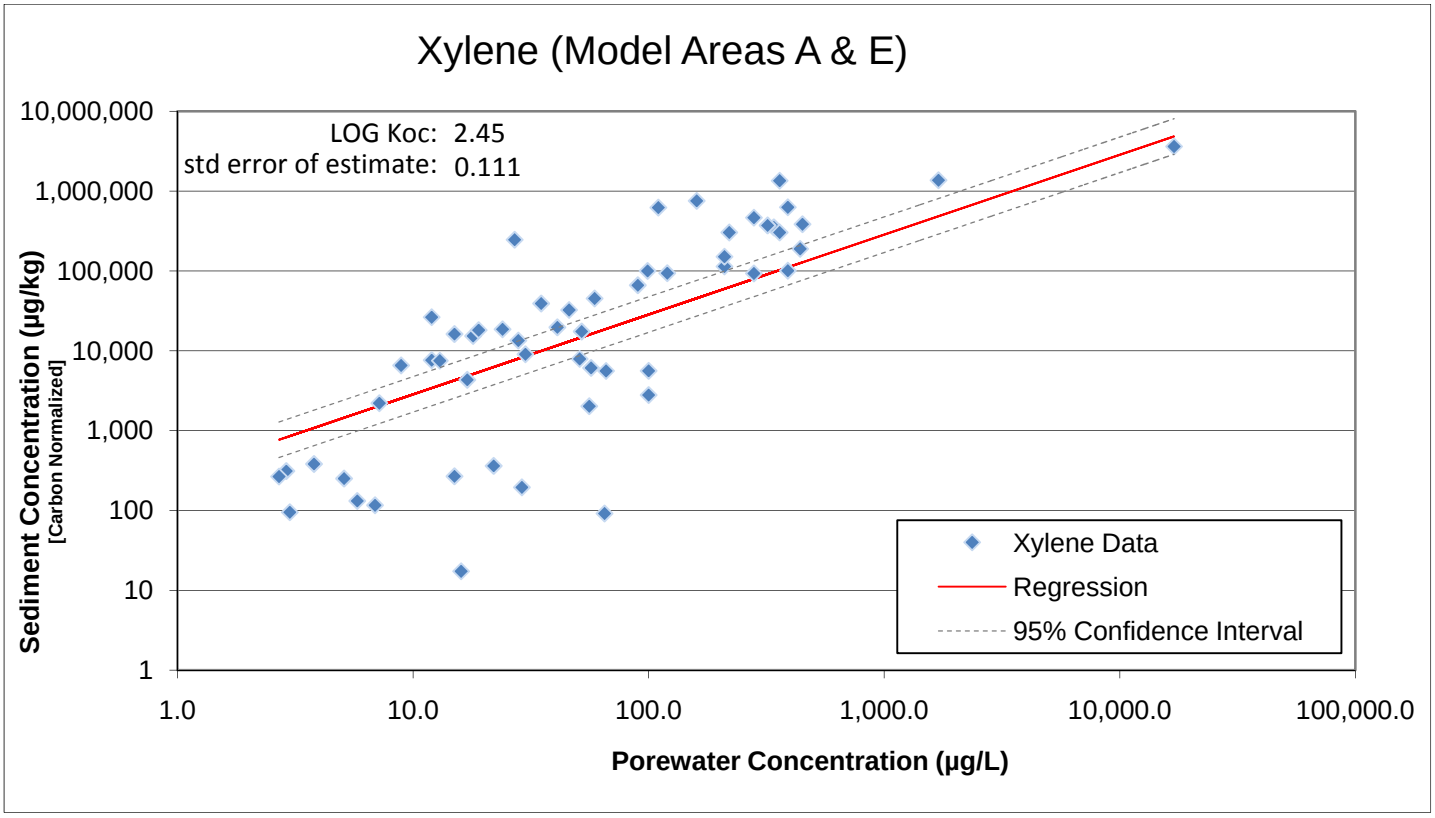

Figure 4. Relationship between *xylene* porewater concentration and carbon-normalized sediment concentration (with log-transformed regression).

CHLOROBENZENE – SMU-1

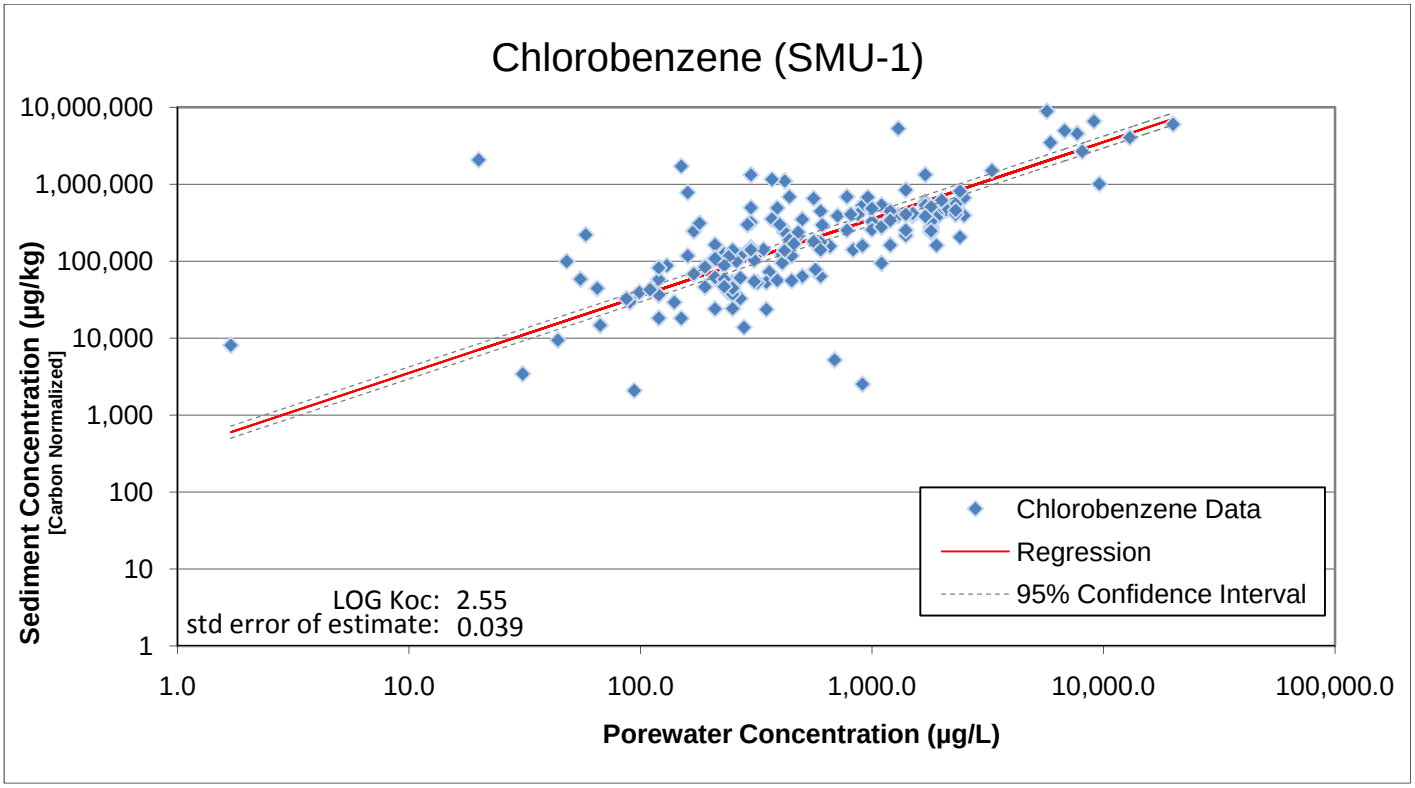

CHLOROBENZENE – Model Areas A & E

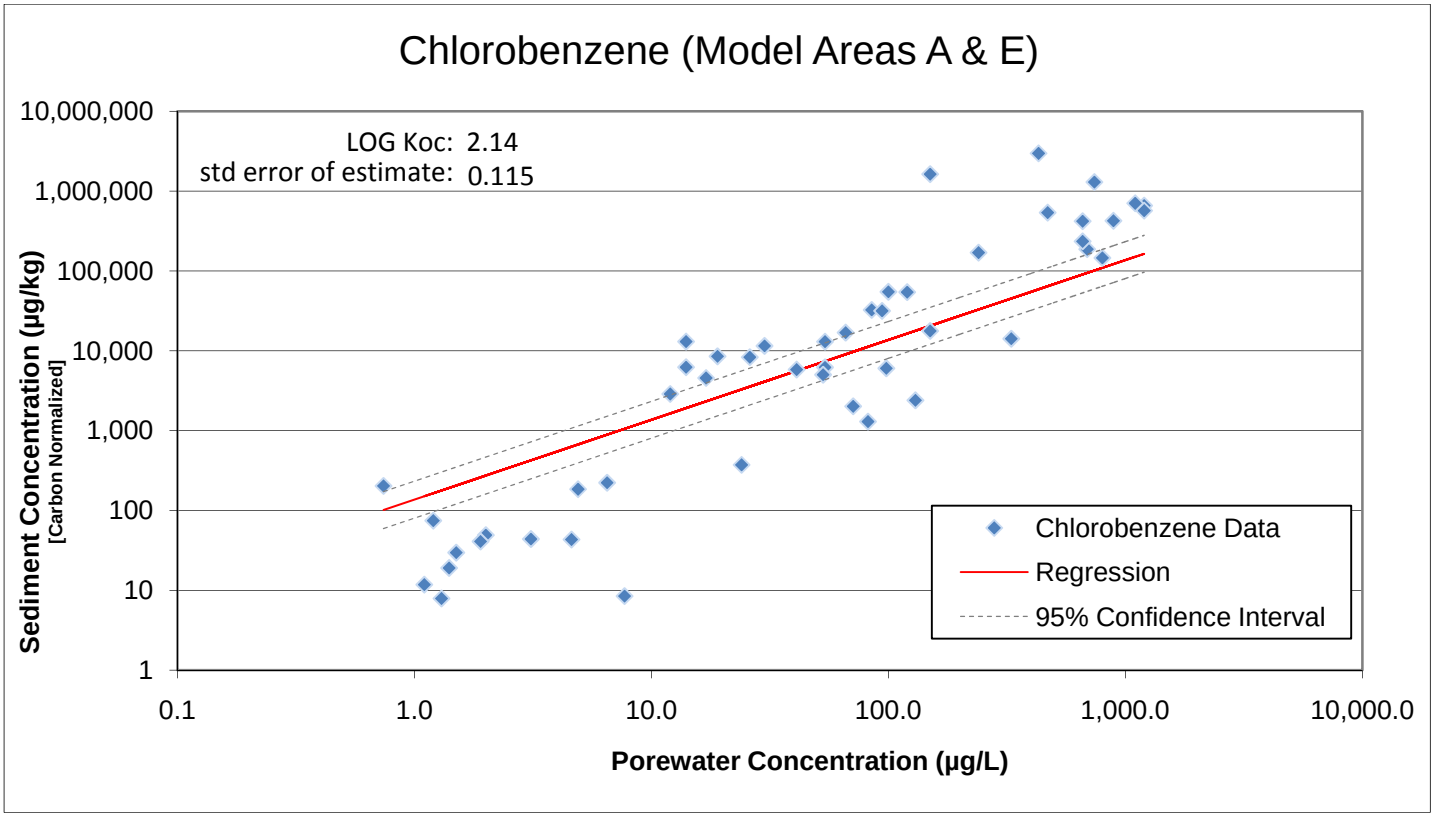

Figure 5. Relationship between *chlorobenzene* porewater concentration and carbon-normalized sediment concentration (with log-transformed regression).

1,2-DICHLOROBENZENE – SMU-1

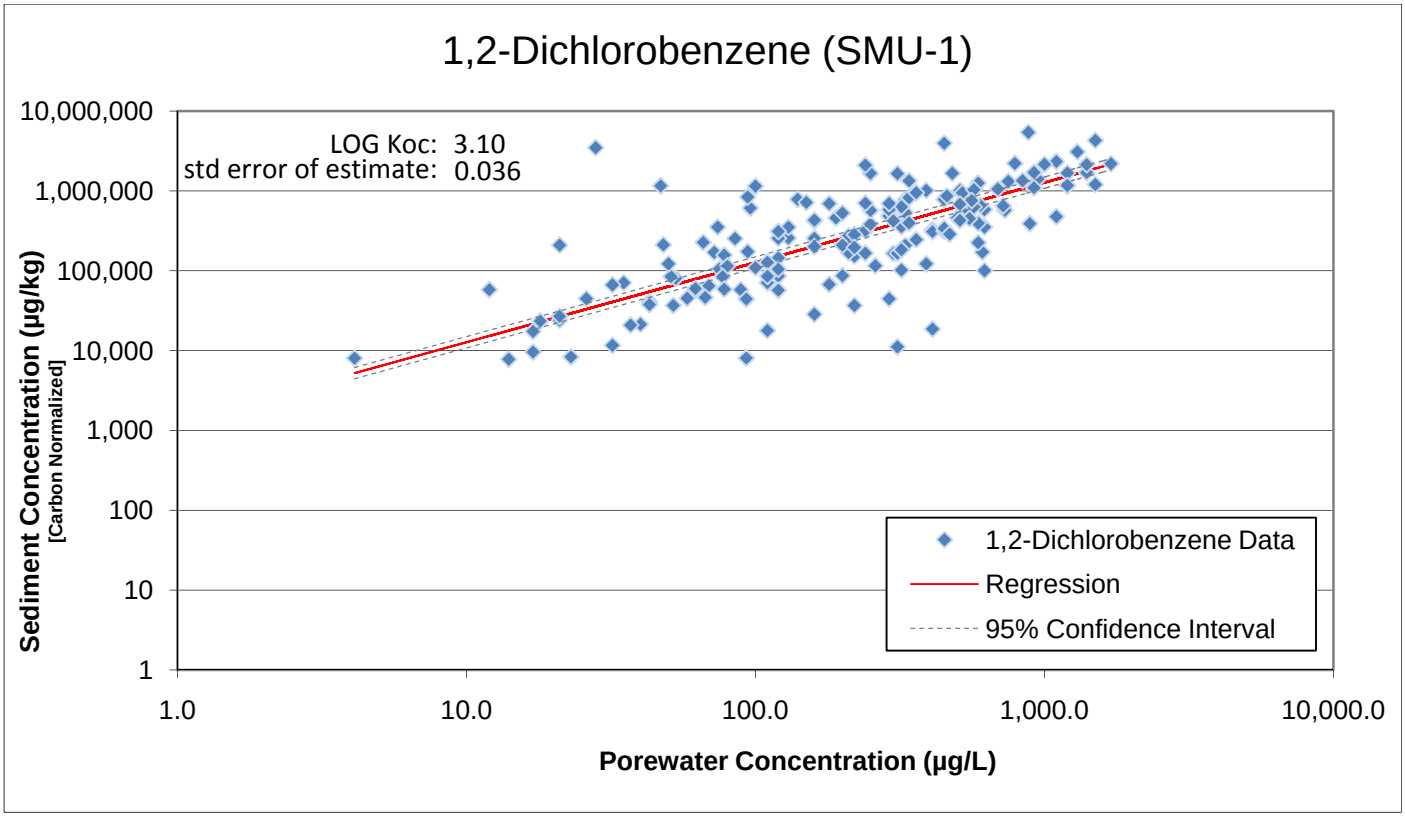

1,2-DICHLOROBENZENE – Model Areas A & E

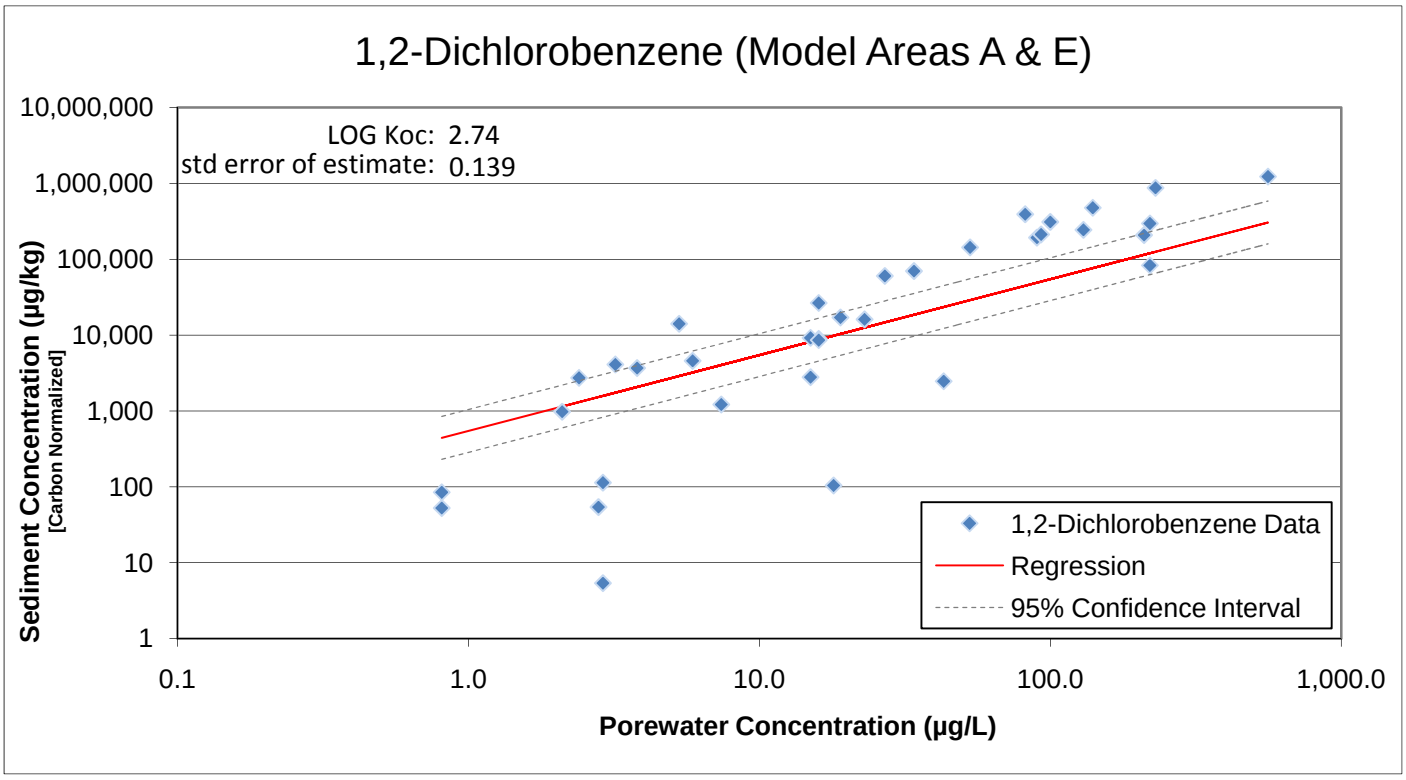

Figure 6. Relationship between *1,2-dichlorobenzene* porewater concentration and carbon-normalized sediment concentration (with log-transformed regression).

1,3-DICHLOROBENZENE – SMU-1

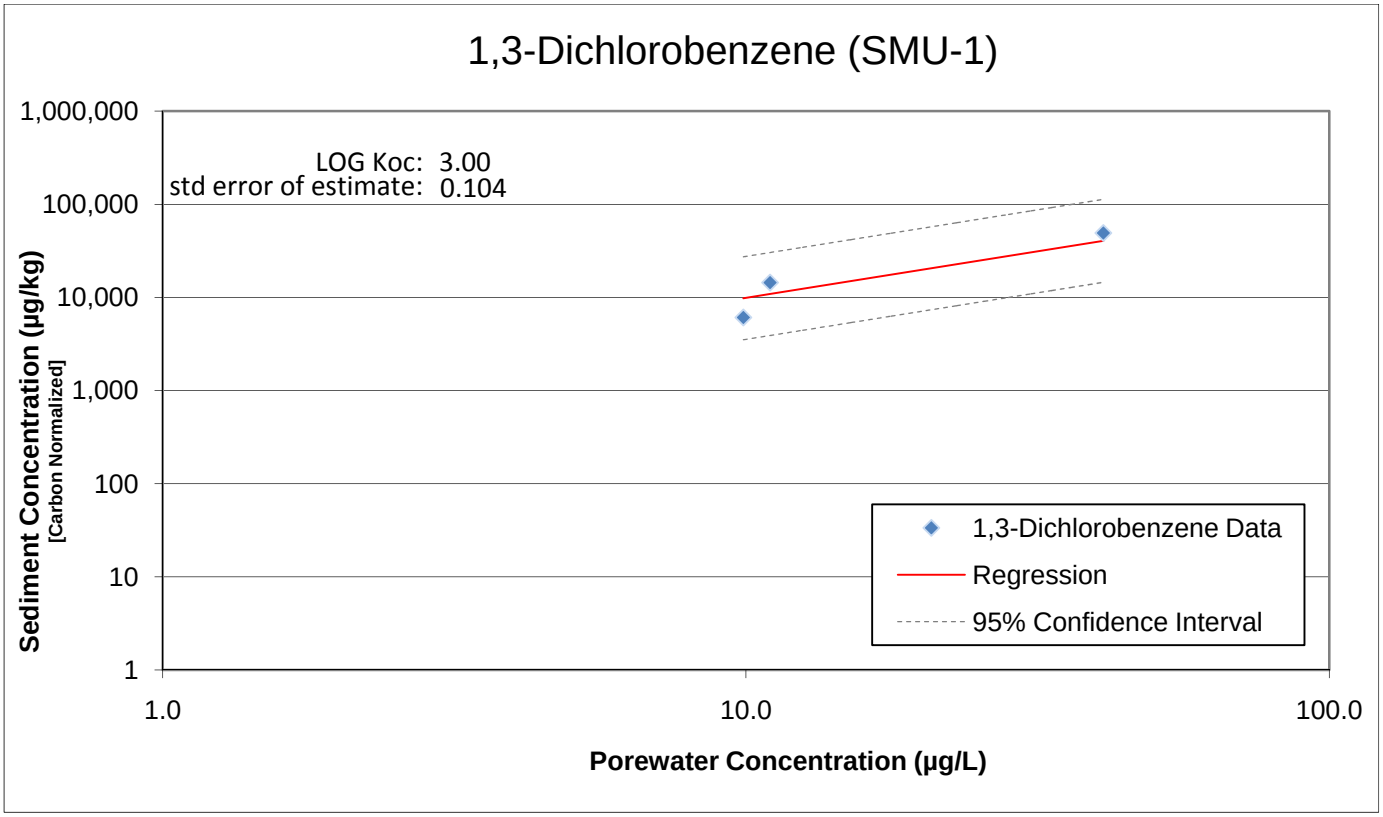

1,3-DICHLOROBENZENE – Model Areas A & E

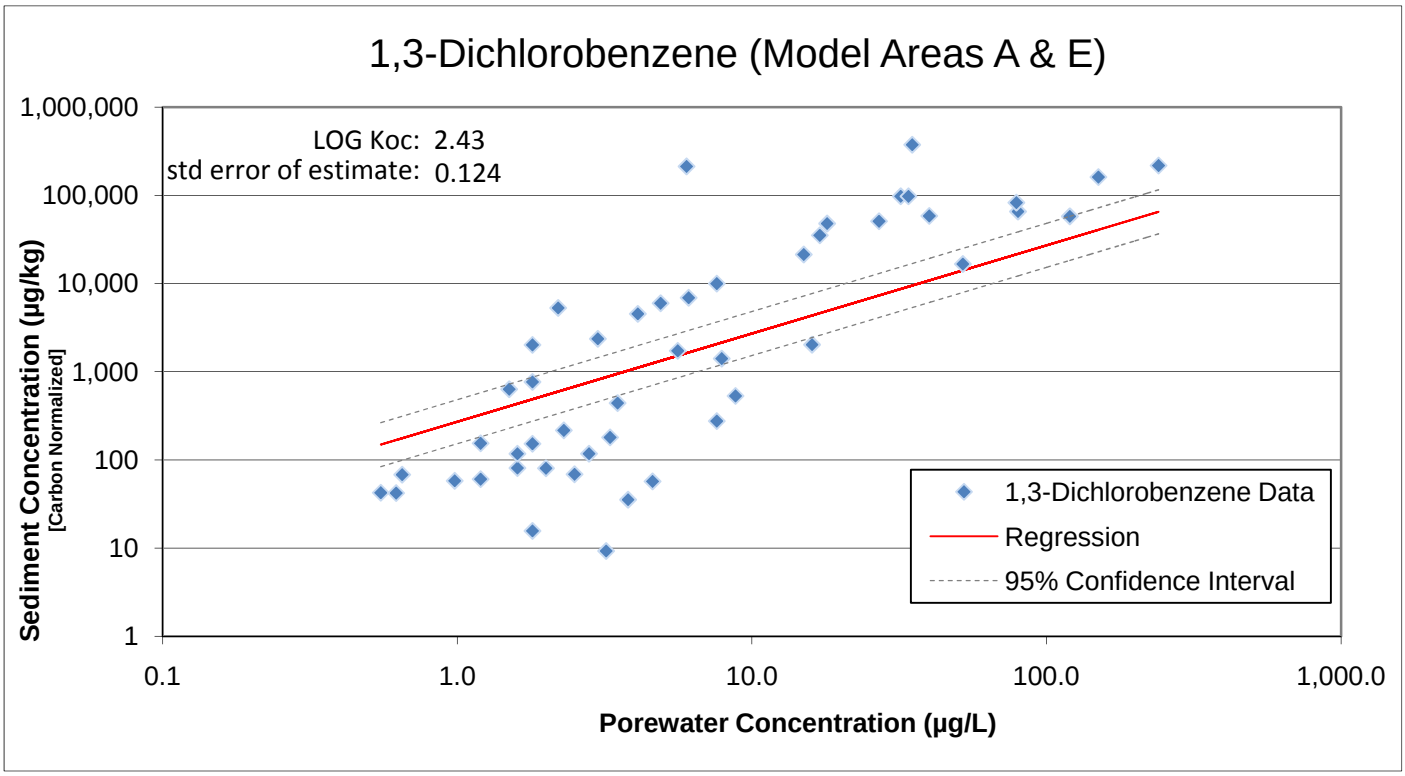

Figure 7. Relationship between *1,3-dichlorobenzene* porewater concentration and carbon-normalized sediment concentration (with log-transformed regression).

1,4-DICHLOROBENZENE – SMU-1

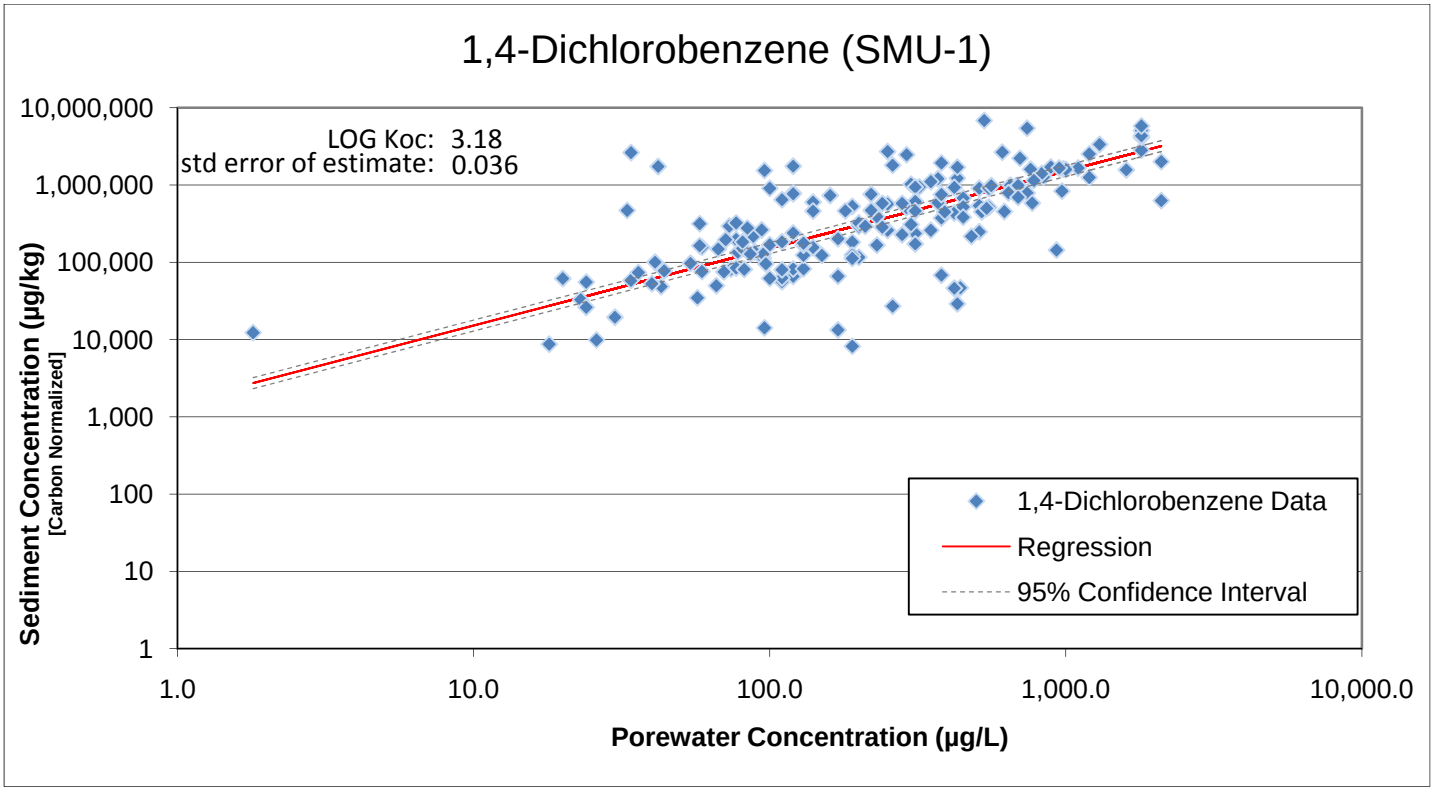

1,4-DICHLOROBENZENE – Model Areas A & E

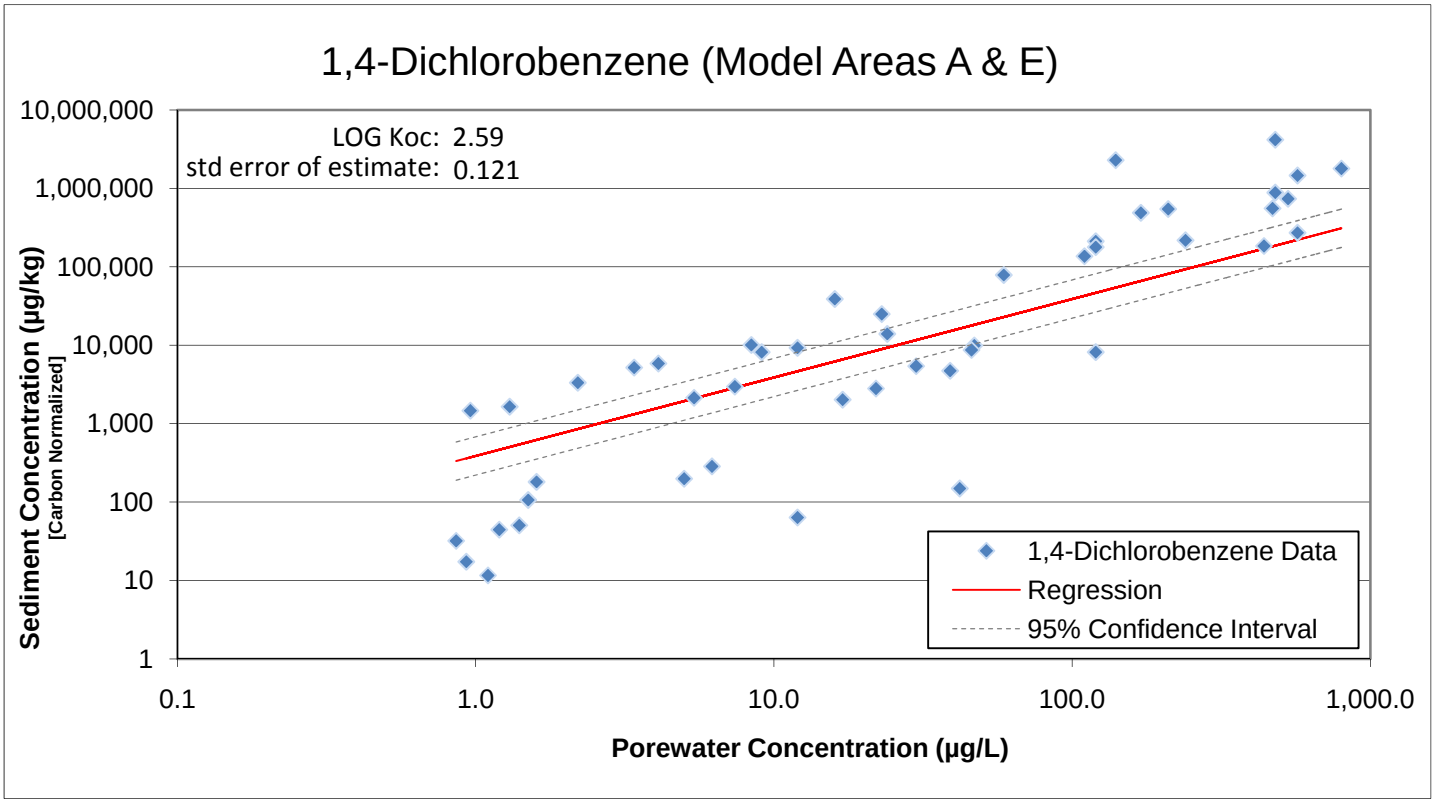

Figure 8. Relationship between *1,4-dichlorobenzene* porewater concentration and carbon-normalized sediment concentration (with log-transformed regression).

NAPHTHALENE – SMU-1

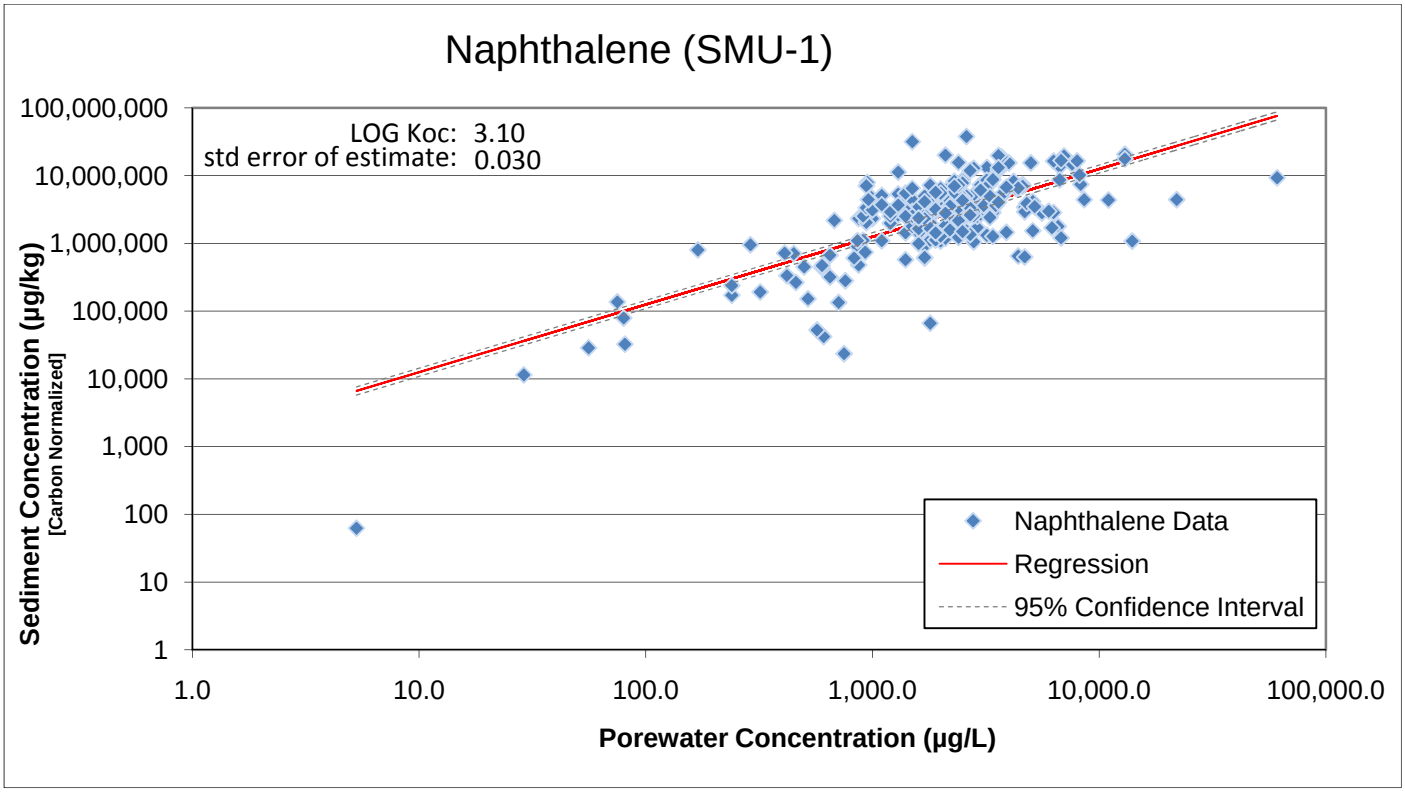

NAPHTHALENE – Model Areas A & E

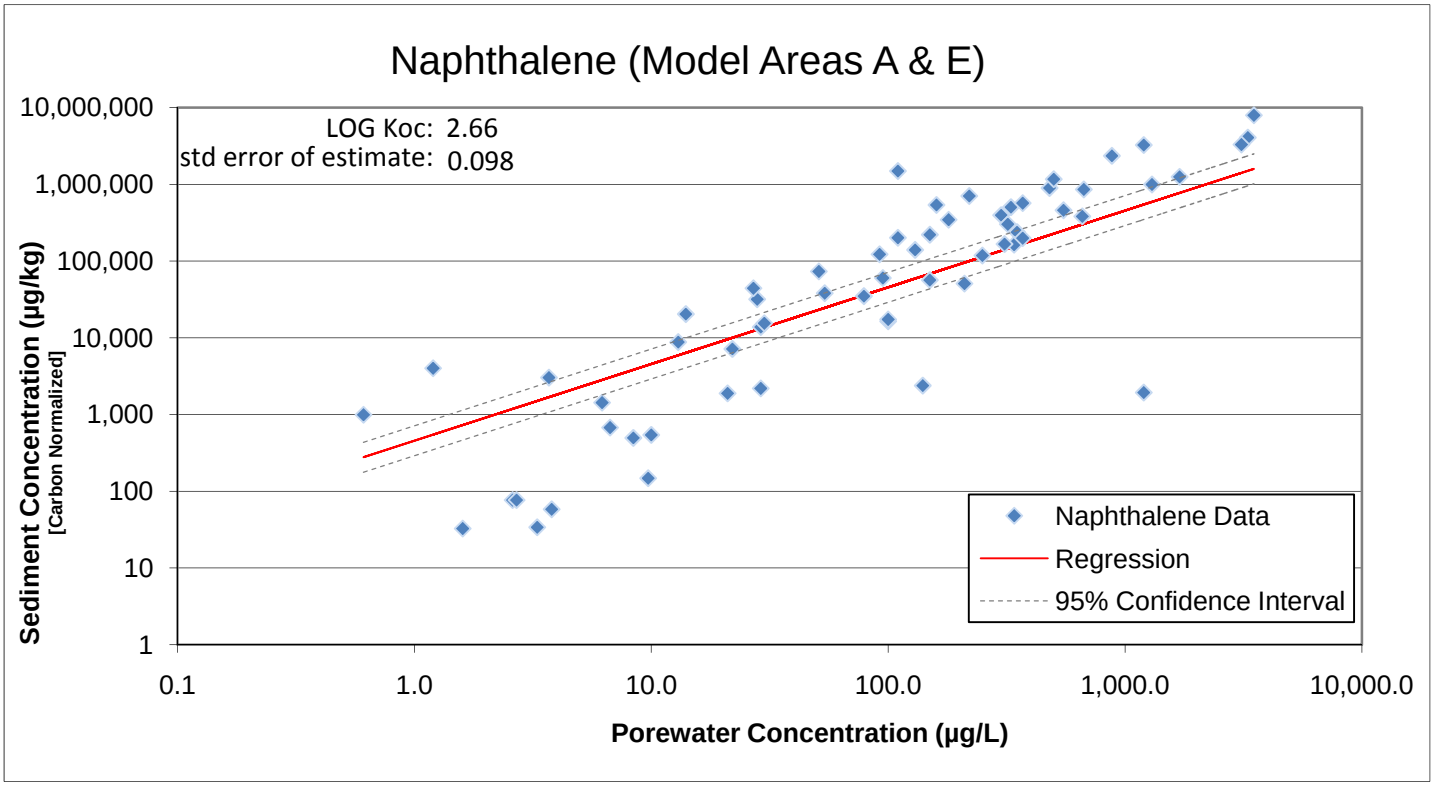

Figure 9. Relationship between *naphthalene* porewater concentration and carbon-normalized sediment concentration (with log-transformed regression).

ADDENDUM 1

Geosyntec consultants

130 Research Lane, Suite 2
Guelph, Ontario, Canada N1G 5G3
PH 519.822.2230
FAX 519.822.3151

TECHNICAL MEMORANDUM

Date: 09 December 2009

To: Edward Glaza – Parsons

Copies to: Caryn E. Kiehl-Simpson and John Nolan – Parsons

From: Tom Krug and David Himmelheber - Geosyntec Consultants
Danny Reible – University of Texas at Austin

Subject: Establishing Representative PAH Sediment-Porewater Partitioning Coefficients Within Sediments for Input into Transport Modeling, Onondaga Lake, Syracuse, New York

---

1. BACKGROUND AND SCOPE

This memorandum has been prepared by Geosyntec Consultants, Inc. (Geosyntec) to provide recommended values for effective sediment-porewater partitioning coefficients (K_{oc}) in lake sediments to be used to calculate sediment porewater concentrations. The values are intended to be incorporated into transport modeling at areas of Onondaga Lake, Syracuse, New York (the "Site") not impacted by in-lake waste deposits (ILWD) that are to be managed with an *in situ* sediment cap. A focused literature review of select datasets was performed to examine the phenomenon of porewater polycyclic aromatic hydrocarbon (PAH) and polychlorinated biphenyl (PCB) concentrations measured in actual sediment samples being lower than expected based upon conventional estimates derived from octanol-water distribution coefficients (K_{ow}) and bulk sediment concentration. Direct measurement of porewater concentrations of these compounds are unavailable, hence the need to make the best prediction of porewater concentration for the purposes of modeling.

One approach of estimating porewater concentrations of hydrophobic contaminants, such as PAHs and PCBs, in sediments has been to measure bulk sediment concentration (C_s), then assume linear partitioning into the aqueous phase (C_w) based on solid-liquid distribution coefficients (K_d). The distribution coefficient has been generalized as the product of the fraction organic carbon (f_{oc}) in the sediment and K_{oc}:

$$C_w = \frac{C_s}{K_d} = \frac{C_s}{K_{oc} \times f_{oc}} \quad (1)$$

While this approach does not account for mass held in the dissolved-phase associated with the sediment solids, the correction is extremely small for highly sorptive compounds such as PAH

and PCB. Therefore, pore water concentrations can be related to bulk sediment concentrations (which is based on mass in all phases) with negligible adjustment. Measured f_{oc} values are site-specific while K_{oc} values are chemical-specific and can either be determined experimentally or calculated based on chemical structure and/or properties (e.g., octanol-water partitioning coefficient [K_{ow}]). Note that K_{ow} values are physical constants of a particular compound but that values of K_{oc} are partially dependent upon the particular compound and are also influenced by environmental conditions (including factors such as the nature of the f_{oc}) and whether compounds are sorbing or desorbing. Modeling conducted to date has used K_{ow} values reported in New York State Department of Environmental Conservation Guidance (NYSDEC, 1999) as estimates of K_{oc} and measured f_{oc} values to estimate the concentrations of PAHs and PCBs in sediment porewater beneath the cap. A growing body of literature indicates that this conventional approach of calculating PAH and PCB porewater concentrations in sediments will overestimate actual PAH or PCB porewater concentrations (for discussions see Arp et al., 2009; Hawthorne et al., 2006; and McGroddy et al., 1996). The primary cause of this discrepancy is that natural sediments are composed of different types of organic carbon, with some phases of organic carbon ("hard" carbon) sorbing hydrophobic contaminants stronger but more slowly than other phases ("soft" carbon). An illustration of how different forms of carbon present in sediments results in different effective K_{oc} values for phenanthrene was compiled by Ghosh et al. (2003) and reproduced in this document as Figure 1. As a result, when PAHs or PCBs are introduced into sediments, a portion of the contaminant is sorbed strongly to the "hard" carbon component of organic matter and effectively resistant to desorption. This desorption-resistance is not inherently incorporated into the conventional K_{oc} x f_{oc} approach of estimating porewater concentrations since compilations of K_{oc} are often based upon short-term sorption experiments in the laboratory or equivalent correlations with K_{ow}. This discrepancy ultimately leads to lower field measurement of porewater PAH concentrations than are predicted by literature K_{oc} values.

A more realistic approach to modeling PAH and PCB transport within sediments is to use measured f_{oc} values and field-derived effective K_{oc} values measured in natural sediment that account for strongly-sorbing fractions of sediment. A compilation of field-derived effective K_{oc} values from several literature sources has been performed.

2. COMPILATION OF DATASETS COMPARING MEASURED PAH POREWATER CONCENTRATIONS WITH ESTIMATED POREWATER CONCENTRATIONS

Figures 2 and 3 present graphs plotting K_{ow} values for PAHs versus field-derived effective K_{oc} values. PAHs included in the analysis are listed in Table 1. Plotted K_{ow} values were obtained from the NYSDEC Guidance Document (1999) for all but three PAH compounds (acenaphthylene, benzo[ghi]perylene, and dibenz[a,h]anthracene) whose K_{ow} values were obtained from Syracuse Research Corporation's (SRC) KowWIN database. The K_{ow} values utilized in this assessment are the same values being employed for modeling efforts to date. The data utilized for the field-derived observed K_{oc} values were actual porewater sampling and

analysis, providing an accurate measurement of aqueous phase PAH concentrations (Arp et al., 2009). Figure 2 contains the compilation of all sediment site data compiled and Figure 3 contains data from sites with freshwater and brackish conditions (i.e., excluding marine sediments).

The K_{ow} values consistently underestimate observed effective K_{oc} values and thus overestimate PAH porewater concentrations associated with sediment containing a known concentration of PAH compared with the field-derived values. On average, the field-derived PAH K_{oc} values are greater than the K_{ow} values currently utilized in modeling efforts by 1.07 ± 0.14 log units (average ± 95% confidence interval) when examining all the data, and 1.05 ± 0.15 when considering just freshwater and brackish sediment sites. Figures 2 and 3 indicate that adjusting the log K_{ow} values currently employed in modeling efforts by one log unit, or a factor of 10, closely approximates the statistical best-fit lines in both Figures 2 and 3 and falls within the 95% confidence bands of each respective regression line.

3. COMPILATION OF DATASETS COMPARING MEASURED PCB POREWATER CONCENTRATIONS WITH ESTIMATED POREWATER CONCENTRATIONS

Figures 4 and 5 presents graphs of K_{ow} values for PCBs versus field-derived effective K_{oc} values from Arp et al 2009. PCBs included in the analysis are presented in Table 2. Plotted K_{ow} values in Figures 4 and 5 were obtained from the Hawker et al 1988 and Lu et al 2007 respectively.

The K_{ow} values consistently underestimate observed effective K_{oc} values and thus overestimate PCB porewater concentrations associated with sediment containing a known concentration of PCB compared with the field-derived values. On average, the field-derived PCB K_{oc} values are greater than the literature K_{ow} values by a factor of five. Figures 4 and 5 indicate that adjusting the K_{ow} values currently employed in modeling efforts by a factor of five, closely approximates the statistical best-fit lines in both Figures 4 and 5 and falls within the 95% confidence bands of each respective regression line.

4. RECOMMENDATIONS

The literature review described above and relevant experience at other sediment sites supports the use of corrected PAH and PCB K_{oc} values to most accurately model and predict porewater PAH and PCB concentrations within the Onondaga Lake sediment in the absence of direct measurements. Based on the data presented in Figures 2 and 3 an increase in effective K_{oc} values of 10 from PAH K_{ow} values is recommended for derivation of PAH porewater concentrations in the non-ILWD impacted sediments at this time. Based on the data presented in Figures 4 and 5 an increase in effective K_{oc} values of 5 from PCB K_{ow} values is recommended for derivation of PCB porewater concentrations in the non-ILWD impacted sediments.

5. REFERENCES

Arp, H.P.H., Breedveld, G.D., and Cornelissen, G., 2009. Estimating the in situ sediment-porewater distribution of PAHs and chlorinated aromatic hydrocarbons in anthropogenic impacted sediments. *Environ. Sci. Technol.. 43*, 5576–5585.

Cornelissen, G., Gustafsson, O., Bucheli, T. D., Jonker, M. T. O., Koelmans, A. A., and VanNoort, P. C.M., 2005. Extensive sorption of organic compounds to black carbon, coal, and kerogen in sediments and soils: Mechanisms and consequences for distribution, bioaccumulation, and biodegradation. *Environ. Sci. Technol., 39* (18), 6881–6895.

Ghosh, U., Zimmerman, J.R., and Luthy, R.G., 2003. PCB and PAH speciation among particle types in contaminated harbor sediments and effects on PAH bioavailability. *Environ. Sci. Technol.*, *37*, 2209–2217.

Hawker, D.W., and Connell, D.W., 1988. Octanol-water partition coefficients of polychlorinated biphenyls congeners. *Environ. Sci. Technol*., 22:382-385.

Hawthorne, S.B., Grabanski, C.B., and Miller, D.J., 2006. Measured partitioning coefficients for parent and alkyl polycyclic aromatic hydrocarbons in 114 historically contaminated sediments: Part 1. K_{oc} values. *Environ. Toxicol. Chem.*, *25* (11), 2901-2911.

Lohmann, R., MacFarlane, J. K., and Gschwend, P. M., 2005. Importance of black carbon to sorption of native PAHs, PCBs, and PCDDs in Boston and New York Harbor sediments. *Environ. Sci. Technol., 39* (1), 141–148.

Lu, X., Reible, D.D., and Fleeger, J.W., 2006. Bioavailability of polycyclic aromatic hydrocarbons in field-contaminated Anacostia River (Washington, DC) sediment. *Environ. Toxicol. Chem., 25,* (11), 2869-2874.

Lu, W., Chen, Y., Liu, M., Chen, X. and Hu, Z., 2007. QSPR prediction of n-octonal/water partitioning coefficient for polychlorinated biphenyls. *Chemosphere,* 69 (2007), 469-478.

McGroddy, S. E., Farrington, J. W., and Gschwend, P. M., 1996. Comparison of the in situ and desorption sediment-water partitioning of polycyclic aromatic hydrocarbons and polychlorinated biphenyls. *Environ. Sci. Technol., 30* (1), 172–177.

New York State Department of Environmental Conservation (NYSDEC), 1999. Technical Guidance for Screening Contaminated Sediments. Division of Fish, Wildlife and Marine Resources.

Table 1 - Literature Values for Kow and Koc for Polycyclic Aromatic Hydrocarbons

Data Source in Arp et al, 2009	**CAS #**	**Compound**	**Average Log Koc** Arp et al, 2009	**Log Kow** NYSDEC, 1999	**Log Kow** SRC
7	208-96-8	Acenaphthylene	5.11	ns	3.94
9	208-96-8	Acenaphthylene	4.48	ns	3.94
10	208-96-8	Acenaphthylene	4.47	ns	3.94
4	120-12-7	Anthracene	6.24	4.45	
6	120-12-7	Anthracene	6.08	4.45	
7	120-12-7	Anthracene	5.75	4.45	
9	120-12-7	Anthracene	5.41	4.45	
14	120-12-7	Anthracene	6.61	4.45	
15	120-12-7	Anthracene	5.26	4.45	
1	56-55-3	Benz[a]anthracene	7.14	5.61	
4	56-55-3	Benz[a]anthracene	7.38	5.61	
6	56-55-3	Benz[a]anthracene	6.77	5.61	
7	56-55-3	Benz[a]anthracene	6.55	5.61	
8	56-55-3	Benz[a]anthracene	6.95	5.61	
9	56-55-3	Benz[a]anthracene	6.45	5.61	
14	56-55-3	Benz[a]anthracene	7.81	5.61	
6	50-32-8	Benzo(a)pyrene	7.03	6.04	
1	50-32-8	Benzo[a]pyrene	7.77	6.04	
4	50-32-8	Benzo[a]pyrene	8.37	6.04	
7	50-32-8	Benzo[a]pyrene	6.68	6.04	
8	50-32-8	Benzo[a]pyrene	7.96	6.04	
9	50-32-8	Benzo[a]pyrene	6.85	6.04	
11	50-32-8	Benzo[a]pyrene	7.25	6.04	
12	50-32-8	Benzo[a]pyrene	6.79	6.04	
13	50-32-8	Benzo[a]pyrene	6.15	6.04	
14	50-32-8	Benzo[a]pyrene	7.81	6.04	
4	205-99-2	Benzo[b]fluoranthene	7.99	6.04	
6	205-99-2	Benzo[b]fluoranthene	7.06	6.04	
8	205-99-2	Benzo[b]fluoranthene	7.42	6.04	
9	205-99-2	Benzo[b]fluoranthene	6.91	6.04	
15	205-99-2	Benzo[b]fluoranthene	6.59	6.04	
1	191-24-2	Benzo[ghi]perylene	8.25	ns	6.70
4	191-24-2	Benzo[ghi]perylene	9.01	ns	6.70
6	191-24-2	Benzo[ghi]perylene	7.58	ns	6.70
7	191-24-2	Benzo[ghi]perylene	7.13	ns	6.70
8	191-24-2	Benzo[ghi]perylene	7.84	ns	6.70
9	191-24-2	Benzo[ghi]perylene	6.94	ns	6.70
14	191-24-2	Benzo[ghi]perylene	8.91	ns	6.70
15	191-24-2	Benzo[ghi]perylene	6.67	ns	6.70
4	207-08-9	Benzo[k]fluoranthene	8.16	6.04	
6	207-08-9	Benzo[k]fluoranthene	7.25	6.04	
8	207-08-9	Benzo[k]fluoranthene	7.41	6.04	
9	207-08-9	Benzo[k]fluoranthene	6.90	6.04	
12	207-08-9	Benzo[k]fluoranthene	6.74	6.04	
15	207-08-9	Benzo[k]fluoranthene	6.41	6.04	

notes:

ns - not specified

Table 1 - Literature Values for Kow and Koc for Polycyclic Aromatic Hydrocarbons

Data Source in Arp et al, 2009	CAS #	Compound	Average Log Koc Arp et al, 2009	Log Kow NYSDEC, 1999	Log Kow SRC
4	53-70-3	Dibenz[a,h]anthracene	8.06	ns	6.70
6	53-70-3	Dibenz[a,h]anthracene	7.62	ns	6.70
7	53-70-3	Dibenz[a,h]anthracene	6.82	ns	6.70
9	53-70-3	Dibenz[a,h]anthracene	6.88	ns	6.70
6	206-44-0	Fluorantene	6.25	5.19	
1	206-44-0	Fluoranthene	6.26	5.19	
4	206-44-0	Fluoranthene	6.37	5.19	
7	206-44-0	Fluoranthene	5.79	5.19	
8	206-44-0	Fluoranthene	6.04	5.19	
9	206-44-0	Fluoranthene	5.89	5.19	
13	206-44-0	Fluoranthene	6.43	5.19	
14	206-44-0	Fluoranthene	7.41	5.19	
15	206-44-0	Fluoranthene	6.15	5.19	
16	206-44-0	Fluoranthene	6.34	5.19	
7	86-73-7	Fluorene	4.71	4.18	
9	86-73-7	Fluorene	4.65	4.18	
10	86-73-7	Fluorene	4.17	4.18	
15	86-73-7	Fluorene	4.69	4.18	
16	86-73-7	Fluorene	6.49	4.18	
7	91-57-6	2-Methylnaphthalene	4.56	3.86	
16	91-57-6	2-Methylnaphthalene	7.03	3.86	
7	91-20-3	Naphthalene	4.26	3.37	
9	91-20-3	Naphthalene	3.39	3.37	
10	91-20-3	Naphthalene	3.14	3.37	
1	85-01-8	Phenanthrene	5.87	4.45	
4	85-01-8	Phenanthrene	6.15	4.45	
6	85-01-8	Phenanthrene	5.83	4.45	
7	85-01-8	Phenanthrene	5.20	4.45	
8	85-01-8	Phenanthrene	5.70	4.45	
8	85-01-8	Phenanthrene	5.70	4.45	
9	85-01-8	Phenanthrene	5.30	4.45	
10	85-01-8	Phenanthrene	5.03	4.45	
11	85-01-8	Phenanthrene	5.25	4.45	
12	85-01-8	Phenanthrene	4.76	4.45	
13	85-01-8	Phenanthrene	6.50	4.45	
14	85-01-8	Phenanthrene	6.91	4.45	
15	85-01-8	Phenanthrene	4.99	4.45	
16	85-01-8	Phenanthrene	6.59	4.45	
4	129-00-0	Pyrene	6.38	5.32	
6	129-00-0	Pyrene	5.86	5.32	
7	129-00-0	Pyrene	5.82	5.32	
8	129-00-0	Pyrene	6.05	5.32	
9	129-00-0	Pyrene	5.97	5.32	
10	129-00-0	Pyrene	5.08	5.32	
11	129-00-0	Pyrene	5.90	5.32	
12	129-00-0	Pyrene	5.43	5.32	
13	129-00-0	Pyrene	6.06	5.32	
14	129-00-0	Pyrene	6.71	5.32	
15	129-00-0	Pyrene	5.75	5.32	
16	129-00-0	Pyrene	6.80	5.32	

notes:

ns - not specified

Table 2 - Literature Values for Kow and Koc of PCB Congeners

PCB Congener	Log Kow Hawker et al 1988	Log Kow Lu et al 2007	Ave Log Koc Arp et al 2009
PCB-18	5.24	5.33	5.94
PCB-18	5.24	5.33	5.54
PCB-28	5.67	5.71	6.25
PCB-28	5.67	5.71	6.44
PCB-28	5.67	5.71	7.18
PCB-28	5.67	5.71	6.28
PCB-31	5.67	5.68	6.99
PCB-44	5.75	5.73	6.48
PCB-44	5.75	5.73	5.9
PCB-52	5.84	5.79	6.46
PCB-52	5.84	5.79	6.7
PCB-52	5.84	5.79	7.01
PCB-52	5.84	5.79	6.51
PCB-52	5.84	5.79	6.03
PCB-66	6.2	5.98	6.8
PCB-72	6.26	na	6.01
PCB-77	6.36	na	7.32
PCB-77	6.36	na	6.86
PCB-81	6.36	na	7.38
PCB-95	6.13	5.92	6.35
PCB-101	6.38	na	6.56
PCB-101	6.38	na	7.54
PCB-101	6.38	na	7.71
PCB-101	6.38	na	6.95
PCB-101	6.38	na	6.55
PCB-105	6.65	6.79	8.06
PCB-105	6.65	6.79	7.51

PCB Congener	Log Kow Hawker et al 1988	Log Kow Lu et al 2007	Ave Log Koc Arp et al 2009
PCB-118	6.74	6.57	6.83
PCB-118	6.74	6.57	8.02
PCB-118	6.74	6.57	7.58
PCB-118	6.74	6.57	6.85
PCB-118	6.74	6.57	6.86
PCB-126	6.89	na	7.7
PCB-138	6.83	6.73	8.19
PCB-138	6.83	6.73	8.25
PCB-138	6.83	6.73	7.55
PCB-138	6.83	6.73	7.15
PCB-153	6.92	6.8	8.33
PCB-153	6.92	6.8	8.32
PCB-153	6.92	6.8	7.46
PCB-153	6.92	6.8	7.01
PCB-156	7.18	7.44	8.13
PCB-156	7.18	7.44	7.82
PCB-156	7.18	7.44	7.38
PCB-167	7.27	7.29	7.94
PCB-169	7.42	7.55	7.96
PCB-170	7.27	7.08	8
PCB-180	7.36	7.21	7.35
PCB-180	7.36	7.21	8.31
PCB-180	7.36	7.21	8.3
PCB-180	7.36	7.21	7.86
PCB-187	7.17	6.99	7.79
PCB-195	7.56	7.35	7.85
PCB-204	7.3	7.48	8.24

Figure 1 - Phenanthrene K_{oc} values for different types of organic carbon.
Reproduced from Ghosh et al., 2003.

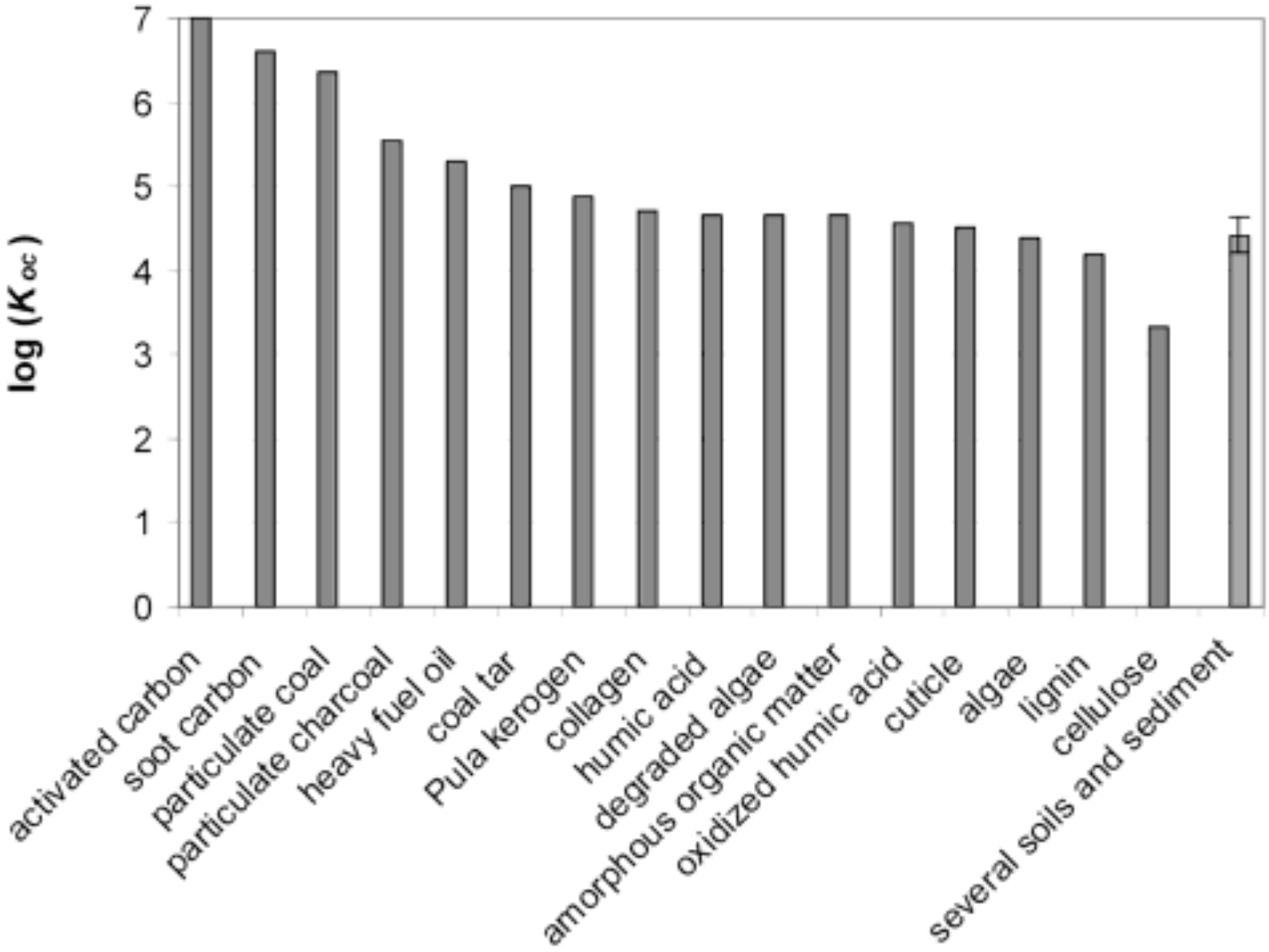

Figure 2 - Log K_{ow} versus Observed K_{oc} All Sediment Site Data

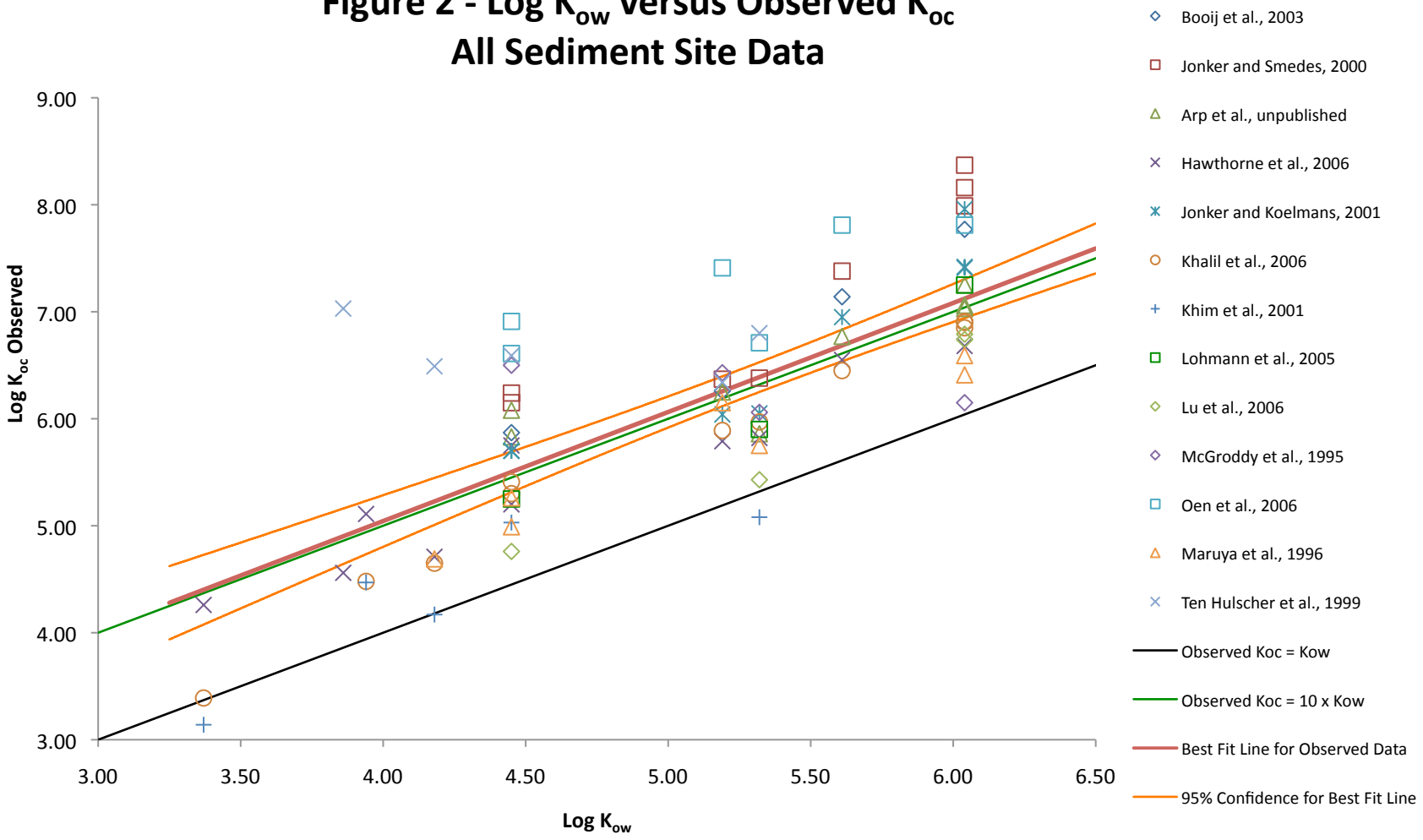

Figure 3 - Log K_{ow} versus Observed K_{oc}
Freshwater to Brackish Sediment Sites

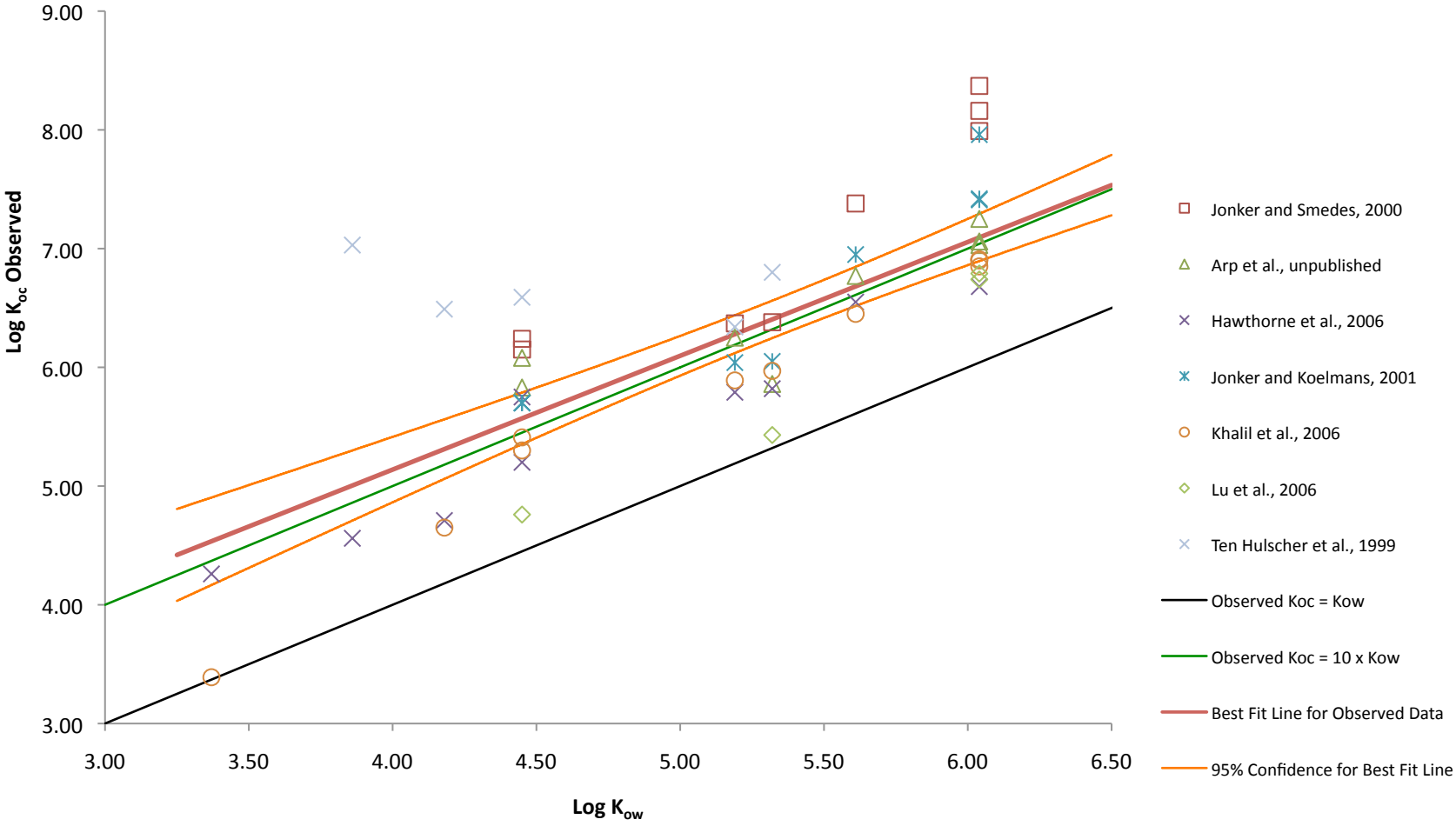

Figure 4 - Log K_{ow} vs Observed Log K_{oc}

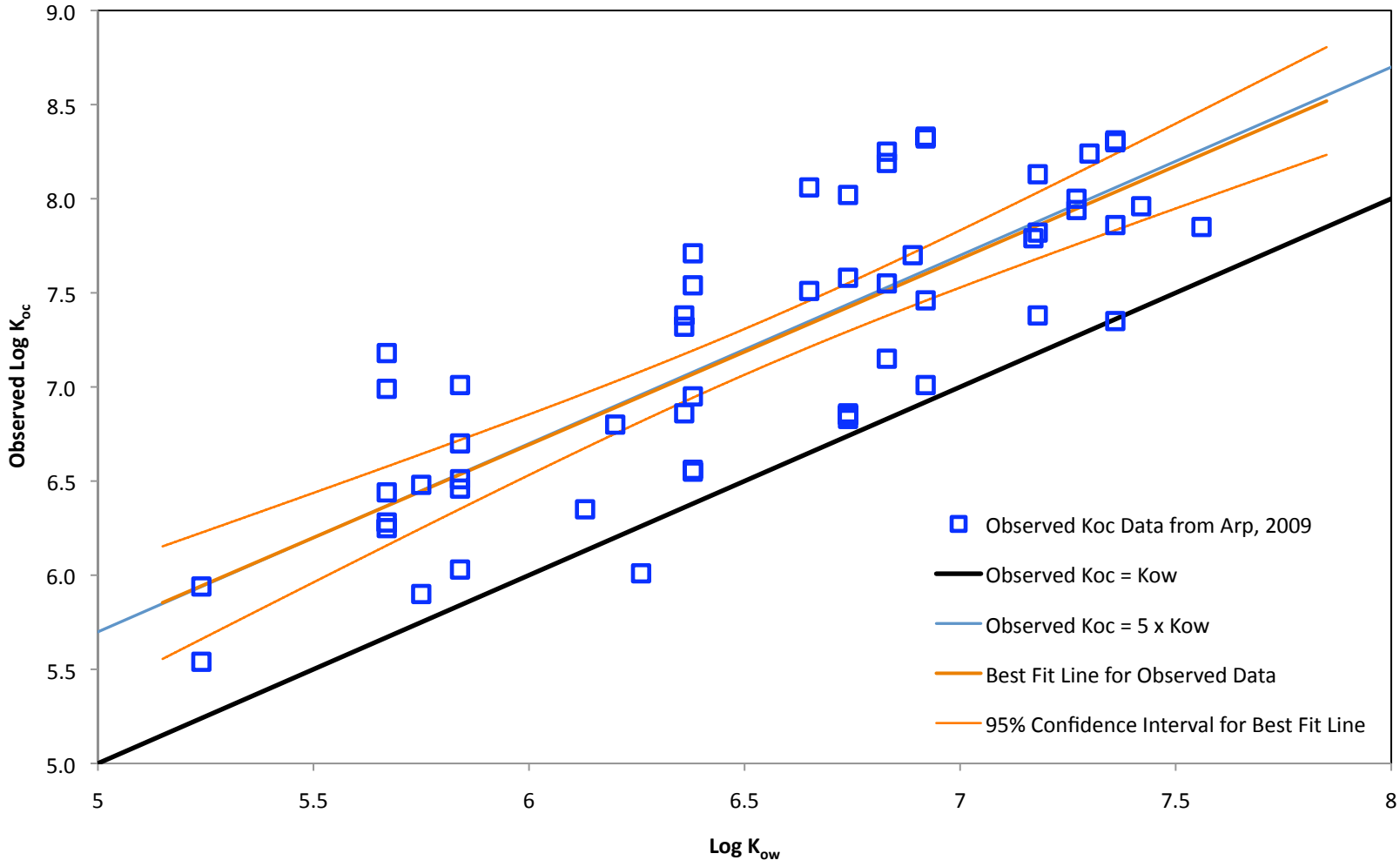

Log K_{ow} values from Hawker, 1988

Figure 5 - Log K_{ow} vs Observed Log K_{oc}

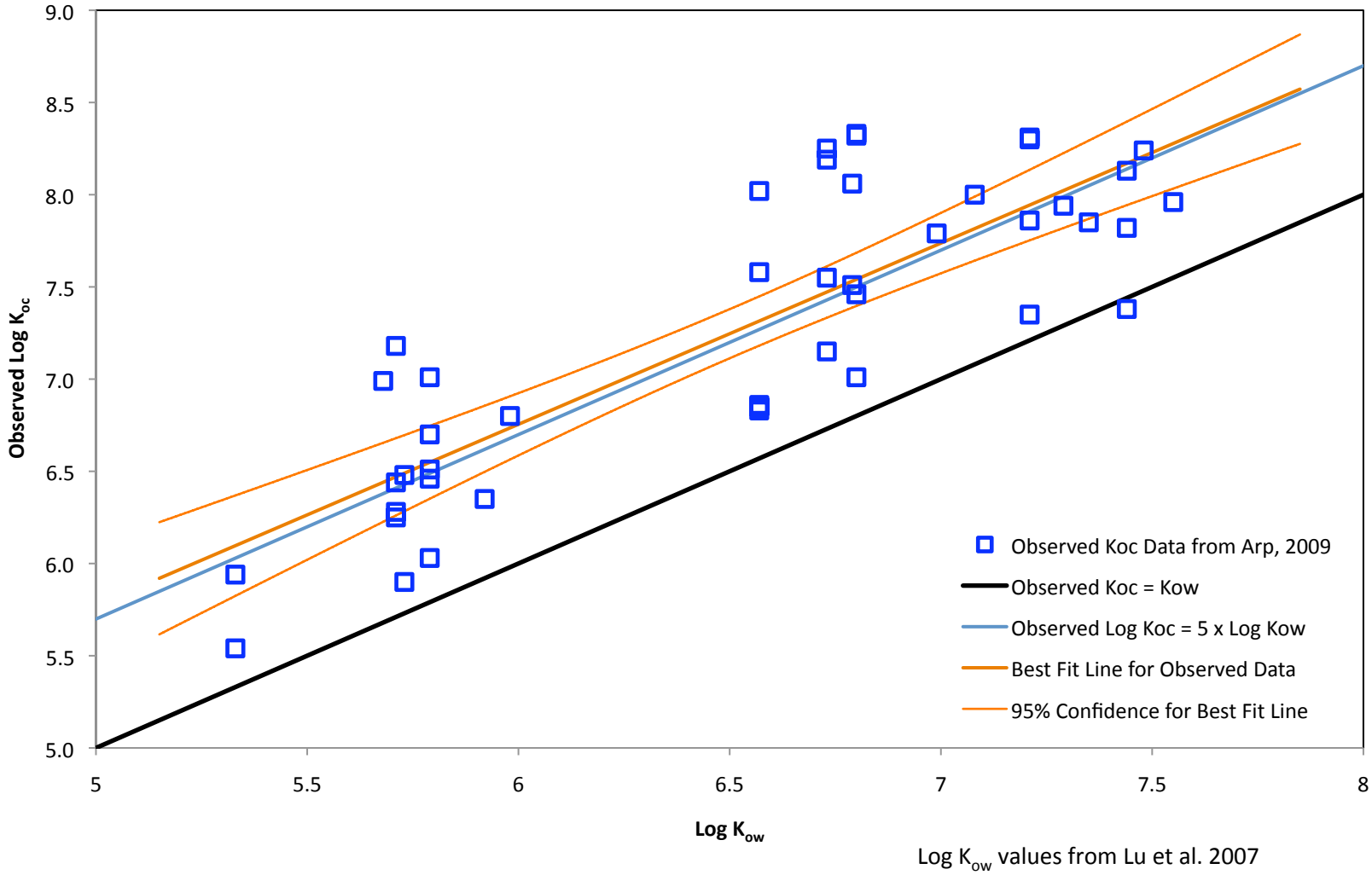

Log K_{ow} values from Lu et al. 2007

ATTACHMENT 3

BIOLOGICAL DEGRADATION RATE EVALUTION

3.1 VOC BIOLOGICAL DECAY RATE EVALUATION

3.2 PHENOL BIOLOGICAL DECAY

ATTACHMENT 3.1

VOC BIOLOGICAL DECAY RATE EVALUATION

Environmental and Water Resources C1786 November 25, 2009
The University of Texas at Austin, Austin TX 78712
Bettie Margaret Smith Chair of Environmental Health Engineering
Phone: 512-471-4642 Email: reible@mail.utexas.edu

To: Caryn Kiehl-Simpson

Parsons

From: Danny Reible and Anthony Smith, University of Texas

Re: Calculation and Summary of Degradation Rates in SMU 6 and 7 Observed in Phase III Addendum 6 Column Tests

Background and Summary

One of the goals of the Phase III column testing was evaluation of fate processes in caps over the Onondaga Lake sediment. This report details the estimation of degradation rates from SMU6 and SMU7 column samples. Sediment cores sent to UT by Parsons were split; half of the material was used in capped sediment column tests and half was sent to TestAmerica, Pittsburgh for pore water generation. Contaminant concentrations measured by TestAmerica were assumed were to be used as the initial sediment concentrations (i.e. the concentrations entering the cap layer) in the column tests. The difference between inlet and outlet concentrations in the columns was to be used to assess fate processes within the cap. The degradation rates calculated in this memorandum are preliminary and will be considered in context with results of future data collection efforts and additional column studies.

The collected sediment samples, however, did not retain a volume of pore water sufficient for analysis except for core 70050. Solid concentration measurements and site-specific partition coefficients, however, could be used to estimate inlet concentrations in several other columns. In addition, effluent contaminant concentrations were generally below the limit of detection. A conservative estimate of fate processes in the columns could be estimated by using the estimated or measured inlet concentrations and assuming that the effluent concentrations were at the detection limit. This report summarizes that analysis.

Overview of Degradation Rate Analysis

Samples 70050A, 70050B, and 70050C yielded pore water volumes sufficient for analysis and estimation of cap layer influent concentrations. Low flow column 70050C demonstrated signs of contamination

during setup, and was not expected to achieve steady state effluent concentrations over the period of testing and was not evaluated for degradation rates. Samples 60098A, 60100A, 60100B, 70048B, and 70048C did not yield pore water volumes sufficient for analysis but solid phase concentrations could be used to estimate porewater concentrations using site-specific partition coefficients. If predicted porewater concentrations were below detection limits (averaged 3.8 µg/L for the column effluent analysis method), a reaction rate was not estimated for those compounds.

Effluent concentrations were consistently above detection limit near the end of testing in only a single column, high flow column 70050A which showed benzene at up to 19 µg/L and 1,4 DCB which reached 5.65 µg/L. In column 70050B, a peak benzene of 14.5 µg/L was detected in the effluent but early in the experimental period suggesting either a sampling artifact or a transient effluent concentration prior to the initiation of effective biodegradation capability. Despite the fact that it was not judged to be indicated of steady state cap behavior, it was employed in the analysis herein to estimate benzene reactivity. In all other columns, effluent concentrations were not detected. The detection limits associated with the column effluent analysis method varied between 3-4.5 µg/L with an average of 3.8 µg/L. If no detectable concentration was observed in the cap effluent, the effluent was presumed to contain 3.8 µg/L of each CPOI for the purposes of getting a preliminary degradation rate assessment. For xylenes and DCB, the rate analysis was focused on the sum of isomers and the detection limit for the sum of the 3 isomers was assumed to be 3*3.8 µg/L or 11.4 µg/L.

In summary, contaminant degradation rates were inferred from columns 60098A, 60100A, 60100B, 70048B, 70048C, 70050A, and 70050B based upon porewater concentrations estimated from solid phase concentrations and assuming detection limits in the effluent. A reaction rate was also inferred from columns 70050A and 70050B based upon measured porewater concentrations from sections of each core. Because it was unknown if the measured or estimated porewater concentration was a better estimate of what was actually moving into the cap for column 70050A and 70050B, both approaches were treated as independent estimates for purposes of this preliminary rate calculation.

Degradation Rate Estimation

The one-dimensional transport equation for an advection-dominated system, given by

$$R_f \, dC/dt = -v \, dC/dx - k \, C \qquad \text{(Eqn 1)}$$

simplifies at steady state to

$$v \, dC/dx = - k \, C \qquad \text{(Eqn 2)}$$

where

v is the interstitial (pore water) velocity (cm/day),

C is the aqueous phase concentration (ug/L),

x is displacement along the flow path (cm), and

k is the first order degradation rate constant ($days^{-1}$).

The parameter "k" is then solved by integration:

$$k = \ln(C_0/C)*(v/x) \qquad \text{(Eqn 3)}$$

where

C_0 is the aqueous phase concentration at x = 0 cm (i.e. entering the cap) (ug/L), and
k, C, v, x as defined previously.

Concentrations at the top of the cap (x = h = 15 cm) are provided from measured effluent concentrations or assumed detection limits and denoted C_{effl}. Eqn 3 becomes

$$k = \ln(C_0/C_{effl})*(v/h) \qquad \text{(Eqn 4)}$$

and estimation of the necessary parameters is described below. The analysis assumes that the concentration within the sediment is initially uniform and uses the maximum concentration in the effluent (or the detection limit) as the quasi-steady effluent concentration from which an effective rate constant can be estimated by Eqn. 4.

Estimation of contaminant concentration entering the sand cap

For columns 70050A and 70050B, porewater concentrations in a portion of the core were available to estimate porewater concentration.

Table 1: Measured sediment porewater concentrations ug/L (TestAmerica analysis)

	Bz	Tol	CB	EtBz	Xyl	13DCB	14DCB	12DCB	SUM	Naph
70050A Inlet, ug/L	130	75	160	23	260	7	230	160	397	1100
70050B, ug/L	61	36	69	8.3	120	<3.3	91	67	158	510

Solid/aqueous partitioning equilibrium was also used to estimate the contaminant concentration entering the sand cap layer of the columns. Solids concentrations (Sw) were determined by TestAmerica (Table 2).

Table 2: Solids loading on sediment samples split from cores and sent to TestAmerica (ug/kg)

	Solids Loading (ug/kg)								
Sample	**Bz**	**Tol**	**CB**	**EtBz**	**Xyl**	**13DCB**	**14DCB**	**12DCB**	**Naph**
60098A	10	11	<9.8	<10	67	<9.2	<9.8	<9.7	1100
60100A	<79	89	<84	140	600	<80	<84	<84	1400
60100B	<90	90	1100	<100	1300	<91	2000	4200	3900
70048B	<1.8	5	<1.9	2.9	73	<1.8	9.8	11	180
70048C	<75	<57	<80	<85	<250	<76	<80	<80	1000
70050A	<530	<410	2200	760	4500	610	6400	2800	34000
70050B	<550	<420	2300	1000	5200	740	9800	4100	56000
70050C	<540	<410	1500	620	3200	<550	5600	2000	45000

Compounds with concentrations less than the minimum detection limit (MDL) were not analyzed further.

The fraction organic carbon was measured by CHN analysis at the Marine Sciences Institute at Port Aransas on samples provided for Phase II tests (Table 3).

Table 3: Fraction organic carbon of Phase II sediment samples analyzed November, 2007.

Sample	foc (%)
60098	0.88
60100	2.64
70048	1.95
70050	5.95

Values of Koc were computed from SMU7 data as presented in the Partitioning[a] Coefficient Memorandum (Parsons, 2008). Mean values are included in Table 4.

Table 4: Mean values for Koc computed from Parsons data.

Koc (L/kg)	
Sample	**Mean**
Bz	99.1
Tol	339.2
CB	356.3
EtBz	879.6
Xyl	783.2
13DCB	1253.5
14DCB	1101.0
12DCB	1211.7
Naph	929.1

The aqueous phase concentration in equilibrium with the sediment solid phase (i.e., the concentration entering the sand cap, C_0) was computed (Eqn 5) for each compound for mean Koc (Table 5).

$$C_0 = Ws / (Koc*foc) \qquad \text{(Eqn 5)}$$

where

Ws is the solid phase loading (ug/kg),
Koc is the organic carbon – water partitioning coefficient (L/kg),
foc is the fraction organic carbon (--), and
C_0 as defined previously.

[a] Parsons, 2008. Partitioning Coefficient Evaluation Memorandum (Cap-18a). Submitted to NYSDEC on behalf of Honeywell, Morristown, NJ. November 2008.

Tables 5: Aqueous phase concentrations in equilibrium with sediment solid phase (C_0) computed using mean value of Koc

	Aqueous Concentration in Equilibium with Solid (ug/L), average Koc								
Sample	**Bz**	**Tol**	**CB**	**EtBz**	**Xyl**	**13DCB**	**14DCB**	**12DCB**	**Naph**
60098A	11.51	3.70			9.76				135.02
60100A		9.92		6.02	28.97				56.99
60100B		10.03	116.77		62.78		68.70	131.09	158.76
70048B		0.76		0.17	4.79		0.46	0.47	9.96
70048C									55.32
70050A			103.80	14.52	96.58	8.18	97.71	38.84	615.16
70050B			108.52	19.11	111.61	9.92	149.62	56.88	1013.21
70050C			70.77	11.85	68.68		85.50	27.75	814.19

Estimation of Effluent Concentrations

Effluent concentrations for all SMU6 and 7 columns (except 70050A/B, as noted above) were below the limit of detection (see Final Report for Phase III Addendum 3 column tests). To provide conservative estimates of degradation rates, the steady-state effluent concentrations of each contaminant for each column were assumed to be at the detection limit which based upon 9 sampling periods (Table 6) was 3.8 ug/L+/- 0.39 µg/L (11.4 ug/L for Xylenes and sum DCBs because they each include three isomers). (Note that the assumption of the highest effluent concentration underestimates the change in concentration between the cap/sediment interface and the top of the cap, providing a conservative estimate of degradation rate.)

Table 6: Average Method Detection Limits reported by DHL Laboratory for specific sampling dates

Date	MDL (ug/L)
3/28/2008	3.66
4/10/2008	3.67
4/25/2008	3.51
5/9/2008	4.06
6/3/2008	3.74
6/26/2008	3.77
7/22/2008	4.65
9/24/2008	4.03
10/28/2008	3.85

Estimation of Column Flow Rates

The hydraulic tracer, fluorescein, was not detected in column effluent and thus does not provide information regarding column pore water velocity. Tracer analysis from SMU1 columns suggests an average pore water velocity of 0.19 cm/day for baseline flow columns. High flow column 70050Bwas approximately 4 times higher, giving power velocities of 0.76 cm/day.

Computation of Degradation Rates

Degradation rates were computed by equation 4 with values of C_0 from Table 1 and 5, C_{effl} = 3.8 ug/L, h = 15 cm, and v = 0.19 cm/day for baseline and 0.76 cm/day for high flow (70050B). Results are summarized in Table 7.

Table 7a: Degradation rates computed using measured pore water concentrations (Co) and assuming effluent concentrations equal to the analytical limit of detection (approx 3.8 ug/L) except when measured effluent concentrations exceeded the detection limit

	Bz	Tol	CB	EtBz	Xyl	13DCB	14DCB	12DCB	SUM DCB	Naph
70050A Inlet, ug/L	130	75	160	23	260	7	230	160	397	1100
Max effluent, ug/L	19	3.80	3.8	3.8	11.4		3.8	3.8	11.4	3.8
rate, day^-1	0.024	0.038	0.047	0.023	0.040		0.052	0.047	0.045	0.072
ln rate	-3.715	-3.276	-3.050	-3.781	-3.229		-2.957	-3.050	-3.102	-2.634
half-life, days	28.4	18.3	14.6	30.4	17.5		13.3	14.6	15.4	9.7
70050B, ug/L	61	36	69	8.3	120	<3.3	91	67	158	510
Max effluent, ug/L	14.5	3.80	3.8	3.8	11.4	3.8	5.65	3.8	13.25	3.8
rate, day^-1	0.0728	0.1139	0.1469	0.0396	0.1193		0.1408	0.1454	0.1256	0.2482
ln rate	-2.620	-2.172	-1.918	-3.229	-2.126		-1.960	-1.928	-2.075	-1.393
half-life	9.5	6.1	4.7	17.5	5.8		4.9	4.8	5.5	2.8

Table 7b: Degradation rates computed using theoretical pore water concentrations assuming equilibrium with solids (average Koc) and effluent concentrations equal to the analytical limit of detection (approx 3.8 ug/L

	Bz	Tol	CB	EtBz	Xyl	13DCB	14DCB	12DCB	SUM DCB	Naph
Max effluent, ug/L	3.8	3.80	3.8	3.8	11.4	3.8	3.8	3.8	11.4	3.8
60098A	11.51	3.70			9.76					135.02
rate, day^{-1}	0.0140									0.0452
ln rate	-4.266									-3.096
half-life (d)	49.4									15.3
60100A		9.92		6.02	28.97					56.99
rate, day^{-1}		0.0122		0.0058	0.0118					0.0343
ln rate		-4.410		-5.145	-4.438					-3.373
half-life (d)		57.0		118.9	58.7					20.2
60100B		10.03	116.77		62.78		68.70	131.09	199.79	158.76
rate, day^{-1}		0.0123	0.0434		0.0216		0.0367	0.0449	0.0363	0.0473
ln rate		-4.398	-3.138		-3.835		-3.306	-3.104	-3.317	-3.052
half-life (d)		56.3	16.0		32.1		18.9	15.5	19.1	14.7
70048B		0.76		0.17	4.79		0.46	0.47	0.92	9.96
rate, day^{-1}										0.0122
ln rate										-4.406
half-life (d)										56.8
70048C										55.32
rate, day^{-1}										0.0339
ln rate										-3.384
half-life (d)										20.4
70050A			103.80	14.52	96.58	8.18	97.71	38.84	144.74	615.16
rate, day^{-1}			0.0419	0.0170	0.0271	0.0097	0.0411	0.0294	0.0322	0.0644
ln rate			-3.173	-4.075	-3.609	-4.634	-3.191	-3.525	-3.436	-2.742
half-life (d)			16.5	40.8	25.6	71.4	16.8	23.5	21.5	10.8
70050B			108.52	19.11	111.61	9.92	149.62	56.88	216.42	1013.21
rate, day^{-1}			0.1698	0.0818	0.1156	0.0486	0.1861	0.1371	0.1491	0.2830
ln rate			-1.773	-2.503	-2.158	-3.023	-1.681	-1.987	-1.903	-1.262
half-life (d)			4.1	8.5	6.0	14.2	3.7	5.1	4.6	2.4

Computation of rate not possible if $C_0 < C_{effl}$

Confirmation of Degradation by Solids Loading

The total mass of contaminant in each column was estimated using the loadings measured by TestAmerica from the split sample from each core. The mass associated with solids was added to the mass in pore water at equilibrium with the sediment (Table 5, above). The following assumptions (bulk density and porosity) and column dimensions were used:

Sediment bulk density (ρ_b) = 1.5 g/cm^3,

Cross-sectional area of column = 18.1 cm^2,

Height of sediment column = 15.0 cm,

Assume sediment porosity = 0.4.

The volume occupied by sediment is 270 cm^3 and the mass of dry sediment is 0.40 kg. The volume of pore water in the sediment layer is 0.11 L. The total contaminant mass in the column at the start of the experiment is computed by

$$M\ (ug) = 0.40\ kg\ dry\ sediment * Ws\ (ug/kg) + 0.11\ L * C_0\ (ug/L) \qquad \text{(Eqn 6)}$$

but the contribution by the aqueous phase is small and may be neglected for simplicity. (To demonstrate this, consider toluene, a comparatively non-sorbing compound, in sample 60098A, which has the lowest foc of all samples at 0.8%. The mass on the solids is 0.4 kg * 11 ug/kg = 4.4 ug, while the mass in the aqueous phase is 0.11 L * 3.7 ug/L = 0.41 ug, one order of magnitude lower. The difference is greater for the other compounds. Note that this simplification is not valid for benzene.)

The mass of contaminant in the column at the time of shutdown was computed similarly. Cap and sediment were sectioned in 5 cm intervals, so assuming the sediment and sand have similar physical characteristics, each interval has a dry mass of 0.13 kg. For non-detects, the contaminant loading was assumed equal to the MDL, as done with the effluent above. This, again, provides a conservative estimate of the contaminant mass degraded during the course of the experiment.

Total mass of each contaminant in each column at the start and finish of the experiment is reported in Table 8. Also reported is the change in mass and the time of column operation.

Table 8: Total contaminant mass in column based on solids loading at the start and finish of the test and the change.

			Total Mass of Contaminant in Column (ug)								
Sample	**deltaT (d)**		**Bz**	**Tol**	**ClBz**	**EtBz**	**Xyl**	**13DCB**	**14DCB**	**12DCB**	**Naph**
		start	4	4.4			26.8				440
		finish	0.8	0.8			0.8				0.8
60098A	280	delta	-3.2	-3.6			-26				-439.2
			-80.00%	-81.82%			-97.01%				-99.82%
		start		35.6		56	240				560
		finish		0.8		0.8	0.8				1.2
60100A	280	delta		-34.8		-55.2	-239.2				-558.8
				-97.75%		-98.57%	-99.67%				-99.79%
		start		36	440		520		800	1680	1560
		finish		1.7	0.8		0.8		0.8	0.8	2.4
60100B	267	delta		-34.3	-439.2		-519.2		-799.2	-1679.2	-1557.6
				-95.28%	-99.82%		-99.85%		-99.90%	-99.95%	-99.85%
		start		2		1.16	29.2		3.92	4.4	72
		finish									2.1
70048B	280	delta		-2		-1.16	-29.2		-3.92	-4.4	-69.9
				-100.00%		-100.00%	-100.00%		-100.00%	-100.00%	-97.08%
		start									400
		finish									1.7
70048C	259	delta									-398.3
											-99.58%
		start			880	304	1800	244	2560	1120	13600
		finish			300.4	300.4	300.4	<300	127.5	300.4	392.4
70050A	280	delta			-579.6	-3.6	-1499.6	NA	-2432.5	-819.6	-13207.6
					-65.86%	-1.18%	-83.31%		-95.02%	-73.18%	-97.11%
		start			920	400	2080	296	3920	1640	22400
		finish			89.5	85.5	415.4	52.5	435.3	156	3785.2
70050B	259	delta			-830.5	-314.5	-1664.6	-243.5	-3484.7	-1484	-18614.8
					-90.27%	-78.63%	-80.03%	-82.26%	-88.90%	-90.49%	-83.10%
	Average Reduction		-80.00%	-93.71%	-85.32%	-69.60%	-93.31%	-82.26%	-95.95%	-90.90%	-96.62%

NA denotes that the mass loss was indeterminate .

The results showed that substantial mass of each contaminant was degraded in the capping columns. These estimates include both contaminants degrading in the sediment and in the cap column. The high degradation rates support the substantial degradation rates estimated in the effluent from the columns.

Discussion

The degradation rate from each column was used to define average rates and confidence limits. There is no evidence to support spatial variations in degradation rate between SMU 6 and7 so the goal of the experiments was to make the best estimate of the expected rate. The best estimate of the reaction rate is the mean of the observations and the uncertainty in that estimate is the uncertainty in the mean. The

observed degradation rates were log transformed effectively assuming that the uncertainty in relative reactivity was uniform, that is, that the fraction (or percent) error in high and low estimates of the reactivity were the same. In addition, the use of log transformed data would insure that non-feasible values (i.e. negative rates) would be excluded from the analysis. The logarithm transformed rates for each compound were averaged and then transformed back to estimate average reaction rate. Confidence limits for the estimated reaction rate were calculated by the following method: The standard deviation of the logarithm of the estimated reaction rates was calculated for each compound. The standard error was then calculated defined by the ratio of the sample standard deviation and the square root of the number (N) of estimates used to define the standard deviation. The standard error is the appropriate metric to define the uncertainty in the best estimate of reactivity, the mean. The 95% confidence limits were then estimated using the average log transformed rate +/- the standard error times the student t value corresponding to degrees of freedom (N-1) and 95% upper and lower confidence limits. A reasonable estimate of the uncertainty distribution of these reaction rates is to assume a log-normal distribution with the estimated 95 % upper and lower confidence limits. Although there is insufficient data currently to test the condition of normality of the log-transformed data, it is expected that greater confidence in the reaction rates will result from the currently ongoing studies. Degradation rates for the six baseline flow columns using average Koc values are summarized in Table 9.

Table 9: Summary of degradation rates computed from baseline flow columns.

	Bz	Tol	CB	EtBz	Xyl	13DCB	14DCB	12DCB	SUM	Naph
Number of Analyses	3	4	5	5	6	2	5	5	5	9
t value - 95%	4.30	3.18	2.78	2.78	2.57	12.71	2.78	2.78	2.78	2.31
Average ln rate, day^-1	-3.53	-3.56	-2.61	-3.75	-3.23	-3.83	-2.64	-2.72	-2.78	-2.82
+/-95% CI	2.08	1.70	0.87	1.22	0.98	10.23	0.88	0.89	0.88	0.76
Average rate, day^-1	0.0292	0.0283	0.0735	0.0236	0.0395	0.0217	0.0712	0.0659	0.0622	0.0599
Halflife days	23.74	24.47	9.43	29.37	17.56	31.89	9.73	10.51	11.14	11.58
95% conf. rate- Low	0.0036	0.0052	0.0308	0.0069	0.0148	0.0000	0.0295	0.0270	0.0259	0.0281
Halflife Low Days	190.26	134.14	22.51	99.74	46.69	888122.94	23.52	25.66	26.79	24.70
95% conf rate- high	0.2340	0.1553	0.1756	0.0801	0.1049	605.3734	0.1722	0.1610	0.1497	0.1277
Halflife High Days	2.96	4.46	3.95	8.65	6.61	0.00	4.03	4.30	4.63	5.43

Half-lives reported above are generally supported by literature values for anaerobic degradation and are also within the range of the reaction rates observed in the slurry experiments.

There exist several sources of uncertainty in the estimated degradation rates. The use of method detection limits in the effluent results in likely underestimates of the rate of degradation. That is, higher rates would be calculated if actual effluent concentrations could be measured. Uncertainty that might lead to lower estimated rates, include heterogeneity and degradation within the sediment which might lower the final effluent concentration due to dispersion and or reductions in the inlet concentration. In addition, the columns may not have been fully reduced. Although sealed, they were operated in air and oxygen may have diffused into column tubing or into the feed water that was pumped into the column during sampling. Some indications of marginally reducing conditions in the cap led to their placement in a nitrogen chamber. No increase in effluent concentrations were noted after placement in the chamber, that is, no observable decrease in reactivity was noted after a return to anaerobic conditions. These rates are preliminary estimates that will allow evaluation of preliminary designs but should be used with the

understanding that final design calculations will be incorporated using on-going column experiments which are expected to provide a more robust data set.

The factors contributing to ambiguity in Phase III tests have been eliminated in Phase IV. The new columns are operated in an anaerobic chamber, eliminating the possibility of oxygen intrusion. Redox will be measured and effluent will be analyzed for methane. Changes to the contaminant concentration entering the sand cap (i.e. C_0) can be detected at a sampling port between the sediment column and the sand cap column. And by balancing the isotope inventory following injection of radio-labeled contaminant into the sand cap column, uncertainty regarding steady state will be diminished. Until this addition rate information is available, the estimated rates presented herein can be used to evaluate preliminary cap designs. It is recommended that modeling distributions examine a lognormal distribution reflecting the 95% upper and lower confidence limits defined above which will capture possibilities outside this range in a Monte Carlo analysis of uncertainty around this input parameter.

ATTACHMENT 3.2

PHENOL BIOLOGICAL DECAY

Geosyntec consultants

130 Research Lane, Suite 2
Guelph, Ontario, Canada N1G 5G3
PH 519.822.2230
FAX 519.822.3151

MEMORANDUM

Date: 09 December 2009

To: Caryn Kiehl-Simpson, P.E. – Parsons

Copies to: Edward Glaza and David A. Smith - Parsons

From: Tom Krug, Dave Major, and Paul Nicholson - Geosyntec Consultants

Subject: Onondaga Lake Sediment Cap - Anaerobic Biodegradation Rates for Phenol

---

This memo has been prepared by Geosyntec Consultants, Inc. (Geosyntec) to provide an analysis of anaerobic biodegradation rates for phenol that can be used as a starting point in modeling of biodegradation in the planned sediment cap at Onondaga Lake. This memorandum presents a summary of the literature biodegradation rates and focuses on those rate studies that were conducted under conditions consistent with redox and temperature levels present in Onondaga Lake.

Table 1 presents a summary of literature anaerobic biodegradation rates for phenol compiled by Aronson and Howard (1997). The table shows both degradation rates (k) and half lives ($t_{1/2}$) from various literature sources for both field and microcosm (laboratory) testing under a variety of redox conditions and temperatures.

Phenol has a high solubility in water and lower tendency for partitioning to solids than many other organic compounds. The octanol-water partitioning coefficient (K_{ow}) for phenol and several other compounds are presented below (NY DEC, 1999).

Compound	**Log of Octanol-Water Partitioning Coefficient (K_{ow})**
Phenol	2.0
Benzene	2.0
Toluene	2.69
Chlorobenzene	2.84
Naphthalene	3.37
Dichlorobenzene	3.38
Fluorene	4.18
Pyrene	5.32

As a result of its low partitioning onto solids, most experiments conducted to evaluate biodegradation rates for phenol monitor the concentration of phenol in the aqueous phase (Godsy, EM et al. 1983; Godsy, EM et al. 1992A; Gibson, S.A., and Suflita, J.M. 1986). The data from these tests are reasonable to use directly in sediment cap modeling because of the relatively low degree of partitioning onto the solids.

Redox conditions and temperature will have a significant impact on the degradation capabilities and rates for organic contaminants such as are present in the sediment at Onondaga Lake. Biodegradation processes under anaerobic but mildly reducing conditions such as nitrate (NO_3) reducing conditions can be significantly different than for the more highly reducing conditions (methanogenic) that are expected to occur in the deep (i.e., below one foot) sediment in a lake. Under mildly anaerobic conditions, the types of microorganisms that can degrade organic contaminants are more varied and degradation pathways will typically be more beneficial to the microorganisms than those available under more highly reducing conditions. Temperature will not generally impact the biodegradation reactions that will take place but cooler temperatures will decrease the rate that biodegradation reactions take place. A typical rule of thumb for the effect of temperature on biodegradation rates is that a ten-degree drop in temperature will decrease degradation rates (increase $t_{1/2}$) by a factor of about two.

Based on the impacts of various conditions discussed above, we selected degradation data from the full data set in Table 1 for a short list of data set for methanogenic conditions. The short list of degradation rates does not include the four methanogenic field and column studies where biodegradation was observed but rate data was not reported or the three methanogenic studies presented in Aronson and Howard (1997) where biodegradation of phenol was not observed. Substantial laboratory microcosm and field study data demonstrate that phenol degrades under anaerobic methanogenic conditions. The studies where degradation was not observed were not laboratory microcosm studies and, as such, are not considered well controlled and reliable relative to the results of microcosm studies and the results of these three tests are not considered in the half-life statistics presented below. We also applied a temperature correction factor based on an assumption that, unless otherwise specified, microcosm tests were conducted at 22°C and field tests were at the temperature expected to occur in the Onondaga Lake sediments. One test conducted at 37°C was excluded because of the difficulty in adjusting data from a temperature 25°C above the anticipated temperature in the sediment.

The table below shows statistics for the focused data set with temperature adjusted half-life values.

Range	3.6 to 116 days
Average	36.5 days
median (50^{th} percentile)	19.5 days
90^{th} percentile	108 days
standard deviation	43 days

Based on a review of the phenol literature, the focused data provided in Table 1 is expected to reflect the range of degradation rates one would expect in the Onondaga Lake sediment cap. Bench testing is underway as part of the Phase V Pre-Design Investigation to develop site-specific data on phenol biodecay which will be incorporated into future model revisions.

REFERENCES

Aronson, D., Howard, P.H., 1997. "Anaerobic Biodegradation of Organic Chemicals in Groundwater: A Summary of Field and Laboratory Studies." Syracuse Research Corporation, North Syracuse, NY.

Gibson, S.A., and Suflita, J.M. 1986. "Extrapolation of Biodegradation Results to Groundwater Aquifers: Reductive Dehalogenation of Aromatic Compounds." Applied and Environmental Microbiology, 52, 681-88.

Godsy, EM et al. 1983. Methanogenesis of phenolic compounds by a bacterial consortium from a contaminated aquifer in St. Louis Park, Minnesota. Bulletin Environ Contam Toxicol. 30: 261-268.

Godsy, EM et al. 1992A. Methanogenic degradation kinetics of phenolic compounds in aquifer-derived microcosms. Biodegradation 2: 211-221.

Healy, J.B., Young, L.Y. 1978. "Catechol and Phenol Degradation by a Methanogenic Population of Bacteria." Applied and Environmental Microbiology, 35, 216-218.

New York State Department of Environmental Conservation (NY DEC), 1999. Technical Guidance for Screening Contaminated Sediments. January 15, 1999.

* * * * *

Enclosures: Table 1 – Anaerobic Biodegradation Rates for Phenol

Table 1: Anaerobic Biodegradation Rates for Phenol

Compound	Redox Conditions	Average Biodegradation Rate (1/day)	Average Biodegradation Half-life (days)	Study type	Reported Temp. (°C)	Temp. Correction	Temp. Adjusted Half life (days)	Reference	Primary Reference
All Data									
Phenol	Fe	0.218	3.2	Microcosm	30°C			Lovely, 1990	
	Fe	>0.027	< 26	In-situ Microcosm				Aronson & Howard, 1997	Nielsen, PH et al. 1995a
	Fe	no biodegradation		In-situ Microcosm				Aronson & Howard, 1997	Nielsen, PH et al. 1995a
	NO3	0.059	11.7	Microcosm	31°C			O'Connor, 1996	
	NO3	0.420	1.7	GW Sample				Aronson & Howard, 1997	Flyvbjerg, J et al. 1993
	NO3	0.430	1.6	GW Sample				Aronson & Howard, 1997	Flyvbjerg, J et al. 1993
	NO3	0.520	1.3	GW Sample				Aronson & Howard, 1997	Flyvbjerg, J et al. 1993
	NO3	0.100	6.9	Microcosm				Aronson & Howard, 1997	Morris, MS. 1988
	NO3	biodegrades		Batch Reactor				Aronson & Howard, 1997	Lyngkilde, J et al. 1992
	NO3/Mn	possible		In-situ Microcosm				Aronson & Howard, 1997	Nielsen, PH et al. 1995a
	NO3/SO4	0.003	239.0	GW Sample				Aronson & Howard, 1997	Francis, AJ 1982
	SO4	0.366	1.9	Microcosm	30°C			Haggblom, 1995	
	SO4	0.051	13.5	Microcosm				Gibson, 1986	
	SO4	0.069	10.0	Microcosm	20°C			Ramanand, 1991	
	SO4	biodegrades		GW Sample				Aronson & Howard, 1997	Flyvbjerg, J et al. 1993
	Methanogenic/Fe/SO4	no biodegradation		Microcosm				Aronson & Howard, 1997	Nielsen, PH et al. 1995a
	Methanogenic/SO4	0.100	6.9	Microcosm				Aronson & Howard, 1997	Morris, MS. 1988
	Methanogenic	0.032	21.7	Field				Aronson & Howard, 1997	Godsy, EM et al. 1992
	Methanogenic	0.053	13.1	Microcosm	37°C			O'Connor, 1996	
	Methanogenic	0.012	57.8	GW Sample				Aronson & Howard, 1997	Godsy, EM et al. 1983
	Methanogenic	0.388	1.8	Microcosm				Healy, 1978	
	Methanogenic	0.077	9.0	Microcosm				Gibson, 1986	
	Methanogenic	0.013	53.3	Microcosm				Aronson & Howard, 1997	Troutman, DE et al. 1984
	Methanogenic	0.068	10.2	Microcosm				Aronson & Howard, 1997	Godsy, EM et al. 1992
	Methanogenic	0.071	9.8	Microcosm				Aronson & Howard, 1997	Arvin, E et al. 1989
	Methanogenic	0.130	5.3	Microcosm				Aronson & Howard, 1997	Godsy, EM et al. 1992A
	Methanogenic	no biodegradation		Batch Reactor				Aronson & Howard, 1997	Lyngkilde, J et al. 1992
	Methanogenic	biodegrades		Column				Aronson & Howard, 1997	Suflita, JM & Miller, GD. 1985
	Methanogenic	no biodegradation		Column				Aronson & Howard, 1997	Haag, F et al. 1991
	Methanogenic	biodegrades		Field				Aronson & Howard, 1997	Goerlitz, DF et al. 1985
	Methanogenic	biodegrades		Field				Aronson & Howard, 1997	Troutman, DE et al. 1984
	Methanogenic	biodegrades		Field				Aronson & Howard, 1997	Godsy, EM et al. 1983
	Methanogenic	no biodegradation		In-situ Microcosm				Aronson & Howard, 1997	Nielsen, PH et al. 1995a
	Methanogenic	>0.11	< 6.3	Microcosm				Aronson & Howard, 1997	Gibson, 1986
	Not provided	no biodegradation		Microcosm				Aronson & Howard, 1997	Klecka, GM et al. 1990a
	Not provided	0.20	3.5	Microcosm				Aronson & Howard, 1997	Smith, JA & Novak, JT. 1987
	Not provided	1.15	0.6	Column				Aronson & Howard, 1997	Lin, CH. 1988

Table 1: Anaerobic Biodegradation Rates for Phenol

Compound	Redox Conditions	Average Biodegradation Rate (1/day)	Average Biodegradation Half-life (days)	Study type	Reported Temp. (°C)	Temp. Correction	Temp. Adjusted Half life (days)	Reference	Primary Reference
Methanogenic Conditions Only									
Phenol	Methanogenic	0.388	1.8	Microcosm		2	3.6	Healy, 1978	
	Methanogenic	0.13	5.3	Microcosm		2	10.7	Aronson & Howard, 1997	Godsy, EM et al. 1992A
	Methanogenic	> 0.11	< 6.3	Microcosm		2	12.6	Aronson & Howard, 1997	Gibson, 1986
	Methanogenic	0.077	9.0	Microcosm		2	18.1	Gibson, 1986	
	Methanogenic	0.071	9.8	Microcosm		2	19.5	Aronson & Howard, 1997	Arvin, E et al. 1989
	Methanogenic	0.068	10.2	Microcosm		2	20.4	Aronson & Howard, 1997	Godsy, EM et al. 1992
	Methanogenic	0.032	21.7	Field		1	21.7	Aronson & Howard, 1997	Godsy, EM et al. 1992
	Methanogenic	0.013	53.3	Microcosm		2	106.6	Aronson & Howard, 1997	Troutman, DE et al. 1984
	Methanogenic	0.012	57.8	GW Sample		2	115.5	Aronson & Howard, 1997	Godsy, EM et al. 1983
						Range	3.6 to 116		
						Mean	36.5		
						10th Percentile	9.2		
						25th Percentile	12.6		
						Median (50th Percentile)	19.5		
						75th Percentile	21.7		
						90th Percentile	108.4		
						Standard Deviation	42.7		

Arvin, E et al. Microbial degradation of oil and creosote related aromatic compounds under aerobic and anaerobic conditions. Int Conf Physiochemical Biol Detoxif Hazard Wastes. 2: 828-847 (1989)
Flyvbjerg, J et al. Microbial degradation of phenols and aromatic hydrocarbons in creosotecontaminated groundwater under nitrate-reducing conditions. J Contam Hydrol 12: 133-150 (1993)
Francis, AJ. Microbial Transformation of Low-Level Radioactive Waste. In: IAEA-SM-257/72. Environmental Migration of Long-Lived Radionuclides. Vienna, Austria: International Atomic Energy Agency pp. 415-429 (1982)
Gibson, SA & Suflita, JM. Extrapolation of biodegradation results to groundwater aquifers: reductive dehalogenation of aromatic compounds. Appl Environ Microbiol 52: 681-688 (1986)
Godsy, EM et al. Methanogenesis of phenolic compounds by a bacterial consortium from a contaminated aquifer in St. Louis Park, Minnesota. Bull Environ Contam Toxicol. 30: 261-268 (1983)
Godsy, EM et al. Methanogenic biodegradation of creosote contaminants in natural and simulated ground-water ecosystems. Ground Water 30(2): 232-242 (1992)
Godsy, EM et al. Methanogenic degradation kinetics of phenolic compounds in aquifer-derived microcosms. Biodegradation 2: 211-221 (1992A)
Goerlitz, DF et al. Migration of wood-preserving chemicals in contaminated groundwater in a sand aquifer at Pensacola, Florida. Environ Sci Technol 19: 955-961 (1985)
Haag, F et al. Degradation of toluene and p-xylene in anaerobic microcosms: evidence for sulfate as a terminal electron acceptor. Environ Toxicol Chem 10: 1379-89 (1991)
Klecka, GM et al. Natural bioremediation of organic contaminants in ground water: Cliffs-Dow Superfund site. Ground Water 28(4): 534-543 (1990A)
Lin, CH. Biodegradation of selected phenolic compounds in a simulated sandy surficial Florida aquifer. Ph.D. Dissertation, University of Florida (1988)
Lyngkilde, J & Christensen, TH. Fate of organic contaminants in the redox zones of a landfill leachate pollution plume (Vejen, Denmark). J Contam Hydrol 10: 291-307 (1992)
Morris, MH. Biodegradation of organic contaminants in subsurface systems: kinetic and metabolic considerations. Ph.D. Dissertation. Virginia Polytechnic Institute and State University (1988)
Smith, JA & Novak, JT. Biodegradation of chlorinated phenols in subsurface soils. Water, Air, and Soil Pollution 33: 29-42 (1987)
Suflita, JM & Miller, GD. Microbial metabolism of chlorophenolic compounds in ground water aquifers. Environ Sci Technol 4: 751-758 (1985)
Troutman, DE et al. Phenolic contamination in the sand-and-gravel aquifer from a surface impoundment of wood treatment wastes, Pensacola, Florida. USGS Water-Resources Investigations Report 84-4230 (1984)

ATTACHMENT 4

MODEL FILES

(PROVIDED ELECTRONICALLY ON ATTACHED CD)